AD NUMBER
ADC000461

CLASSIFICATION CHANGES

TO: **unclassified**

FROM: **confidential**

LIMITATION CHANGES

TO:

Approved for public release, distribution unlimited

FROM:

Distribution authorized to U.S. Gov't. agencies and their contractors; Administrative/Operational Use; NOV 1974. Other requests shall be referred to Office of Naval Research, Attn: Code 102-OSC, Arlington, VA 22217.

AUTHORITY

31 Dec 1980, per document marking; CNO/N772 ltr N772A/6U875630 20 Jan 2006 & ONR ltr 31 Jan 2006

CONFIDENTIAL

Sound Velocity Structure of the Labrador Sea, Irminger Sea, and Baffin Bay During the NORLANT-72 Exercise
[Unclassified Title]

DON F. FENNER AND PAUL J. BUCCA

Naval Oceanographic Office

November 1974

Provisional Technical Report

DEPARTMENT OF THE NAVY
NAVAL OCEANOGRAPHIC OFFICE
Washington, D.C. 20373

CONFIDENTIAL

CONFIDENTIAL

CONFIDENTIAL

REPORT DOCUMENTATION PAGE		READ INSTRUCTIONS BEFORE COMPLETING FORM
1. REPORT NUMBER NOO TR-245	2. GOVT ACCESSION NO.	3. RECIPIENT'S CATALOG NUMBER
4. TITLE *(and Subtitle)* SOUND VELOCITY STRUCTURE OF THE LABRADOR SEA, IRMINGER SEA, AND BAFFIN BAY DURING THE NORLANT-72 EXERCISE (U)		5. TYPE OF REPORT & PERIOD COVERED Provisional
		6. PERFORMING ORG. REPORT NUMBER
7. AUTHOR(s) Don F. Fenner and Paul J. Bucca		8. CONTRACT OR GRANT NUMBER(s)
9. PERFORMING ORGANIZATION NAME AND ADDRESS Naval Oceanographic Office Code 6160 Washington, DC 20373		10. PROGRAM ELEMENT, PROJECT, TASK AREA & WORK UNIT NUMBERS 714-LW-RGA
11. CONTROLLING OFFICE NAME AND ADDRESS Long Range Acoustic Propagation Project Office of Naval Research Code 102-OSC Arlington, VA 22217		12. REPORT DATE November 1974
		13. NUMBER OF PAGES 108
14. MONITORING AGENCY NAME & ADDRESS(*if different from Controlling Office*)		15. SECURITY CLASS. *(of this report)* CONFIDENTIAL
		15a. DECLASSIFICATION/DOWNGRADING SCHEDULE GDS 1980

16. DISTRIBUTION STATEMENT *(of this Report)*

In addition to security requirements which apply to this document and must be met, it may be further distributed by the holder only with specific prior approval of the Director, Long Range Acoustic Propagation Project.

17. DISTRIBUTION STATEMENT *(of the abstract entered in Block 20, If different from Report)*

Approved for public release; distribution unlimited

18. SUPPLEMENTARY NOTES

19. KEY WORDS *(Continue on reverse side if necessary and identify by block number)*

Oceanographic data, sound velocity profiles, bathymetric tracks, deep sound channel axis, critical depth, Labrador Sea, Irminger Sea, Baffin Bay, Davis Strait, Denmark Strait, North Atlantic Current, Labrador Current, West Greenland Current, Baffinland Current, Subarctic Convergence, Polar Front, LRAPP (Long Range Acoustic Propagation Project)

20. ABSTRACT *(Continue on reverse side if necessary and identify by block number)*

During July-September 1972, 439 oceanographic observations were taken in the Labrador Sea, Irminger Sea, and Baffin Bay as part of the NORLANT-72 Exercise. One-third of these observations, mostly expendable bathythermographs (XBTs), were converted into sound velocity profiles using Wilson's equation and historical salinities. These data were adequate for temporal and spatial analysis in the central Labrador Sea and along tracks between this region and the Denmark Strait, Reykjanes Ridge, and the Carey Islands in northern Baffin Bay. Oceanographic data also were adequate to define

DD FORM 1473 1 JAN 73   EDITION OF 1 NOV 65 IS OBSOLETE
S/N 0102-014-6601

20. (cont'd)

meandering of the Subarctic Convergence in the central Labrador Sea throughout the three exercise phases. Sound velocity profiles throughout the exercise area were extremely complex and variable, particularly in the central Labrador Sea and just south of Davis Strait. At one station astride the Subarctic Convergence, the sound velocity at the deep sound channel (DSC) axis varied by 9.5 m/sec over less than 48 hours. In the intense transition zone south of Davis Strait, this parameter varied by 20.9 m/sec over a distance of 155 nm. The depth of the DSC axis was much less variable than the sound velocity at the axis in both regions. Temporal and spatial variability appear to be equally significant as controls over DSC structure throughout the exercise area.

ACKNOWLEDGMENTS

CONTENTS

v

CONTENTS (cont'd)

FIGURES

FIGURES (cont'd)

UNCLASSIFIED

FIGURES (cont'd)

TABLES

TABLES (cont'd)

INTRODUCTION

(C) The NORLANT-72 Exercise was conducted from July through September 1972 in the western North Atlantic Ocean north of 45°N in a region including the Labrador Sea, Irminger Sea, and Baffin Bay. The following ships took part in the exercise:

- USNS SANDS (T-AGOR-6),

- USNS HAYES (T-AGOR-16),

- USNS LYNCH (T-AGOR-7),

- R/V PIERCE,

- R/V LANGEVIN, and

- CFAV QUEST.

Oceanographic data were collected from SANDS, HAYES, and LANGEVIN and from various aircraft for use in determining environmental effects on acoustic propagation. A preliminary analysis of the sound velocity structure of the exercise area was given by Fenner and Bucca (1972) based on a very limited number of data points. This report supplements the preliminary NORLANT-72 sound velocity analyses and includes additional sound velocity/temperature-salinity (T-S) comparisons, making use of 177 additional observations.

DEFINITIONS

(S) For purposes of this report, the depth of the deep sound channel (DSC) axis is defined as the depth of the absolute sound velocity minimum. Critical depth is defined as that depth where the maximum sound velocity at the surface or in the mixed layer recurs, and as such demarcates the bottom of the DSC. Depth excess is defined as the interval between critical depth and the seafloor and is necessary for convergence zone propagation from a near-surface source. All depths are given in meters (m), all distances in nautical miles (nm) and all sound velocities in meters per second (m/sec). All bottom depths have been corrected for variations from a standard sound velocity of 1500 m/sec using the depth correction tables of Matthews (1939). Sound velocity data presented in this report have not been extended below the maximum depth of observed data owing to expected data variability throughout the exercise area.

1

(U) The NORLANT-72 Exercise was divided into the following three phases:

- Phase I: 15-29 July 1972,

- Phase II: 30 July-18 August 1972, and

- Phase III: 22 August-19 September 1972.

These three phases oceanographically correspond to early, middle, and late summer.

DISCUSSION OF ENVIRONMENTAL DATA

A. Data Availability

(U) Table I summarizes the oceanographic data collected during NORLANT-72 by phase, platform, and the following categories:

- Expendable bathythermographs (XBTs), including Sippican Model T-5 probes (1830 m) and T-7 probes (760 m),

- 330-m AN/SSQ-36 airborne expendable bathythermographs (AXBTs),

- Salinity-temperature-depth (STD) profiles,

- Conductivity-temperature-depth-sound velocity (CTD/SV) profiles,

- Sound velocimeter profiles (SVPs), and

- Sea surface temperature (SST) observations.

In addition, current meter measurements were obtained at one location throughout the exercise by the Naval Oceanographic Office (NAVOCEANO). The locations of these various observations are shown in figures 3 through 5 of Fenner and Bucca (1972). Table II gives the location and maximum depth of STDs, CTD/SVs, and SVPs taken by SANDS during all three phases.

(C) Most oceanographic observations collected during NORLANT-72 were either XBTs or AXBTs. Many of these observations were taken within a five-degree square between 50°-55°N and 44°-49°W, in the vicinity of the four primary reference stations (stations A, B, C, and D). However, during Phase I, XBT and AXBT observations were taken by SANDS, HAYES, and various aircraft squadrons to the north and east of the primary operating area (OPAREA). During Phase II, HAYES took a line of XBTs between the primary OPAREA and the Reykjanes Ridge. During Phase III, QUEST and SANDS took a line of XBTs into Baffin Bay.

	T-5 XBT	T-7 XBT	AXBT	STD	CTD/SV	SVP	SST
PHASE I	(15-29 July)						
SANDS	4	41	-	-0-	2	4	(2)
HAYES	15	33	-	-0-	-0-	-0-	-0-
LYNCH	-0-	-0-	-	-0-	-0-	-0-	-0-
VXN-8	-	-	51	-	-	-	-
VP-24	-	-	68	-	-	-	-
PHASE II	(30 July-18 August)						
SANDS	17	29	-	3	-0-	5	(2)
HAYES	2	7	-	-0-	-0-	-0-	-0-
LANGEVIN	8	-0-	-	-0-	-0-	-0-	-0-
PIERCE	-0-	-0-	-	-0-	-0-	-0-	-0-
VP-405	-	-	23	-	-	-	-
PHASE III	(22 August-19 September)						
SANDS	5	40	-	-0-	4	1	(2)
QUEST	-0-	64	-	-0-	-0-	-0-	-0-
VP-405	-	-	12	-	-	-	-
POST PHASE III	(18-20 October)						
LYNCH	-0-	-0-	-	-0-	-0-	-0-	-0-
TOTALS	52	214	154	3	6	10	-

Notes: ● (2) indicates observation every 2 hours
 ● - indicates not applicable

TABLE I. SUMMARY OF NORLANT-72 OCEANOGRAPHIC DATA (U)

STATION NUMBER	DATE (1972)	TIME (GMT)	PHASE	LAT (N)	LONG (W)	MAXIMUM DEPTH (m)
CTD/SV 1	17 Jul	1530	I	52°00'	44°44'	1008
CTD/SV 2	18 Jul	2255	I	53°55'	44°50'	649
SVP 1	19 Jul	1800	I	53°55'	44°49'	2772
SVP 2	20 Jul	2114	I	55°48'	43°23'	3087
SVP 3	22 Jul	0330	I	58°42'	38°25'	2935
SVP 4	24 Jul	0200	I	55°50'	34°01'	1403
SVP 5	31 Jul	020C.	II	53°59'	44°51'	3234
STD 1	31 Jul	0500	II	54°02'	44°56'	1498
STD 2	1 Aug	2100	II	51°56'	45°10'	1513
SVP 6	2 Aug	0015	II	51°52'	45°14'	3602
SVP 7	2 Aug	2034	II	52°58'	44°48'	3619
STD 3	3 Aug	0025	II	52°57'	44°51'	1490
SVP 8	12 Aug	1545	II	53°48'	45°00'	3577
SVP 9	17 Aug	1100	II	52°00'	45°00'	3367
CTD/SV 3	24 Aug	2315	III	50°56'	42°12'	2958
CTD/SV 4	30 Aug	0615	III	57°04'	51°57'	2995
CTD/SV 5	31 Aug	2115	III	53°58'	44°46'	2972
CTD/SV 6	3 Sep	1800	III	51°59'	44°50'	2970
SVP 10	4 Sep	0200	III	52°00'	44°57'	3700

Notes: ● Upcasts and downcasts available for STDs and SVPs, downcasts only available for CTD/SVs
● Times and positions are for downcasts in all cases

TABLE II. USNS SANDS STD, CTD/SV, AND SVP OBSERVATIONS (U)

B. Treatment of Data

(U) Most sound velocity data presented in this report were calculated from XBT or AXBT temperature traces and historical salinity values using the equation of Wilson (1960). In all, 163 XBT or AXBT traces were converted into sound velocity profiles. Salinity correction factors for use in Wilson's equation were determined at 10-m depth increments in all cases. The XBT or AXBT traces were machine digitized at 10- to 15-m depth increments. Therefore, the salinity correction factor lying at the depth closest to the given temperature point was used in calculating the sound velocity for that point. Only three salinity profiles collected during the exercise were used in the calculation of sound velocities, one at station A, one at station B, and one midway between these stations. The remainder of the salinity profiles used in the sound velocity calculations were taken from historical summer data.

C. Relative Data Accuracy

(U) Six different instrument types were used to collect environmental data during NORLANT-72: SVPs, STDs, CTD/SVs, T-5 XBTs, T-7 XBTs, and AXBTs. Only two of these, the SVP and CTD/SV, measure sound velocity directly. Both systems have an accuracy of ±0.3 m/sec. In addition, the SVP system has a maximum resolution of ±0.3 m/sec at the lowering rates used in NORLANT-72. The STD system has a temperature accuracy of ±0.02°C, and a salinity accuracy of ±0.02°/oo, leading to an overall calculated sound velocity accuracy of ±0.2 m/sec, disregarding any inaccuracies in Wilson's equation. The T-5 and T-7 XBTs have a temperature accuracy of about ±0.02°C, which results in a calculated sound velocity accuracy of about ±0.7 m/sec, assuming that historical salinities are correct and that there are no inaccuracies in Wilson's equation. Finally, the AXBTs have a temperature accuracy of ±0.3°C (±0.5°F), which results in a minimum calculated sound velocity accuracy of about ±1.2 m/sec. During NORLANT-72, SANDS STD and SVP upcasts and downcasts were equally valid in terms of accuracy and repeatability.

(U) Figure 1 shows a comparison of sound velocities derived from data measured by various systems at approximately the same time and location. There is generally good agreement between the various measurement systems considering the wide variability in system accuracies and the large-scale oceanographic variability encountered in the NORLANT-72 area (Fenner and Bucca, 1972). Sound velocities below the DSC axis calculated from XBTs appear to be 0.5 to 1.0 m/sec higher than sound velocities calculated from STD data or sound velocities measured by an SVP or CTD/SV system for the three positions
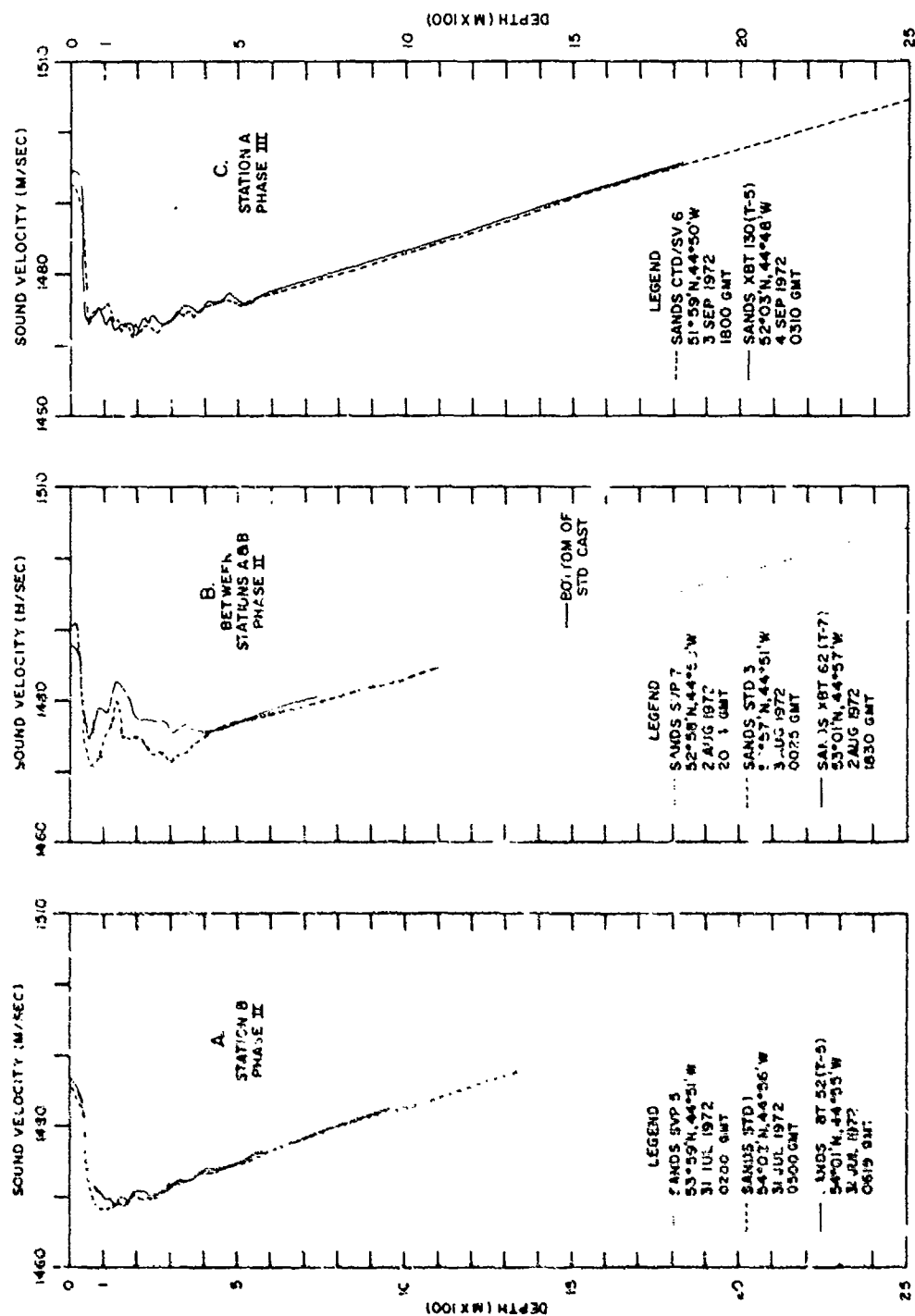
FIGURE 1. COMPARISON OF SVP, STD, CTD/SV, AND XBT DATA (U)

analyzed. This is not due to a salinity error, since an identical
salinity was used to calculate sound velocities for both the STD and
XBT shown in figure 1A and a second identical salinity was used for
those in figure 1B. The higher XBT sound velocities may be due partially
to an error in Wilson's equation, as originally suggested by Carnvale,
et al. (1968).

(U) The extreme variability between the sound velocity profile
calculated using SANDS XBT 62 and the other two profilers shown in
figure 1B is perfectly possible, since all three observations lay
astride the Subarctic Convergence during Phase II. Temperature
variations of 0.5°C across distances of less than 10 nm are common
along the Subarctic Convergence, particularly at depths between 200
and 400 m. A 0.5°C variation in temperature can produce a sound
velocity variation in excess of 2.0 m/sec in the 4° to 6°C temperature
range (NAVOCEANO, 1962). Physically, the XBT-derived sound velocity
profile shown in figure 1B probably is the result of an intrusion of
warmer North Atlantic Central Water under the Subarctic Convergence.

OCEANOGRAPHIC OVERVIEW OF NORLANT-72 AREA

(U) As previously stated by the authors (Fenner and Bucca, 1972),
the NORLANT-72 area is "one of the most complex oceanographic regions
found in the North Atlantic Ocean". Figures 2, 3, and 4A show a
generalized picture of surface circulation in the exercise area during
Phases I, II, and III, respectively. Figure 4B shows the general
surface circulation of Davis Strait and Baffin Bay (Phase III, only).
Figures 2, 3, and 4A also show the position of the Subarctic Convergence
during each of the three phases of the exercise.

(U) The Subarctic Convergence can be considered as the oceanographic
boundary (front) between the cold, dilute circulation of the Labrador
Current and the warmer, more saline circulation of the North Atlantic
Current (an offshoot of the Gulf Stream). The position of this feature
as shown in figures 2, 3, and 4A is based on temperature contours at a
depth of 100 m since this front often is masked at the surface by
summer insolation. The position of the Subarctic Convergence varied
between the three phases of NORLANT-72, particularly in the region
where it separates the warm-water circulation of a semipermanent
North Atlantic Current gyre from the colder circulation of the Labrador
Sea gyre. However, if equal amounts of data were available farther to
the north, the Subarctic Convergence probably would be equally variable
in shape along its entire extent. This front can extend to depths
greater than 1000 m off Grand Banks (Fenner and Bucca, 1971), and
probably extends to maximum depths of about 500 m in the exercise area.
Sound velocity profiles astride or on opposite sides of the Subarctic
Convergence can display substantial variations over relatively small
distances or time periods (figure 1B).
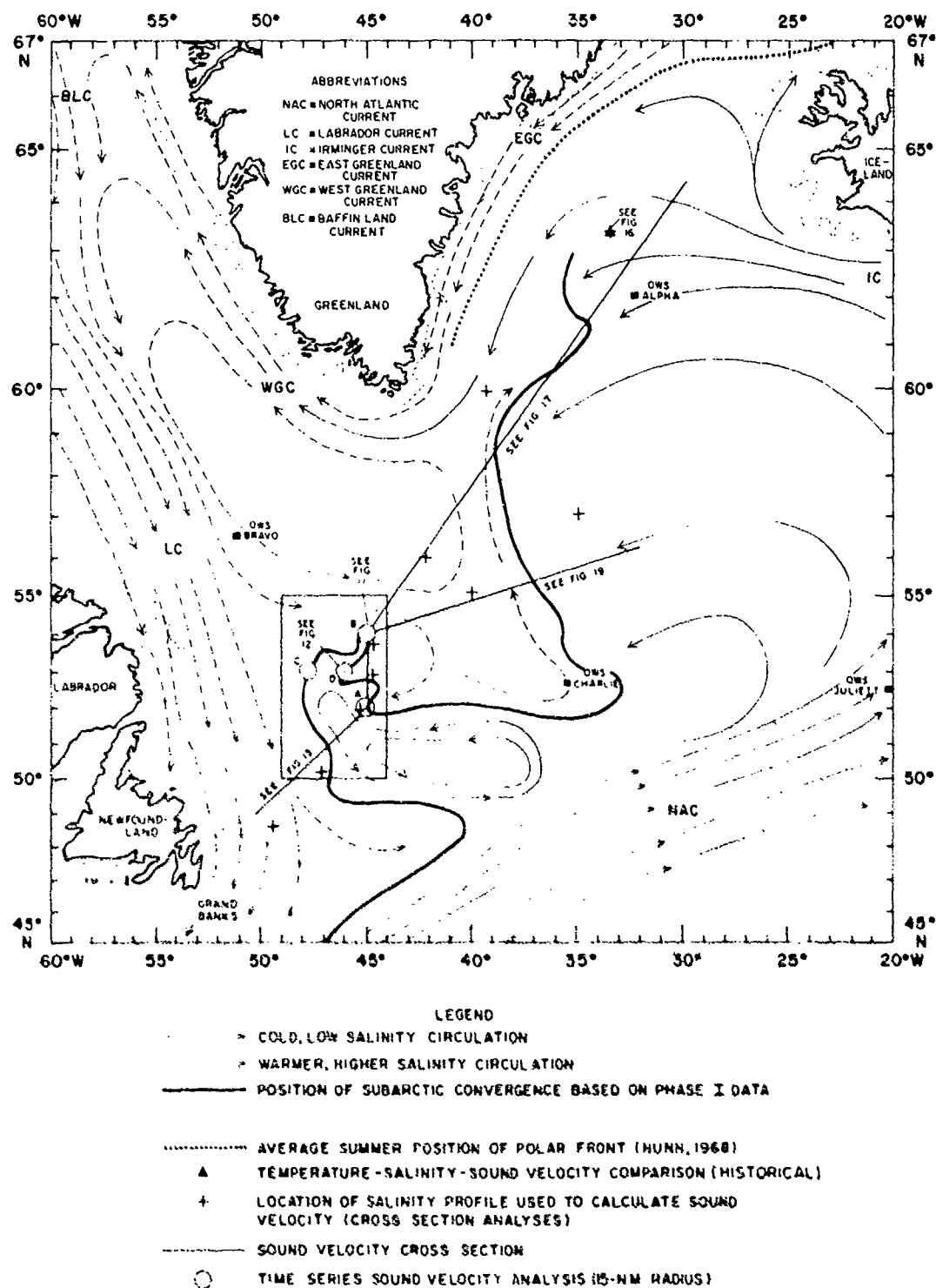
FIGURE 2. GENERALIZED SURFACE CIRCULATION AND INDEX OF SOUND VELOCITY
ANALYSES FOR NORLANT-72 PHASE I (U)

8
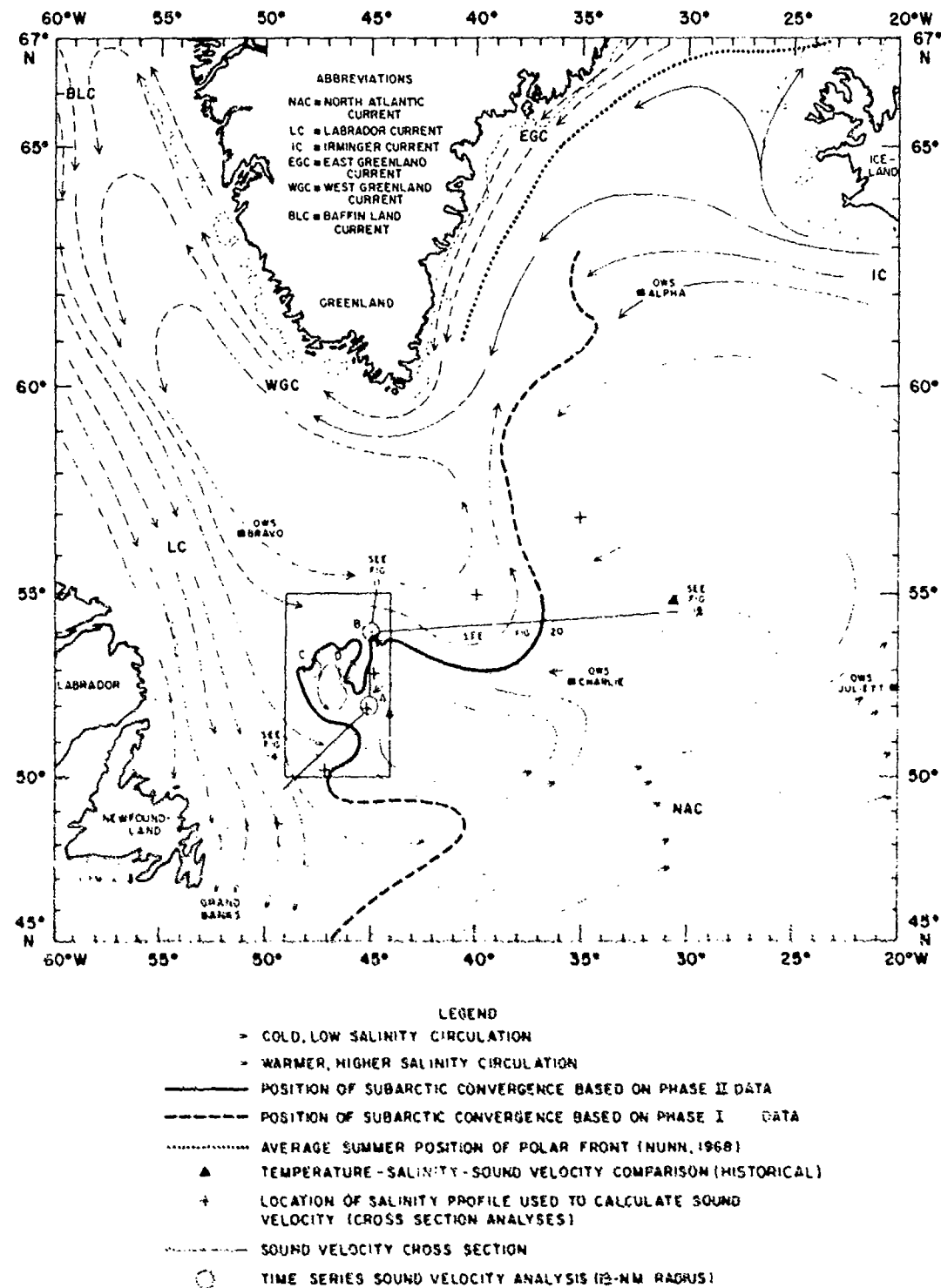
FIGURE 3. GENERALIZED SURFACE CIRCULATION AND INDEX OF SOUND VELOCITY ANALYSES FOR NORLANT-72 PHASE II (U)
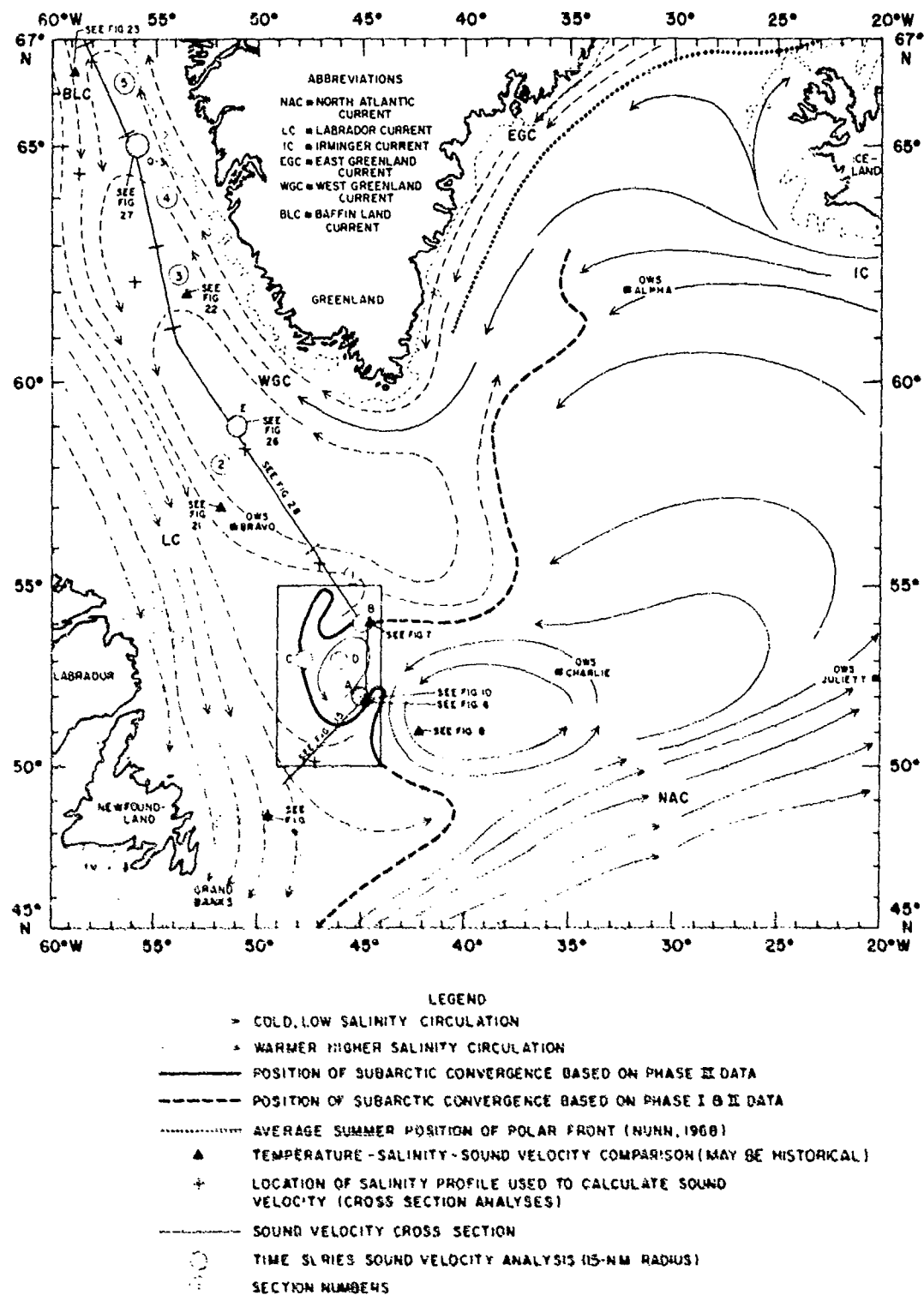
FIGURE 4A. GENERALIZED SURFACE CIRCULATION AND INDEX OF SOUND VELOCITY ANALYSES FOR NORLANT-72 PHASE III (U)

LEGEND

········► COLD, LOW SALINITY CIRCULATION

▲ TEMPERATURE - SALINITY - SOUND VELOCITY COMPARISON (HISTORICAL)

+ LOCATION OF SALINITY PROFILE USED TO CALCULATE SOUND
VELOCITY (CROSS SECTION ANALYSES)

——— SOUND VELOCITY CROSS SECTION

(s) SECTION NUMBER
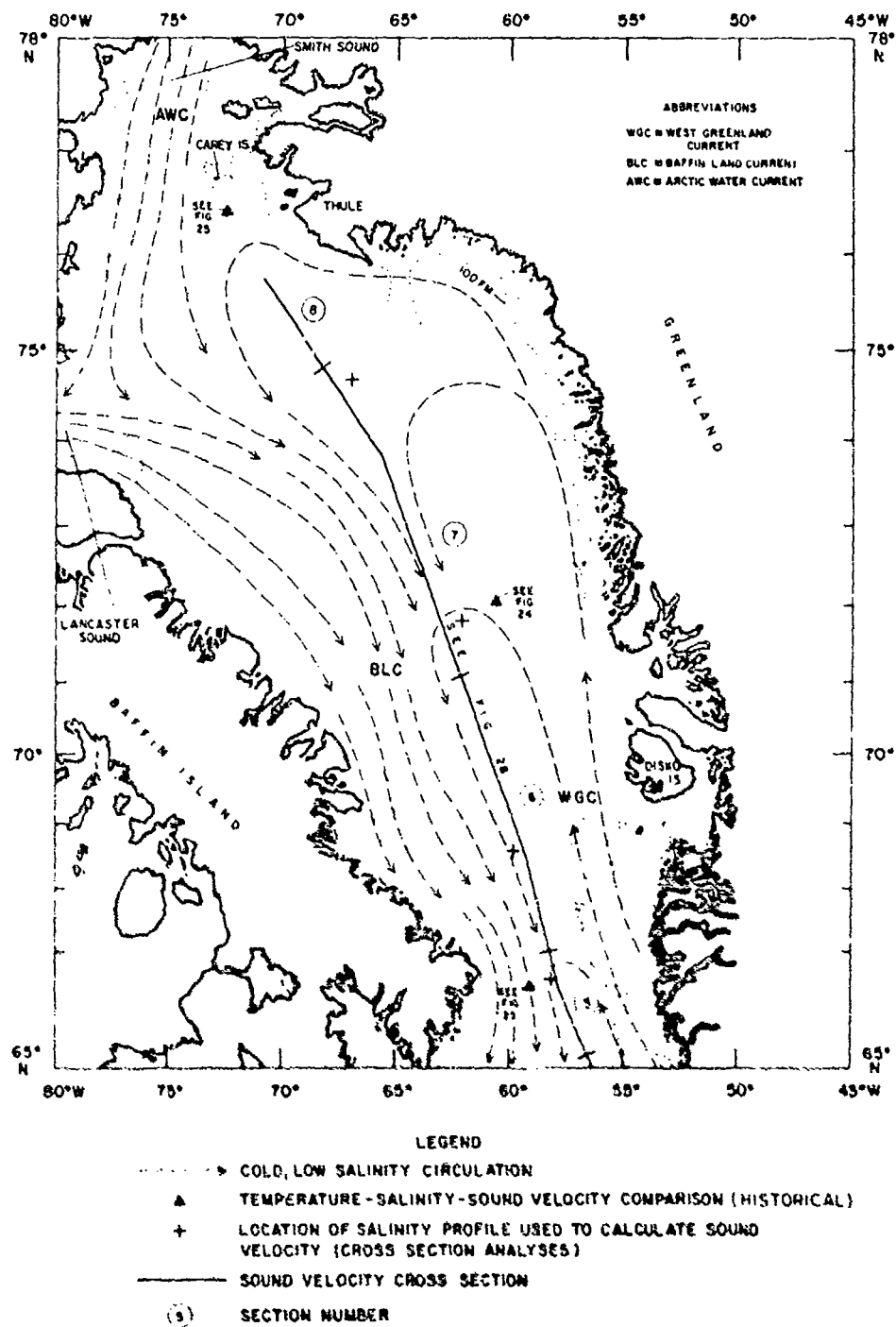
FIGURE 4B. GENERALIZED SURFACE CIRCULATION AND INDEX OF SOUND VELOCITY
ANALYSES FOR NORLANT-72 PHASE I.I, CONTINUED INTO BAFFIN BAY (U)

(U) Farther to the north, the Polar Front separates the cold, dilute waters of the East Greenland Current from the warmer, more saline waters of the Irminger Current (an offshoot of the North Atlantic Current). Since the Subarctic Convergence does not close with the Polar Front during summer months (Nunn, 1968), warmer, more saline waters of the Irminger Current turn to the south in the Irminger Sea and eventually round the southern tip of Greenland to form the West Greenland Current. This current is warmer and more saline than the Labrador Sea gyre, and hence causes higher sound velocities in the upper 1000 m of the water column. The West Greenland Current is apparent as a subsurface flow well into Baffin Bay. This intrusion of Atlantic waters into Baffin Bay also has pronounced effects on sound velocity structure.

(C) Figures 2, 3, 4A, and 4B also are indices of the various sound velocity analyses contained in this report (cross sections and time series analyses). In addition, these figures show the locations of T-S/sound velocity comparisons, salinity profiles used in calculating sound velocities from XBT traces, and various Ocean Weather Stations (OWS) found in the NORLANT-72 exercise area. Since the exercise area is so diverse oceanographically, the various sound velocity analyses will be discussed as follows:

● Sound velocity structure of the primary OPAREA,

● Sound velocity structure between station B and Denmark Strait (northeast of primary OPAREA),

● Sound velocity structure between station B and the Reykjanes Ridge (east of primary OPAREA), and

● Sound velocity structure between station B and the Carey Islands, Baffin Bay (northwest of primary OPAREA).

Each of these sections is proceeded by a short discussion of the general oceanography for the region involved making use of T-S/sound velocity comparisons. Direct comparison of sound velocity structures between the NORLANT-72 phases is possible only for station B, for the tracks southwest of station B, and for the tracks between station B and the Reykjanes Ridge.

SOUND VELOCITY STRUCTURE OF PRIMARY OPAREA

A. General Oceanography

(C) The primary OPAREA for the NORLANT-72 Exercise was a five-degree square between 50°-55°N and 44°-49°W. This area contained the four primary reference stations (stations A, B, C, and D) and is outlined in figures 2, 3, and 4A. The primary OPAREA was dominated by the

meandering Subarctic Convergence during all three phases of the exercise. Figure 5 shows temperature contours at a depth of 100 m for the primary OPAREA and the position of the Subarctic Convergence for each of the three exercise phases. The Subarctic Convergence occurred between the 5° and 6°C isolines at a depth of 100 m based on a rigorous inspection of NORLANT-72 XBT data. During Phase I of NORLANT-72, the Subarctic Convergence passed through all four of the primary reference stations. During Phase II, this front passed through stations C and D, but separated station A (warm side of front) from station B (cold side of front). During Phase III, the Subarctic Convergence passed through stations A and C, but separated station B (cold side) from station D (warm side). The meandering nature of the Subarctic Convergence caused marked changes in sound velocity structures throughout the primary OPAREA over relatively small distances and time periods during all three phases of the exercise.

(U) The following T-S/sound velocity comparisons have been chosen to illustrate the very complex oceanography of the primary OPAREA:

- Figure 6, located at station A,

- Figure 7, located at station B,

- Figure 8, located in the North Atlantic Current gyre, and

- Figure 9, located in the Labrador Current north of Grand Banks.

The data shown in figures 6, 7, and 8 were collected during Phase III of the exercise. Therefore, figure 6 shows an observation lying just on the warm side (almost astride) the Subarctic Convergence, while figure 7 shows an observation lying on the cold side of this front.

(U) Three major surface and near-surface water masses are found in the primary OPAREA: very cold, very dilute Labrador Current Water (LCW); much warmer, much more saline North Atlantic Central Water (NACW) which is carried by the North Atlantic Current; and a water mass with intermediate characteristics called Atlantic Subarctic Water (ASaW) (Sverdrup, et al., 1942). Within the North Atlantic Current, NACW is found between depths of about 200 and 1600 m. Within the Labrador Current, LCW is found between the surface and about 1000 to 1200 m depth. However, ASaW is a surface water mass that can overlie either NACW or LCW in the region on either side of the Subarctic Convergence. All of these water masses intermix at various depths along the Subarctic Convergence, leading to very complicated T-S relationships and equally complex and spurious sound velocity structures.
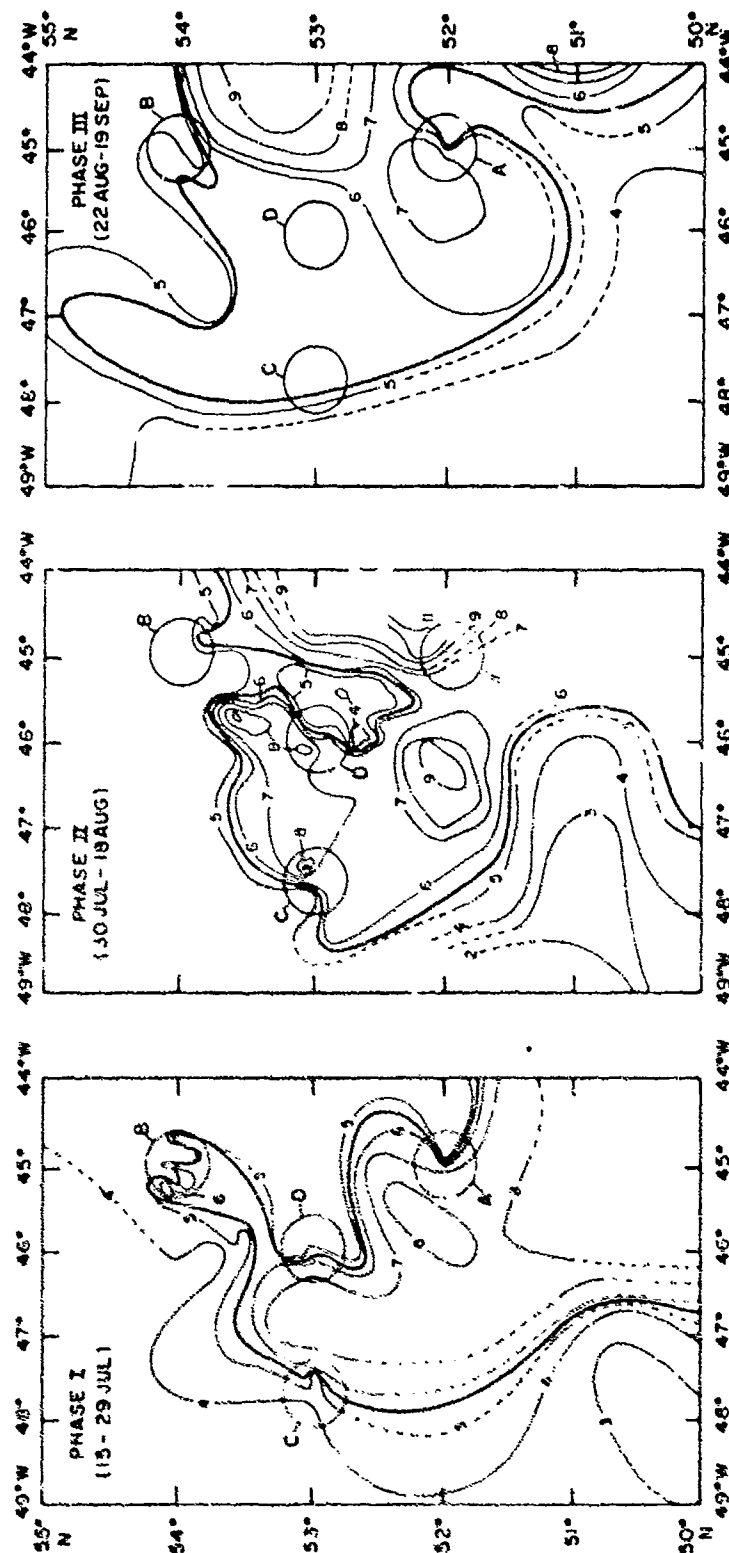
LEGEND: ———— APPROX. POSITION OF SUBARCTIC CONVERGENCE

NOTES: • TEMPERATURE IN °C
       • CIRCLES AROUND STATIONS A THRU D HAVE 15-NM RADIUS
       • DASHED LINES INDICATE LESSER DATA RELIABILITY

FIGURE 5. TEMPERATURE PATTERN AT 100 METERS
DEPTH NEAR NORLANT-77 PRIMARY
REFERENCE STATIONS (U)

(U) The primary OPAREA also is influenced by Arctic Intermediate Water (AIW) that probably is formed north and west of the Subarctic Convergence by sinking of ASaW. To the south and east of the Subarctic Convergence, AIW is characterized by a salinity minimum at depths between about 800 and 1800 m (Bubnov, 1968). However, this water mass does not profoundly affect sound velocity structures.

(U) At greater depths, the entire North Atlantic Ocean is occupied by North Atlantic Deep and Bottom Water. This water mass generally leads to a predictable positive sound velocity gradient below depths of 2000 to 2500 m. However, in the primary OPAREA, cold, dilute Norwegian Sea Overflow Water (NSOW) can cause a gradient change in the deep profile (lower velocities near the bottom). The effects of NSOW on near-bottom sound velocities has been studied in detail in the Irminger Sea by Guthrie (1964).

(U) At station A (figure 6), ASaW overlies an intrusion of NACW between 260 and 700 m. The DSC axis (260 m) coincides with the bottom of the ASaW layer, while the NACW intrusion causes a sound velocity perturbation at 500 m. The two separate AIW cores at 900 and 1300 m do not result in any appreciable change in the positive sound velocity gradient below the DSC axis. Below about 2200 m, the predictable positive sound velocity gradient is altered by NSOW. At 3000 m, the sound velocity is nearly 2.0 m/sec less than that found at station B (figure 7). The irregular sound velocity structure above the DSC axis at station A is a result of local mixing and turbulence in the ASaW layer that is common on the warm side of the Subarctic Convergence.

(U) At station B (figure 7) ASaW overlies a layer of LCW between 160 and 800 m. Below 800 m depth, no AIW cores are observable in the NACW layer, indicating that AIW may be in the process of formation north and west of the Subarctic Convergence. The DSC axis (160 m) again coincides with the bottom of the ASaW layer. Several sound velocity perturbations are found within the LCW layer, one of them (at 240 m) roughly corresponds with the depth of the LCW core. There is no noticeable change in the deep positive sound velocity gradient due to NSOW effects at station B. The more regular (smoother) sound velocity structure above the DSC axis is common in the Labrador Sea gyre, and is a further indication that this station lay on the cold side of the Subarctic Convergence during Phase III of the exercise.
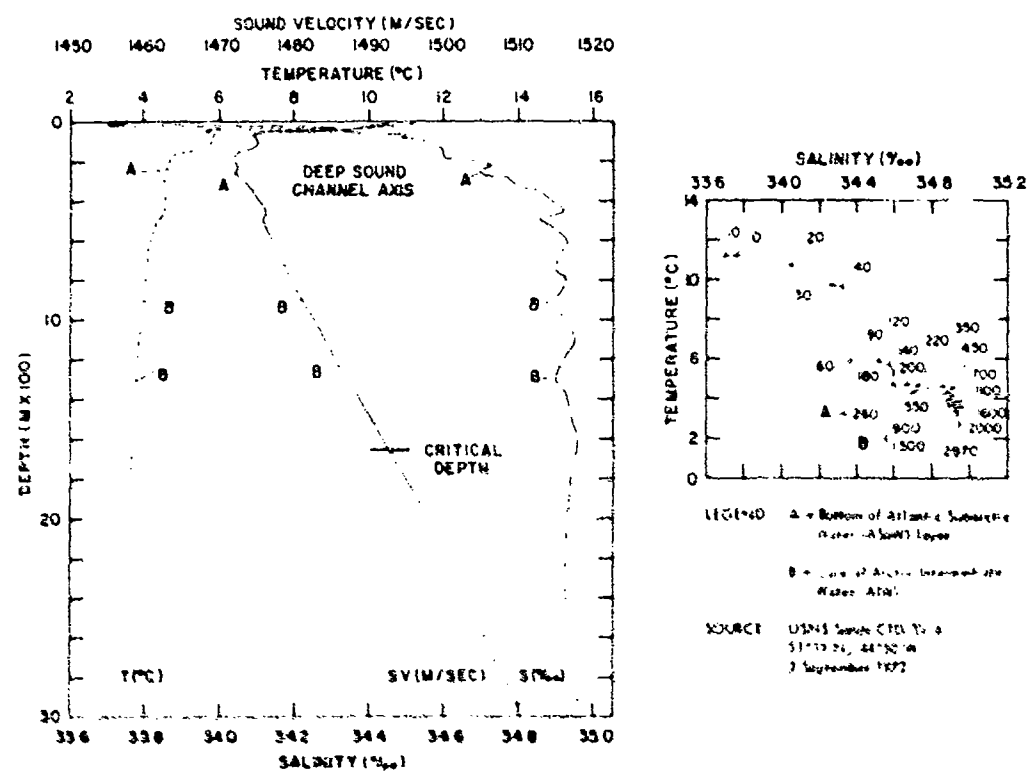
FIGURE 6. TEMPERATURE-SALINITY-SOUND VELOCITY
PROFILES AND T-S DIAGRAM AT STATION A
DURING PHASE III (U)

SOUND VELOCITY (M/SEC)
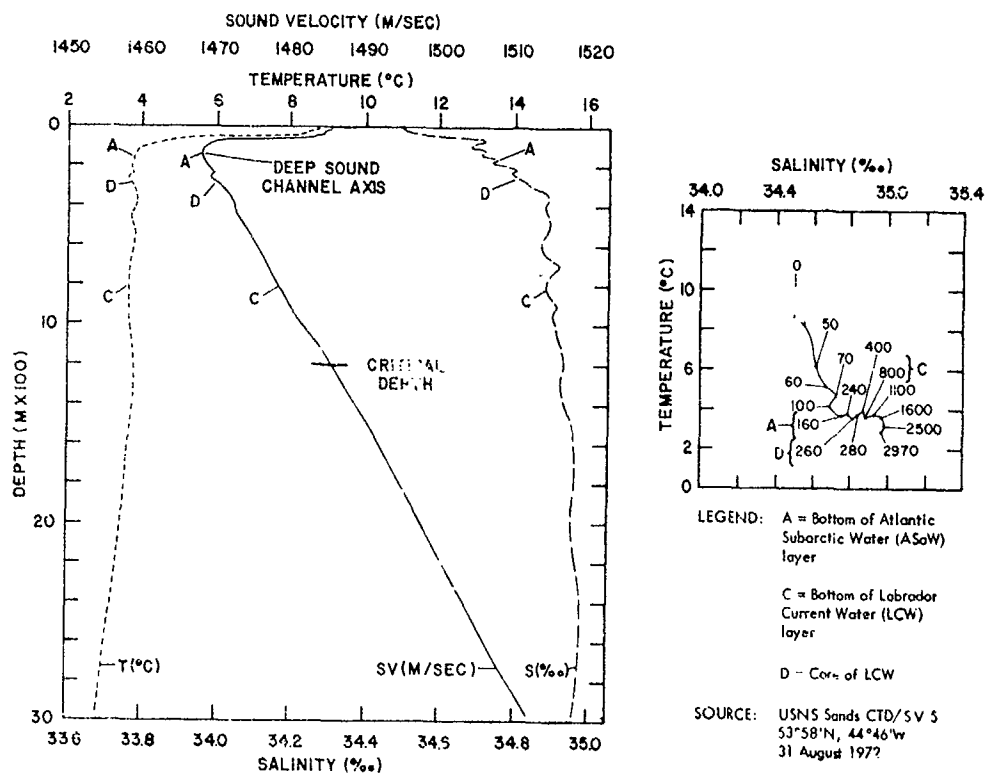
FIGURE 7. TEMPERATURE-SALINITY-SOUND VELOCITY
PROFILES AND T-S DIAGRAM AT STATION B
DURING PHASE III (U)

17

(U) In the North Atlantic Current gyre (figure 8), the upper 100 m of the water column is dominated by a low-salinity layer (less than 35°/oo) that most likely represents warmed LCW transported across the Subarctic Convergence. The salinity at 50 m shown in figure 8 corresponds well with the salinity at the depth of the LCW core shown in figure 9. Low-salinity surface water of apparent Labrador Current origin has been found during summer as far east as OWS CHARLIE by Husby (1968). However, this low-salinity lens has only minor effects on the sound velocity profile. Between 100 and 540 m, the sound velocity profile is extremely complex owing to mixing of ASaW and NACW. This mixing is a result of intrusion of NACW into a layer of ASaW that extends to 540 m. In this layer, repeated sound velocity maxima apparently correspond to intrusions of NACW, whereas sound velocity minima correspond approximately to cores of relatively unmixed ASaW. The DSC axis (350 m) corresponds to the ASaW cell with the lowest salinity, rather than to the bottom of the ASaW layer. The two separate AIW cores at 900 and 1300 m have only a slight effect on the positive sound velocity gradient below the DSC axis. Below about 2200 m, NSOW has a pronounced effect on the positive sound velocity gradient. At about 3000 m, the sound velocity is nearly 2.0 m/sec less than at station A (figure 6) and nearly 4.0 m/sec less than that at station B (figure 7).

(U) In the Labrador Current north of the Grand Banks (figure 9), LCW occupies the upper 1000 m of the water column. The DSC axis (50 m) coincides with the LCW core (temperature minimum in a layer of increasing salinity). The sound velocity gradient change at about 360 m depth is caused by a temperature maximum at the core of a NACW intrusion into the Labrador Current. At a depth of 1400 m, the sound velocity shown in figure 9 is about 2.0 m/sec less than that shown in figures 6, 7 and 8. This may be due to the preferential flow of NSOW under the Labrador Current shown by Worthington (1970).

(U) In summary, the overall sound velocity structure of the primary OPAREA is most complex in the North Atlantic Current gyre (figure 8), least complicated in the Labrador Current (figure 9), and of intermediate complexity at stations A and B (figures 6 and 7, respectively). In the upper 2000 m of the water column, the sound velocity at most depths is greatest in the North Atlantic Current gyre, least in the Labrador Current, and intermediate at stations A and B. Sound velocities during Phase III of NORLANT-72 are generally greater at station A than at station B, since station B lies on the cold side of the Subarctic Convergence rather than in the North Atlantic Current gyre. The effects of NSOW in decreasing near-bottom sound velocities are more pronounced in the North Atlantic Current gyre than at station B, indicating a possible NSOW flow under this gyre. The DSC axis has the greatest depth and sound velocity in the North Atlantic Current gyre, has the least depth and sound velocity in the Labrador Current, and is intermediate in terms of both depth and sound velocity at stations A and B. Generally speaking, sound velocity at
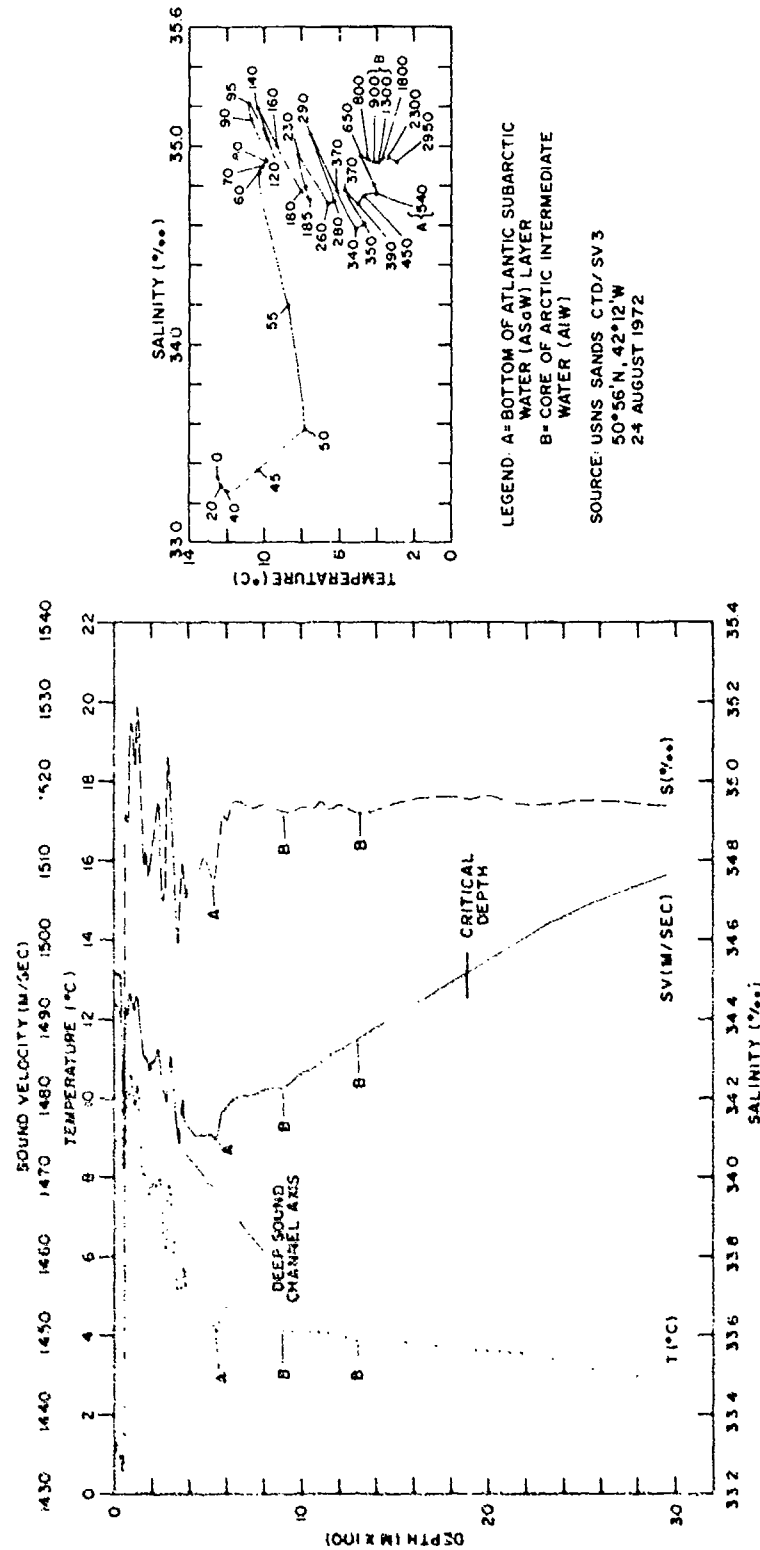
FIGURE 8. TEMPERATURE-SALINITY-SOUND VELOCITY PROFILES AND T-S DIAGRAM IN NORTH ATLANTIC CURRENT GYRE DURING PHASE III (U)

LEGEND: A = BOTTOM OF ATLANTIC SUBARCTIC WATER (ASoW) LAYER
B = CORE OF ARCTIC INTERMEDIATE WATER (AIW)

SOURCE: USNS SANDS CTD/ SV 3
50°56'N, 42°12'W
24 AUGUST 1972
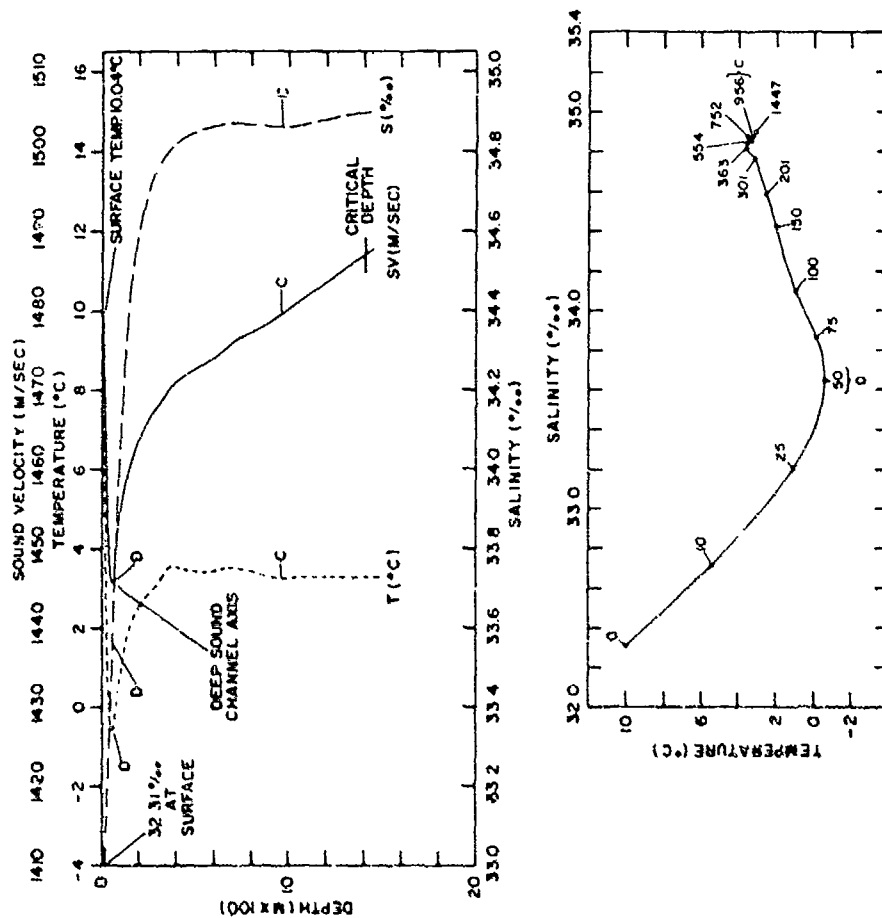
FIGURE 9. HISTORICAL SUMMER TEMPERATURE–SALINITY–SOUND VELOCITY PROFILES AND T-S DIAGRAM IN LABRADOR CURRENT NORTH OF GRAND BANKS (U)

CONFIDENTIAL

the DSC axis is greater than 1472 m/sec in the North Atlantic Current gyre, less than 1472 m/sec in the Labrador Sea gyre, and between 1440 and 1460 m/sec in the main flow of the Labrador Current.

B. Variability of Sound Velocity at Station A

(C) During Phases I and III of NORLANT-72, station A lay astride the Subarctic Convergence. During Phase II, this station lay in the North Atlantic Current gyre (see figure 5). Adequate data were available during Phase III to analyze the variability of sound velocity within a 15-nm radius of station A for a 10-hour period during 3-4 September. Figure 10 shows a time series plot and contoured presentation of sound velocity data at station A during Phase I for the upper 2000 m and 1000 m of the water column, respectively. The observations used in figure 10 are identified in table III. Their locations relative to the average Phase III position of the Subarctic Convergence are shown in an insert to figure 10. Profiles 1, 2, and 5 are in the colder Labrador Sea gyre; profiles 4 and 6 are in the warmer North Atlantic Current gyre; and profile 3 lies astride the Subarctic Convergence.

(C) The sound velocity variability shown in figure 10 is a result of temporal and spatial variability in the environment. The maximum depth of the DSC axis (340 m) occurred on profile 4 (warm side of front), while the maximum sound velocity at the axis (about 1475 m/sec) occurred on profile 3 (astride front). The minimum depth of the axis (150 m) also occurred on profile 3 (astride front), whereas the minimum sound velocity at the DSC axis (about 1470 m/sec) was on profile 5 (cold side of front). Over the 10-hour occupation, the depth of the DSC axis varied by 190 m, while the sound velocity at the axis varied by 4.3 m/sec. This is a rather substantial amount of variation, but is not unexpected in the vicinity of the Subarctic Convergence. The irregular shapes of the sound velocity isolines shown in figure 10 are the result of intrusions of various water masses through the Subarctic Convergence and local turbulence along this front. During this occupation of station A, the critical depth varied between 1600 and 1780 m due to changes in near-surface sound velocity. Since the corrected bottom depth at station A is approximately 4080 m, there was adequate depth excess during Phase III for convergence zone propagation from a near-surface source. The following table summarizes statistics on the maximum sound velocity in the mixed layer (MLV), depth of the DSC axis (DSCD), sound velocity at the DSC axis (DSCV), and critical depth (CD) for the Phase III occupation of station A:

21

FIGURE 10. VARIABILITY OF SOUND VELOCITY AT STATION A
DURING PHASE III (U)
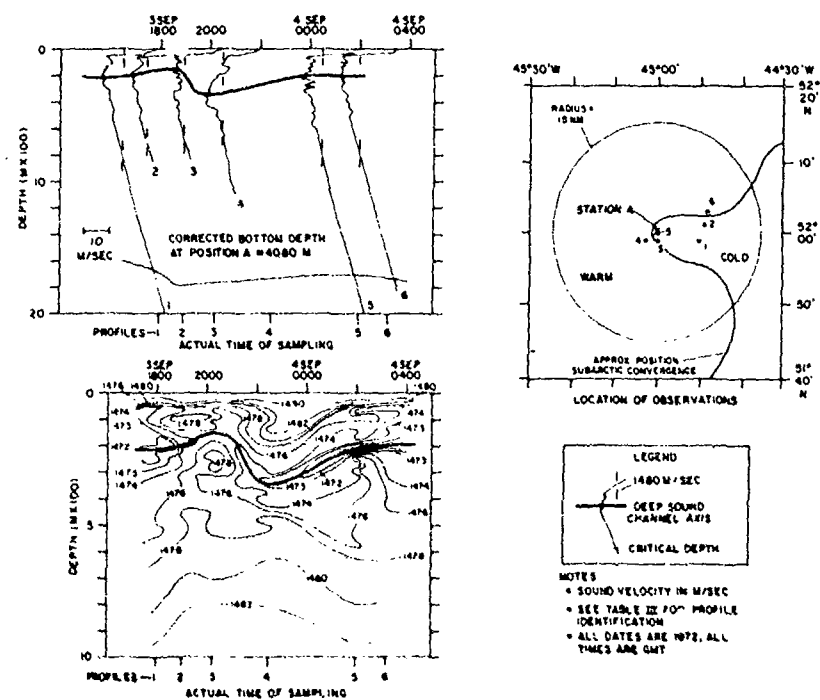
PROFILE	OBSERVATION	DATE (1972)	TIME (GMT)	LAT (°N)	LONG (°W)	RANGE FROM STATION A (nm)
1	SANDS CTD/SV 6 (D)	3 Sep	1800	51°59'	44°50'	6
2	SANDS XBT 127	3 Sep	1900	52°01'	44°49'	9
3	SANDS XBT 128	3 Sep	2015	51°59'	45°00'	1
4	SANDS XBT 129	3 Sep	2230	51°59'	45°03'	2
5	SANDS XBT 110	4 Sep	0200	52°00'	45°00'	0
6	SANDS XBT 130	4 Sep	0310	52°03'	44°48'	10

Notes: • Nominal position of station A is 52°00'N, 45°00'W
        • (D) indicates downcast

TABLE III. IDENTIFICATION OF OBSERVATIONS USED IN PHASE III
TIME SERIES STUDY AT STATION A (U)

	MINIMUM	MEAN	MAXIMUM	RANGE	NO. OF OBS.
MLV (m/sec)	1492.6	1493.7	1494.6	2.0	6
DSCD (m)	150	220	340	190	6
DSCV (m/sec)	1470.4	1472.4	1474.4	4.3	6
CD (m)	1660	1730	1780	120	6

(C) During Phase I of NORLANT-72, variation in sound velocity structure at station A should be quite similar to that shown in figure 10, since the Subarctic Convergence passed through station A during both Phases I and III. The depth and sound velocity of the DSC axis during Phase I should be similar to those found during Phase III. Critical depths during Phase I should be several hundred meters shallower than those for Phase III because of lower near-surface temperatures. During Phase II, the sound velocity structure at station A should be even more complex than that for Phase III, since the station lay well into the North Atlantic Current gyre. The depth and velocity of the DSC axis should be greater during Phase II than during Phase III due to higher temperatures expected in the North Atlantic Current gyre. Critical depths during Phase II should be a few hundred meters deeper than those shown in figure 10 owing to higher near-surface temperatures in the gyre. However, convergence zone propagation from a near-surface source is ensured during all three phases at station A.

C. Variability of Sound Velocity at Station B

(C) During Phase I of NORLANT-72, station B lay astride the Subarctic Convergence, while during Phases II and III this station lay just on the cold side of this front in the Labrador Sea gyre (figure 5). Data were adequate during Phase I to analyze the variability of sound velocity within a 15-nm radius of station B for a 64-hour period during 17-20 July. During Phase II, a similar analysis was made for a 60-hour period during 12-15 August. Figure 11 shows a time series plot and a contoured presentation of sound velocity data at station B for both Phases I and II. The time series plots are for the upper 2000 m of the water column and the contoured presentation for the upper 1000 m of the water column. The observations used in figure 11 are identified in table IV. The locations of these observations relative to the average Phase I and II positions of the Subarctic Convergence are shown in an insert to figure 11.
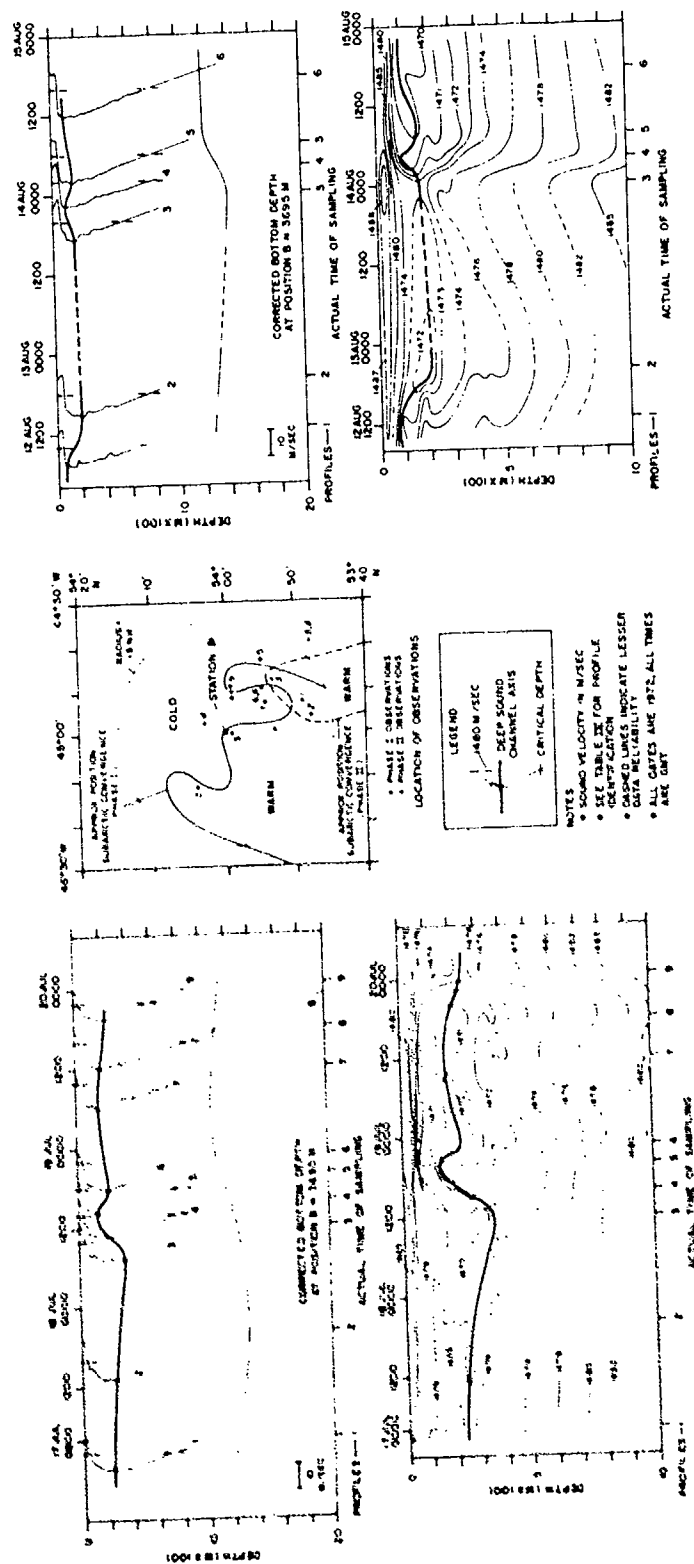
FIGURE 11. VARIABILITY OF SOUND VELOCITY AT STATION B
DURING PHASE I AND PHASE II (U)

25

PROFILE	OBSERVATION	DATE (1972)	TIME (GMT)	LAT (°N)	LONG (°W)	RANGE FROM STATION B (nm)
1	HAYES XBT 7	17 Jul	0800	53°53'	44°59'	7
2	HAYES XBT 8	17 Jul	2009	54°04'	45°12'	8
3	SANDS XBT 15	18 Jul	1200	53°59'	45°00'	1
4	SANDS XBT 16	18 Jul	1600	53°59'	44°50'	5
5	SANDS XBT 17	18 Jul	2000	53°55'	44°44'	11
6	SANDS CTD/SV 2 (D)	18 Jul	2255	53°55'	44°50'	8
7	SANDS XBT 18	19 Jul	1200	53°54'	44°53'	7
8	SANDS SVP 1 (U)	19 Jul	1800	53°55'	44°50'	8
9	SANDS XBT 20	20 Jul	0037	53°59'	44°49'	6

PHASE II

1	SANDS XBT 76	12 Aug	1230	53°49'	44°53'	12
2	SANDS XBT 78	12 Aug	2000	53°48'	44°56'	12
3	SANDS XBT 79	14 Aug	0000	53°53'	44°48'	10
4	SANDS XBT 80	14 Aug	0400	54°03'	44°58'	3
5	SANDS XBT 81	14 Aug	0715	53°48'	44°40'	17
6	SANDS XBT 82	14 Aug	1720	53°48'	44°40'	17

Notes: ● Nominal position of station B is 54°00'N, 45°00'W
● (U) indicates upcast, (D) indicates downcast

TABLE IV. IDENTIFICATION OF OBSERVATIONS USED IN PHASE I AND PHASE II TIME SERIES STUDIES AT STATION B (U)

(U) During Phase I, profiles 1, 2, 3, and 9 were in the warmer North Atlantic Current gyre; profiles 5, 6, 7, and 8 were in the colder Labrador Sea gyre; and profile 4 lay astride the Subarctic Convergence. Therefore, variation in sound velocity during Phase I at station B again is a result of temporal and spatial variability in the environment. The maximum depth of the DSC axis (360 m) occurred for profile 3 (warm side of front), while the maximum sound velocity at the axis (about 1474 m/sec) occurred for profile 1 (also on warm side of front). The minimum depth of the axis (150 m) was found on profile 5 and the minimum sound velocity at the axis (about 1469 m/sec) on profile 6. Profiles 5 and 6 were on the cold side of the Subarctic Convergence. Over the 64-hour occupation, the depth of the DSC axis varied by 210 meters and the sound velocity at the axis varied by 4.3 m/sec. Such a variation is expected along the Subarctic Convergence. The effect of the Subarctic Convergence on the sound velocity isolines below the axis can be seen between profiles 8 and 9 on the contoured section. Profile 8 lay on the cold side of the front, while profile 9 was on the warm side of the front. Therefore, the various isolines tend upwards as the distance between isolines is compressed. During the Phase I occupation of station B, critical depth varied between 1070 m (cold side of front) and 1340 m (warm side of front).

(U) During Phase II, profiles 1, 2, and 3 were in the warmer North Atlantic Current gyre while profiles 4, 5, and 6 were in the colder Labrador Sea gyre, thereby resulting in a mixture of temporal and spatial variability in sound velocity structures. The maximum depth of the DSC axis (200 m) occurred on profile 2, while the maximum sound velocity at the axis (about 1473 m/sec) occurred on profile 3. Both profiles were on the warm side of the Subarctic Convergence. The minimum depth of the axis (80 m) occurred for profile 1 (warm side of convergence), whereas the minimum sound velocity at the axis (about 1470 m/sec) was found on profile 6 (cold side of convergence). Over the 60-hour occupation, the depth of the DSC axis varied by only 120 m and the sound velocity at the axis varied by 3.5 m/sec. The effect of the Subarctic Convergence on the sound velocity isolines below the axis can be seen between profiles 3 and 4 on the contoured section. Since profile 3 was on the warm side of the front and profile 4 on the cold side, the sound velocity isolines tend downwards as the distance between the various isolines is compressed. During the Phase II occupation of station B, critical depth varied between 1210 m (cold side of front) and 1400 m (warm side of front).

(U) The following table summarizes sound velocity profile statistics for the Phase I and Phase II occupations of station B:

	MINIMUM	MEAN	MAXIMUM	RANGE	NO. OF OBS.
MLV (m/sec)					
I	1483.5	1485.1	1488.3	4.8	9
II	1486.4	1487.4	1489.4	3.0	6
DSCD (m)					
I	150	230	360	210	9
II	80	130	200	120	6
DSCV (m/sec)					
I	1469.3	1471.5	1473.6	4.3	9
II	1469.7	1471.3	1473.3	3.6	6
CD (m)					
I	1070	1180	1340	270	9
II	1210	1280	1400	190	6

Both the depth and sound velocity of the DSC axis had a greater variation during Phase I than during Phase II. This effect can be explained by the relative position of the Subarctic Convergence during the two phases. During Phase II, station B was more strongly influenced by the colder, more stable Labrador Sea gyre. During Phase I, station B was influenced more or less equally by the Labrador Sea gyre and the warmer, less stable North Atlantic Current gyre. The lesser mean depth and sound velocity of the DSC axis during Phase II are further indications that station B lay generally north of the Subarctic Convergence during this phase. The mean critical depth during Phase I was 100 m shoaler than during Phase II, despite the increased influence of the North Atlantic Current gyre. This is caused by less surface insolation during Phase I. The smaller variation in critical depth during Phase II indicates more uniform surface insolation later in the summer.

(C) During Phase III of NORLANT-72, the sound velocity structure at station B should be quite similar to that shown in figure 11 for Phase II. However, critical depths during Phase III should be a few hundred meters deeper than those found during Phase II because of increased surface insolation. During all three phases, there was adequate depth excess at station B to ensure convergence zone propagation from a near-surface source.

D. Variability of Sound Velocity at Station D

(C) During Phase I of NORLANT-72, station D lay astride the Subarctic Convergence (figure 5). During this phase, data were adequate to analyze the variability of sound velocity within a 15-nm radius of station D for a 142-hour period during 19-25 July. Figure 12 shows a time series plot and a contoured presentation of sound velocity data at station D during Phase I. The time series plot is for the upper 2000 m of the water column, the contoured presentation for the upper 1000 m of the water column. The observations used in figure 12 are identified in table V. The locations of these observations relative to the average Phase I position of the Subarctic Convergence are shown in an insert to figure 12.

(C) The majority of the profiles used in figure 12 were on the cold side of the Subarctic Convergence, the exceptions being profile 1 in the North Atlantic Current gyre and profile 2 astride the front. During the 142-hour occupation, 131 hours are represented by profiles located in the colder Labrador Sea gyre. Over the occupation as a whole, the maximum depth of the DSC axis (380 m) and the maximum sound velocity at the axis (1476.2 m/sec) occurred for profile 1. The minimum depth of the axis (100 m) occurred on profile 17, while the minimum sound velocity at the axis (1466.7 m/sec) was on profile 4. Both these profiles were on the cold side of the Subarctic Convergence. Over the occupation as a whole, the depth of the DSC axis varied by 280 m. Over a period of less than 48 hours, the sound velocity at the axis varied by 9.5 m/sec. This latter variation is larger than that encountered at station B during either Phase I or Phase II (figure 11) or that encountered at station A during Phase III (figure 10). The magnitude of this variation does not appear to be a function of the length of occupation or placement of stations relative to the Subarctic Convergence. Therefore this large variation must be caused by greater oceanographic variability at station D during Phase I of the exercise. This variability probably is related to the proximity of station D to the center of the North Atlantic Current gyre during Phase I (figure 5). During the total occupation, critical depth at station D varied between 1200 m (profile 2) and 1440 m (profile 22), a variation related to changes in near-surface sound velocity. Since the corrected bottom depth at station D is approximately 3880 m, there was adequate depth excess during Phase I to ensure convergence zone propagation from a near-surface source.

(U) During 131 hours of the occupation, all profiles lay within the colder Labrador Sea gyre and were not subject to spatial variations induced by the relative position of the Subarctic Convergence. Therefore, these profiles offer an opportunity to examine truly temporal variability in the primary OPAREA. During these 131 hours, the depth of the DSC axis varied from 100 to 220 m, while the sound velocity at the axis varied between 1466.7 and 1471.7 m/sec.
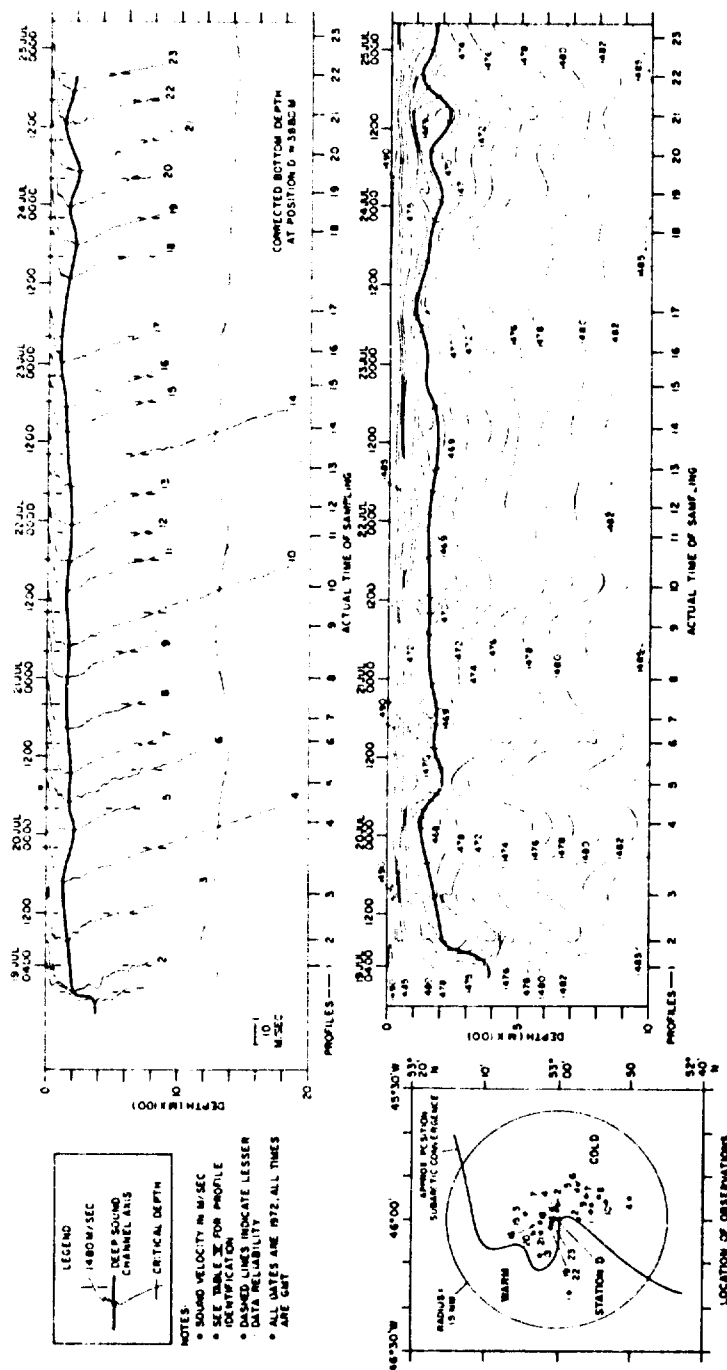
FIGURE 12. VARIABILITY OF SOUND VELOCITY AT STATION D DURING PHASE I (U)

PROFILE	OBSERVATION	DATE (1972)	TIME (GMT)	LAT (°N)	LONG (°W)	RANGE FROM STATION D (nm)
1	HAYES XBT 15	19 Jul	0400	52°58'	46°17'	10
2	HAYES XBT 16	19 Jul	0800	52°57'	46°00'	3
3	HAYES XBT 17	19 Jul	1500	53°04'	45°49'	4
4	HAYES XBT 18	20 Jul	0219	52°50'	45°55'	10
5	HAYES XBT 19	20 Jul	0800	52°57'	45°53'	5
6	HAYES XBT 19A	20 Jul	1430	52°57'	45°52'	6
7	HAYES XBT 20	20 Jul	1800	52°56'	45°55'	5
8	HAYES XBT 21	21 Jul	0000	52°54'	45°55'	6
9	HAYES XBT 22	21 Jul	0800	52°55'	45°57'	5
10	HAYES XBT 23	21 Jul	1400	52°53'	45°56'	7
11	HAYES XBT 24	21 Jul	2140	52°55'	45°58'	4
12	HAYES XBT 25	22 Jul	0200	53°00'	45°57'	2
13	HAYES XBT 26	22 Jul	0800	53°02'	46°09'	6
14	HAYES XBT 27	22 Jul	1410	53°00'	45°58'	1
15	HAYES XBT 28	22 Jul	2045	53°02'	46°01'	2
16	HAYES XBT 29	23 Jul	0200	53°03'	46°02'	3
17	HAYES XBT 30	23 Jul	0800	53°01'	45°58'	1
18	HAYES XBT 32	23 Jul	2000	53°01'	46°00'	1
19	HAYES XBT 33	24 Jul	0200	53°01'	46°02'	1
20	HAYES XBT 34	24 Jul	0800	53°03'	46°03'	4
21	HAYES XBT 35	24 Jul	1400	53°02'	46°03'	3
22	HAYES XBT 36	24 Jul	2000	53°01'	46°02'	1
23	HAYES XBT 37	25 Jul	0200	53°01'	46°01'	1

Note: Nominal position of station D is 53°00'N, 46°00'W

TABLE V.   IDENTIFICATION OF OBSERVATIONS USED IN PHASE II
TIME SERIES STUDY AT STATION D (U)

This variation appears to have a 10- to 12-hour periodicity that probably is due to internal waves generated along the horizontal front that marks the bottom of the ASaW layer. At station D, this front lay at the approximate depth of the DSC axis. Further evidence of internal motion is seen in the form of the 1472 through 1480 m/sec sound velocity isolines below the axis. According to LaFond (1962) internal waves commonly are observed along horizontal water mass boundaries. These internal waves frequently have a period approximating that of the tide. In the southern Labrador Sea, the tides generally are diurnal (NAVOCEANO, 1965a). Therefore, internal waves appear to be responsible for some part of the variability in sound velocity observed at station D during Phase I of NORLANT-72.

(U) The total variability in the depth of the DSC axis observed at station D during Phase I was 280 m. This variability is a result of temporal and spatial changes in sound velocity structure. During the 131-hour period when all observations lay in the Labrador Sea gyre, the depth of the DSC axis varied by only 120 m. The total variability in sound velocity at the axis observed during Phase I at station D was 9.5 m/sec. During the 131-hour period when all observations lay on the cold side of the Subarctic Convergence, the sound velocity at the axis varied by 5.0 m/sec. Therefore, about 45% of the total variation in DSC structure can be attributed to temporal variability (internal waves). The remaining variation (55%) probably is due to changes in the position of the Subarctic Convergence. Internal waves probably are responsible for about half of the variability observed at other reference stations in the primary OPAREA, particularly if these stations either lay astride or near the Subarctic Convergence.

E. Sound Velocity Structure from Station B to Station A to Grand Banks

(C) During all three phases of NORLANT-72, data were adequate to construct sound velocity cross sections from station B to station A (due south) and then southwest towards Grand Banks. During Phase I (figure 2) both stations A and B lay astride the Subarctic Convergence, and the Labrador Sea gyre intruded between these stations. The front between the North Atlantic Current gyre and the Labrador Current was about 95 nm southwest of station A. During Phase II (figure 3), station B lay just north of the Subarctic Convergence and station A lay in the North Atlantic Current gyre. However, the first 30 nm of the cross section south of station B overlay this front. During Phase II the front between the North Atlantic Current gyre and the Labrador Current occurred about 45 nm southwest of station A. During Phase III (figure 4A), station B again lay just north of the Subarctic Convergence and station A lay astride this front on the other side of the North Atlantic Current gyre. The front between this gyre and the Labrador Current occurred about 75 nm southwest of station A during Phase III. Therefore, in respect to the station B to station A to Grand Banks track, the North Atlantic Current gyre was best developed during Phase III and least developed during Phase I.

CONFIDENTIAL

(U) Figure 13 shows a series of 15 sound velocity profiles plotted at their position of observation normal to the station B to station A to Grand Banks track during Phase I and a contoured cross section of these same data. The plot of sound velocity profiles versus distance extends to 2000 m depth, the contoured cross section to a depth of 1000 m. The observations used in figure 13 are identified in table VI. The bathymetric profile shown on figure 13 is from NAVOCEANO North Atlantic Regional (NAR) chart 4.

(C) During Phase I, surface sound velocities along the station B to station A to Grand Banks track varied from less than 1472 to greater than 1490 m/sec. A mixed layer was found on most profiles at a depth of 10 to 30 m. The depth of the DSC axis varied from 50 m in the Labrador Current (profile 14) to 350 m in the North Atlantic Current gyre (profile 7). The sound velocity at the axis varied from about 1455 to about 1475 m/sec between these same two profiles. Critical depth increased from 900 m at station B to 1200 m at a range of about 140 nm from station B (in the North Atlantic Current gyre) and then decreased to 120 m in the Labrador Current at a range of about 325 m. The critical depth then increased to 630 m at the end of the track due to increased surface insolation over the edge of Grand Banks. Depth excess along the entire section was adequate to ensure convergence zone propagation from a near-surface source. However, convergence zone propagation was impeded farther to the southwest by the shallower bathymetry of the Grand Banks continental slope.

(U) Sound velocity structure along the entire Phase I track was very complex and variable because of intrusions of water masses through the meandering Subarctic Convergence. The cells with sound velocities less than 1472 m/sec at about 30 nm from station B and at station A were caused by intrusions of ASaW and/or LCW into the North Atlantic Current gyre. The influence of this gyre to the north and southwest of station A is seen in the domed structure of the sound velocity isolines below the DSC axis. The strong temperature minimum in the LCW core off Grand Banks caused a tongue with sound velocities less than 1460 m/sec at ranges greater than 240 nm from station B. The two cells with sound velocities greater than 1478 m/sec (described by profiles 11 and 14) were caused by intrusions of NACW into the Labrador Current. These NACW intrusions led to perturbations in the positive sound velocity gradient below the DSC axis.

(C) Figure 14 shows a series of 14 sound velocity profiles plotted at their position of observation normal to the station B to station A to Grand Banks track during Phase II and a contoured cross section of these same data. The observations used in figure 14 are identified in table VII. Surface sound velocities along the Phase II

CONFIDENTIAL

FIGURE 13. SOUND VELOCITY STRUCTURE FROM STATION B TO STATION A TO GRAND BANKS DURING PHASE I (U)

34

PROFILE	OBSERVATION	DATE (1972)	TIME (GMT)	LAT (°N)	LONG (°W)
1	SANDS XBT 20	20 Jul	0037	33°59'	44°49'
2	SANDS XBT 14	18 Jul	0800	52°23'	45°02'
3	HAYES XBT 6	17 Jul	0400	53°13'	45°04'
4	SANDS XBT 13	18 Jul	0400	52°40'	44°55'
5	HAYES XBT 5	17 Jul	0000	52°28'	45°04'
6	SANDS CTD/SV 1 (D)	17 Jul	1530	52°00'	44°44'
7	HAYES XBT 3	16 Jul	0803	51°32'	45°54'
8	HAYES XBT 2	16 Jul	0400	51°06'	46°25'
9	HAYES XBT 1A	16 Jul	0003	50°53'	47°01'
10	SANDS XBT 4	17 Jul	0040	50°44'	47°17'
11	SANDS XBT 3	16 Jul	2230	50°29'	47°22'
12	HAYES XBT 1	15 Jul	2000	50°13'	47°50'
13	SANDS XBT 45	29 Jul	2045	50°20'	49°05'
14	SANDS XBT 1	16 Jul	1430	49°22'	48°33'
15	VP-24 AXBT 9	21 Jul	0106	48°45'	49°36'

Note: (D) indicates downcast

TABLE VI.   IDENTIFICATION OF OBSERVATIONS USED IN STATION B TO
STATION A TO GRAND BANKS CROSS SECTION (PHASE I) (U)
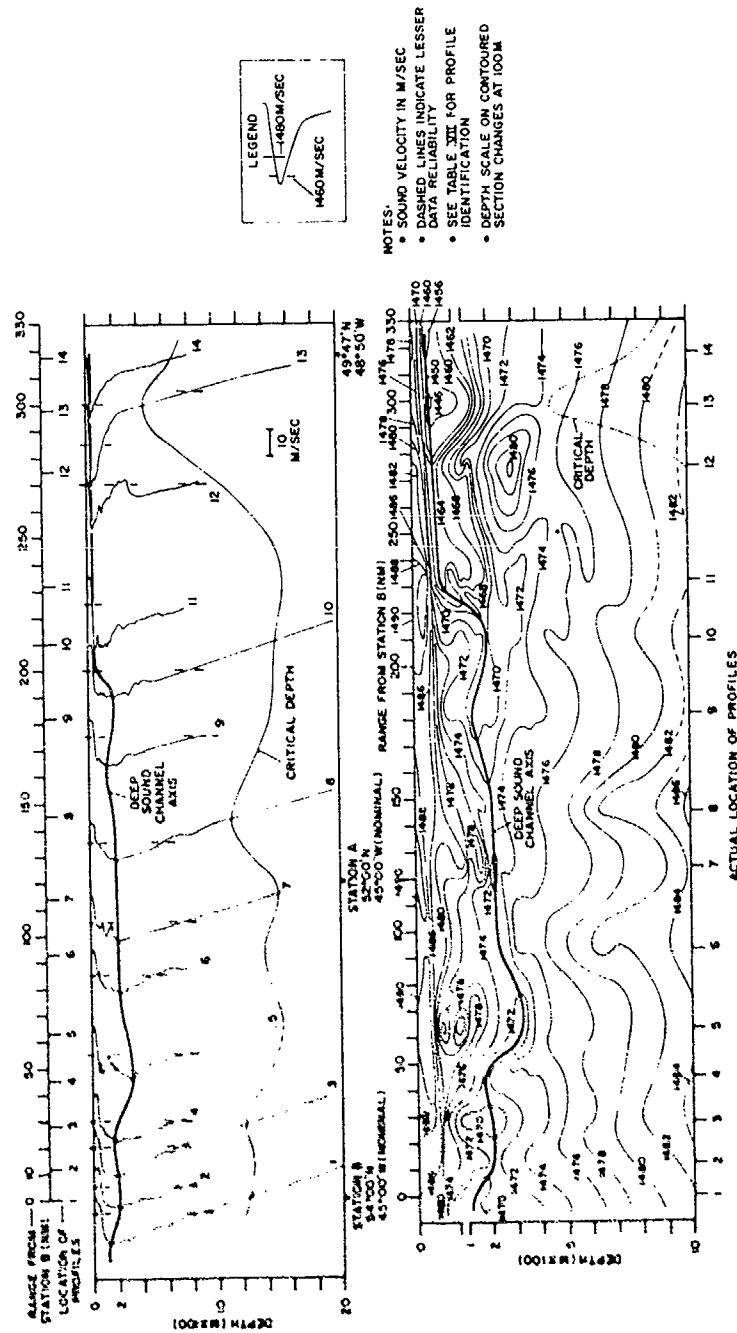
FIGURE 14. SOUND VELOCITY STRUCTURE FROM STATION B TO STATION A TO GRAND BANKS DURING PHASE II (U)

PROFILE	SANDS OBSERVATION	DATE (1972)	TIME (GMT)	LAT (°N)	LONG (°W)
1	SVP 5 (U)	31 Jul	0420	53°59'	44°51'
2	XBT 78	12 Aug	2000	53°48'	44°56'
3	XBT 55	31 Jul	2040	53°32'	45°02'
4	XBT 85	15 Aug	1605	53°21'	44°54'
5	STD 3 (D)	3 Aug	0025	52°57'	44°51'
6	XBT 87	16 Aug	0415	52°27'	45°17'
7	STD 2 (D)	1 Aug	2100	51°56'	45°10'
8	XBT 49	30 Jul	1200	52°33'	46°37'
9	XBT 67	6 Aug	2256	51°18'	46°18'
10	XBT 73	11 Aug	0800	51°39'	47°42'
11	XBT 68	7 Aug	0400	50°45'	47°14'
12	XBT 68A	7 Aug	0800	50°19'	48°02'
13	XBT 71	10 Aug	2216	50°31'	49°15'
14	XBT 70	7 Aug	1600	49°47'	48°50'

Note: (U) indicates upcast, (D) indicates downcast

TABLE VII.   IDENTIFICATION OF OBSERVATIONS USED IN STATION B TO
STATION A TO GRAND BANKS CROSS SECTION (PHASE II) (U)

track varied from about 1475 to greater than 1490 m/sec. A mixed layer at depths of 20 to 50 m was found on most profiles. The depth of the DSC axis varied between 40 m in the Labrador Current (profile 14) and 320 m in the North Atlantic Current gyre (profile 5). The sound velocity at the axis varied from less than 1445 m/sec for profile 13 about 1473 m/sec for profiles 6 and 8. Critical depth varied between 1140 and 1550 m along the first 240 nm of the track and then rapidly decreased to 450 m in the Labrador Current at a range of about 300 nm from station B. Critical depth then increased to the southwest as a result of increased surface insolation over the edge of Grand Banks. Depth excess along the entire Phase II track was adequate to ensure convergence zone propagation from a near-surface source.

(U) Sound velocity structure along the Phase II track was even more complex and variable than that found during Phase I (figure 13). This is due to the greater development of the unstable North Atlantic Current gyre during Phase II. A cell with sound velocities less than 1472 m/sec occurred at station A despite the fact that this station lay well into the gyre. This is clear evidence of an ASaW and/or LCW intrusion under the Subarctic Convergence. In addition, two tongues with sound velocities less than 1472 m/sec intruded under the Subarctic Convergence, one from the north and one from the southwest of station A. This second tongue was associated with the Labrador Current. The Labrador Current itself apparently did not extend as far northeast of Grand Banks during Phase II as during Phase I, since sound velocities less than 1460 m/sec were not found at ranges less than about 290 nm from station B during Phase II. However, the core of the Labrador Current apparently was colder during Phase II than during Phase I. The influence of the North Atlantic Current gyre is apparent in the vicinity of station A in the domed structure of the 1476 through 1484 m/sec sound velocity isolines. A NACW intrusion into the Labrador Current resulted in a cell with sound velocities greater than 1480 m/sec at about 270 nm from station B (profile 12). This intrusion was more pronounced during Phase II than the intrusion found during Phase I at approximately the same location.

(C) Figure 15 shows a series of 12 sound velocity profiles plotted at their position of observation normal to the station B to station A to Grand Banks track during Phase III and a contoured cross section of these same data. The observations used in figure 15 are identified in table VIII. The bathymetric profile shown on the extreme right-hand side of figure 15 is identical to that of figure 13. Surface sound velocities along the Phase III track varied from about 1486 to about 1496 m/sec. A mixed layer at depths between 20 and 70 m was found on all profiles except profile 12. Surface sound velocities during Phase III were greater than those during either Phase I or Phase II, indicating increased effects of surface insolation during
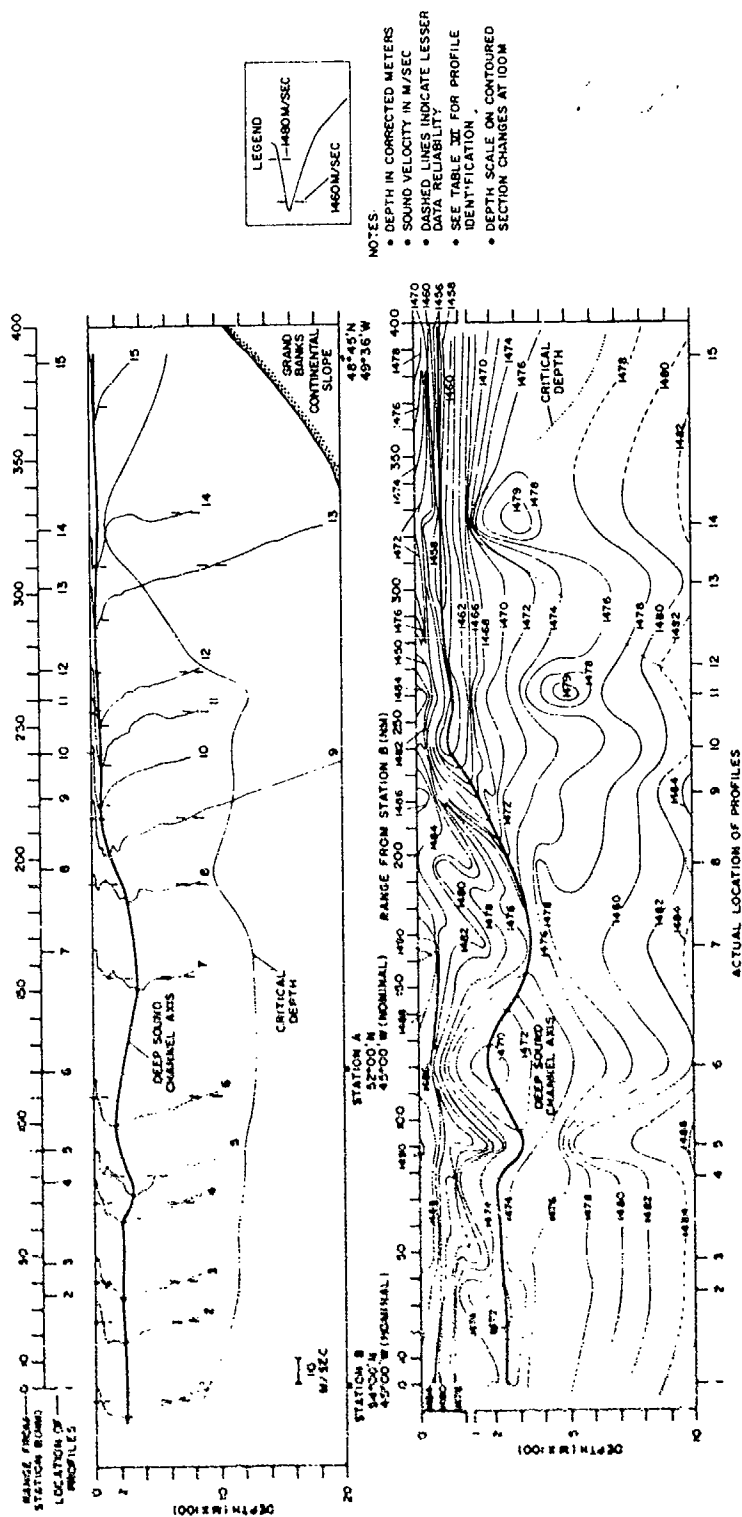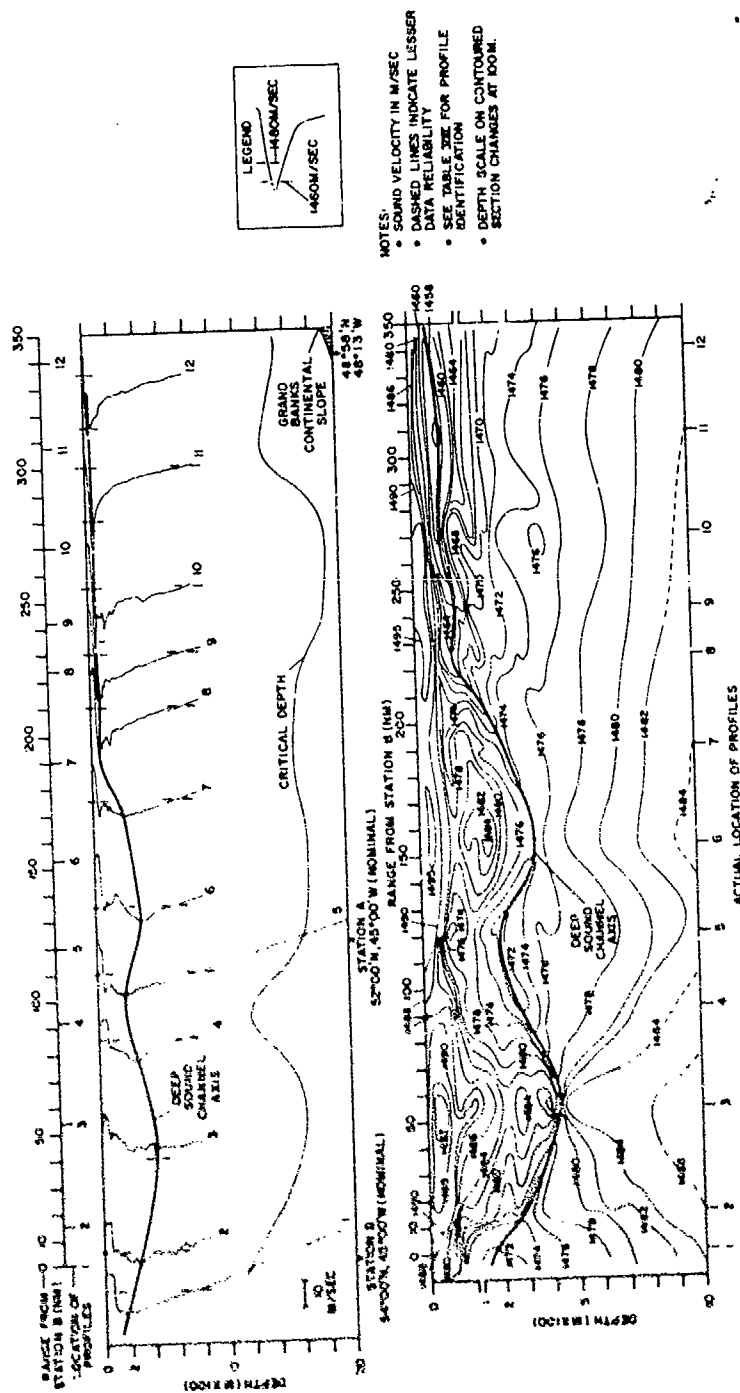
FIGURE 15. SOUND VELOCITY STRUCTURE FROM STATION B TO
STATION A TO GRAND BANKS DURING PHASE III (U)

PROFILE	SANDS OBSERVATION	DATE (1972)	TIME (GMT)	LAT (°N)	LONG (°W)
1	XBT 122	1 Sep	0010	53°58'	44°46'
2	XBT 123	1 Sep	0400	53°47'	44°41'
3	XBT 125	1 Sep	0805	53°03'	44°44'
4	XBT 126	1 Sep	1200	52°23'	44°40'
5	CTD/SV 6 (D)	3 Sep	1800	51°59'	44°50'
6	XBT 132	9 Sep	0400	51°59'	46°02'
7	XBT 133	9 Sep	0800	51°31'	46°42'
8	XBT 134	9 Sep	1200	51°10'	47°23'
9	XBT 95	24 Aug	0420	49°55'	45°54'
10	XBT 93	24 Aug	0000	49°37'	46°40'
11	XBT 136	9 Sep	2000	50°06'	48°54'
12	XBT 91	23 Aug	1600	48°58'	48°13'

Note: (D) indicates downcast

TABLE VIII. IDENTIFICATION OF OBSERVATIONS USED IN STATION B TO
STATION A TO GRAND BANKS CROSS SECTION (PHASE III) (U)

September. The depth of DSC axis varied between 30 m on profile 12 (Labrador Current) and 420 m on profile 3 (center of well-developed North Atlantic Current gyre). The sound velocity at the axis varied between about 1449 m/sec on profile 11 and about 1480 m/sec on profile 3. A minimum critical depth of 1160 m was found at station B and a maximum critical depth of 1900 m was found at a range of about 270 nm from station B in the region dominated by the Labrador Current. Critical depths were greater during Phase III than during the other two phases, again indicating the strong and continued effects of surface insolation during September. During Phase III, depth excess was adequate for convergence zone propagation from a near-surface source over most of the track. However, convergence zone formation was impeded by the shallower bathymetry of the Grand Banks continental slope at the southwest end of the track.

(U) Sound velocity structure along the Phase III track was even more complicated and variable than that during Phase II (figure 14), owing to maximum development of the unstable North Atlantic Current gyre that dominated the first 195 nm of the track. Cells with sound velocities less than 1472 m/sec were found at station B and at ranges greater than 195 nm from station B. Sound velocities less than 1460 m/sec occurred at ranges greater than about 250 nm from station B (similar to situation for Phase I, figure 13). However, the North Atlantic Current gyre was the primary oceanographic influence along the station B to station A to Grand Banks track during Phase III. This gyre caused the closure of the 1480 m/sec sound velocity isolines on either side of profile 3 (midway between stations A and B) and resulted in a cell with sound velocities greater than 1480 m/sec above the DSC axis to the southwest of station A. The unstable nature of the North Atlantic Current gyre is evident in the convoluted form of the greater than 1480 m/sec sound velocity isolines north of station A. The NACW intrusion into the Labrador Current during Phases I and II at a range of about 270 nm also occurred during Phase III (lens with sound velocities greater than 1476 m/sec), but in a much diminished form.

(U) As previously mentioned, the overall sound velocity structure along the station B to station A to Grand Banks track was most complicated and variable during Phase III, least complicated and variable during Phase I, and of intermediate complexity and variability during Phase II. This is directly related to the North Atlantic Current gyre that was best developed during Phase III and least developed during Phase I. The following table summarizes sound velocity profile statistics over the track as a whole during the three phases of NORLANT-72:

	MINIMUM	MEAN	MAXIMUM	RANGE	NO. OF OBS.
MLV (m/sec)					
I	1471.7	1484.3	1490.8	19.1	15
II	1474.7	1485.4	1490.6	15.9	14
III	1486.7	1492.6	1498.0	11.3	12.
DSCD (m)					
I	50	170	350	300	15
II	40	150	320	280	14
III	30	190	420	390	12
DSCV (m/sec)					
I	1455.4	1466.1	1475.4	20.0	15
II	1444.6	1456.7	1473.3	28.7	14
III	1449.3	1467.3	1480.2	30.9	12
CD (m)					
I	120	980	1280	1160	15
II	450	1240	1550	1100	14
III	1160	1340	1900	740	12

Both the mean depth and sound velocity of the DSC axis were greatest and most variable during Phase III, in keeping with the maximum development of the North Atlantic Current gyre. The relatively similar mean sound velocity at the DSC axis during all three phases indicates a similarity in water mass types over the track as a whole. Mean critical depth was greatest during Phase III and least during Phase I, as expected, because of increasing surface insolation over the course of the exercise. However, critical depth was least variable during Phase III and most variable during Phase I, indicating that surface insolation was most uniform over the track during Phase III and least uniform during Phase I. The statistics on the maximum sound velocity in the mixed layer show this same trend.

F. Summary of Sound Velocity Structure Near Stations A and B

(C) Station A was occupied during Phase III of the exercise (figure 10) and station B was occupied during Phases I and II (figure 11). In addition, a line of data from station B south to station A has been analyzed during all three phases of NORLANT-72 (figures 13, 14 and 15). Because of the various acoustic exercises carried out in the vicinity of these two stations throughout the exercise, the overall sound velocity structure near these two stations is briefly summarized in the following section.

(U) Sound velocity profile statistics over the station B to station A track for Phases I, II, and III of the exercise are as follows:

	MINIMUM	MEAN	MAXIMUM	RANGE	NO. OF OBS.
MLV (m/sec)					
I	1484.7	1488.0	1490.2	5.5	6
II	1485.9	1488.9	1490.6	4.7	7
III	1487.7	1492.1	1498.0	10.3	5
DSCD (m)					
I	180	230	310	130	6
II	120	200	320	200	7
III	160	260	420	260	5
DSCV (m/sec)					
I	1469.0	1472.0	1473.2	4.2	6
II	1468.2	1470.9	1473.1	4.9	7
III	1471.3	1473.9	1480.2	8.9	5
CD (m)					
I	900	1140	1280	380	6
II	1220	1370	1530	310	7
III	1160	1400	1660	500	5

Minimum values of these four parameters generally occurred at station B (northern end of track), while maximum values were found at the center of the variable North Atlantic Current gyre. All four parameters had greatest mean values and largest variations during Phase III, coincident with the greatest development of this gyre. During Phase II, the mean values of depth and sound velocity of the DSC axis were less than those during either Phase I or Phase III, indicating a greater influence of the colder Labrador Sea gyre on that portion of the primary OPAREA near stations A and B. This was caused by a tongue of the Labrador Sea gyre that extended well into the North Atlantic Current gyre parallel to the track during Phase Ii (figure 3). In most cases, variability of all four parameters along the track during Phases I and II was greater than the variability at station B during the two phases. Similarly, the variability along the track during Phase III was greater than that at station A during this phase. This indicates that the greatest overall variability in sound velocity structure occurred between stations A and B during all three phases of the exercise. This variability was caused by the unstable North Atlantic Current gyre.

(U) Maximum variability in sound velocity at the DSC axis over the station B to station A track (8.9 m/sec during Phase III) is of the same magnitude as the temporal and spatial variability of this parameter at station D during Phase I (9.5 m/sec). Station D was located in close proximity to the center of the North Atlantic Current gyre during Phase I (figure 2). During Phase III, this gyre was found along most of the station B to station A track (figure 4A). About half the total variability in DSC structure at station D during Phase I is attributable to temporal variations induced by internal waves, the other half to changes in the position of the Subarctic Convergence. This same situation also applies along the station B to station A track during Phase III. It is likely that about half the variability in DSC structure in the vicinity of stations A and B over the course of NORLANT-72 was temporal in nature. The other half probably was caused by meandering of the Subarctic Convergence. In addition, variability in DSC structure in the vicinity of stations A and B over the course of the exercise probably was most extreme in regions close to the center of the relatively unstable North Atlantic Current gyre.

SOUND VELOCITY STRUCTURE NORTHEAST OF PRIMARY OPAREA

A. General Oceanography

(C) During Phase I of the NORLANT-72 Exercise, SANDS and various aircraft took a line of XBTs and AXBTs to the northeast between station B and Denmark Strait. This track crossed the Subarctic Convergence at ranges of about 10, 330, 470, and 535 nm from station B (figure 2). Between ranges of 10 and 330 nm, the track lay within the relatively cold, dilute Labrador Sea gyre. North of 535 nm, the track lay in the warmer, more saline Irminger Current. Between 330 and 535 nm, the track paralleled the Subarctic Convergence in a transitional region between the Labrador Sea gyre and the Irminger Current. Two T-S/sound velocity comparisons illustrate the dissimilar oceanographic conditions at opposite ends of the track (figure 7 at station B and figure 16 in the Irminger Sea). The data shown in figure 7 were collected during Phase III of the exercise, and represent conditions in the Labrador Sea gyre (cold side of Subarctic Convergence). The data shown in figure 16 represent historical conditions in the Irminger Current at approximately that point where it breaches the Subarctic Convergence and turns to the south.

(U) At station B (figure 7), ASaW overlies a layer of LCW between 160 and 800 m that in turn overlies a layer of NACW. The depth of the DSC axis (160 m) coincides with the bottom of the ASaW layer. No AIW cores are observable in the NACW layer, and there is no noticeable change in the deep positive sound velocity gradient attributable to NSOW. In the Irminger Sea (figure 16), warm, saline Irminger Current Water (a derivant of NACW) does not have nearly as marked a thermocline or halocline as observed at station B, resulting in a nearly isovelocity layer between depths of 100 and 600 m. The
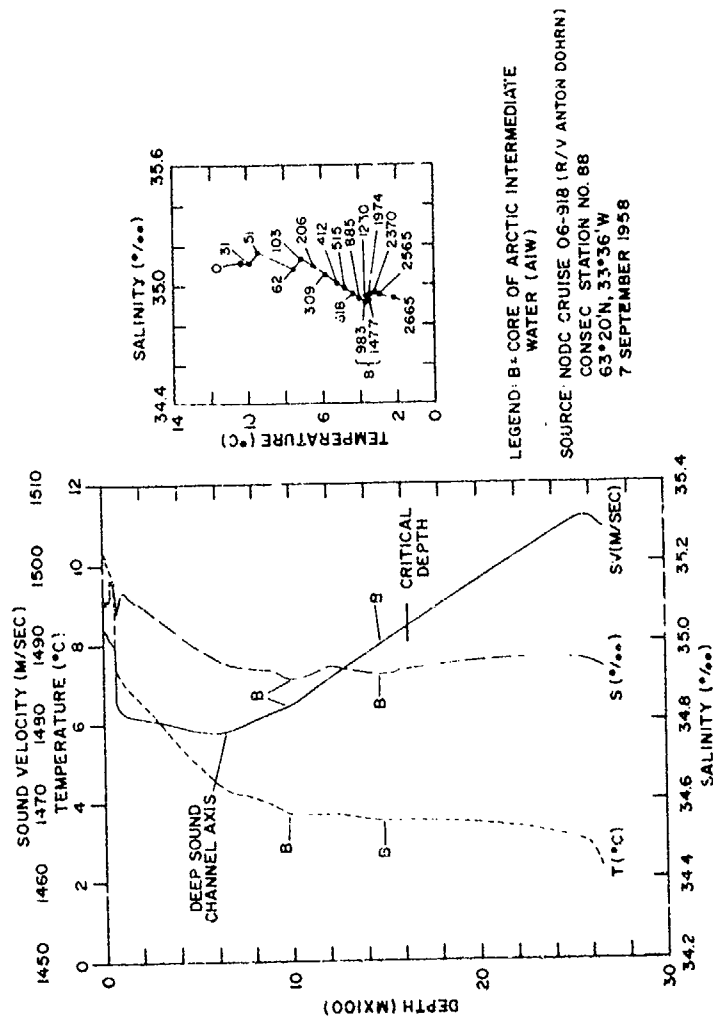
FIGURE 16. HISTORICAL SUMMER TEMPERATURE-SALINITY-SOUND VELOCITY PROFILES AND T-S DIAGRAM IN IRMINGER SEA (U)

depth of DSC axis (620 m) coincides with the bottom of the Irminger
Current Water layer. Below the axis, two cores of AIW are found at
980 m and 1480 m. These cores are separated by a salinity maximum
that probably corresponds to the core of well-mixed Mediterranean
Intermediate Water (MIW). A core of well-mixed MIW has been shown
under the Irminger Current as oxygen minimum by Worthington and
Wright (1970). However, neither the AIW core nor the suspected MIW
core cause an appreciable change in the positive sound velocity gradient
below the DSC axis. Below about 2200 m, NSOW causes a reversal in the
near-bottom positive sound velocity gradient. The effects of NSOW are
particularly evident in the Irminger Sea since this region lies just
south of Denmark Strait, through which NSOW enters the North Atlantic
Ocean. During summer, near-surface sound velocities in the Irminger
Sea can be up to 10 m/sec higher than those in the Labrador Sea gyre
because of warmer sea surface temperatures. Greater near-surface
sound velocities and the near-bottom effects of NSOW combine to in-
crease critical depth at the northern end of the station B to Denmark
Strait track.

B. Sound Velocity Structure Between Station B and Denmark Strait

(U) Figure 17 shows a series of 15 sound velocity profiles
plotted at their position of observation normal to the station B to
Denmark Strait track during Phase I of NORLANT-72 and a contoured
cross section of these same data. The sound velocity profiles ex-
tend to greater than 3000 m depth, and the contoured cross section to
1000 m depth. The observations used in figure 17 are identified in
table IX. The bathymetric profile shown in this figure between 0 and
330 nm was taken by SANDS during the exercise. The remainder of the
bathymetric profile is from NAVOCEANO NAR chart 4.

(C) Surface sound velocities varied from about 1473 m/sec in
the center of the Labrador Sea gyre to more than 1490 m/sec at the
northern end of the track. A variable mixed layer was found at ranges
less than about 350 nm from station B, but generally was absent further
to the north. The depth of the DSC axis varied from 70 m in the
Labrador Sea gyre (profile 4) to about 600 m in the Irminger Current
(profile 14). Sound velocity at the axis varied from less than 1465
to more than 1480 m/sec between these same two profiles. The DSC
structures shown for profiles 13, 14, and 15 are speculative since
these profiles are based on shallow AXBT data. Critical depth de-
creased from 1150 m at station B (in North Atlantic Current gyre) to
520 m at a range of about 310 nm from station B, and then increased
to about 1640 m at the northern end of the track. Depth excess along
the entire track was adequate for convergence zone propagation from a
near-surface source. However, further north, the shallower bathymetry
of the Denmark Strait sill should impede convergence zone propagation.
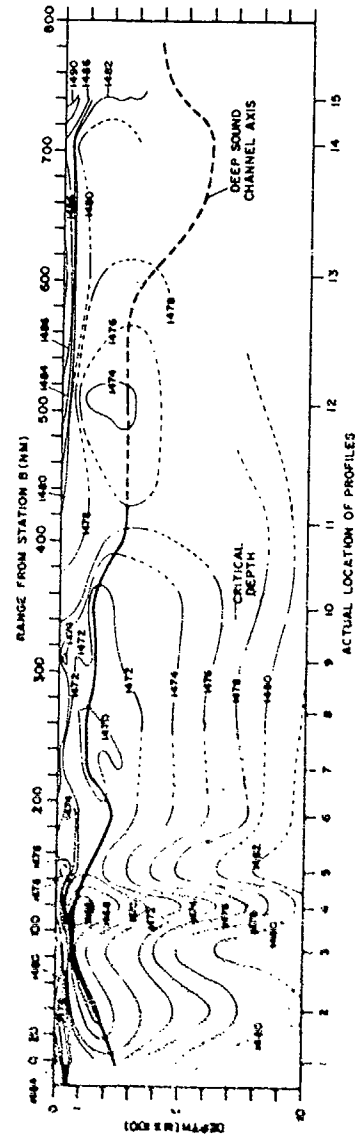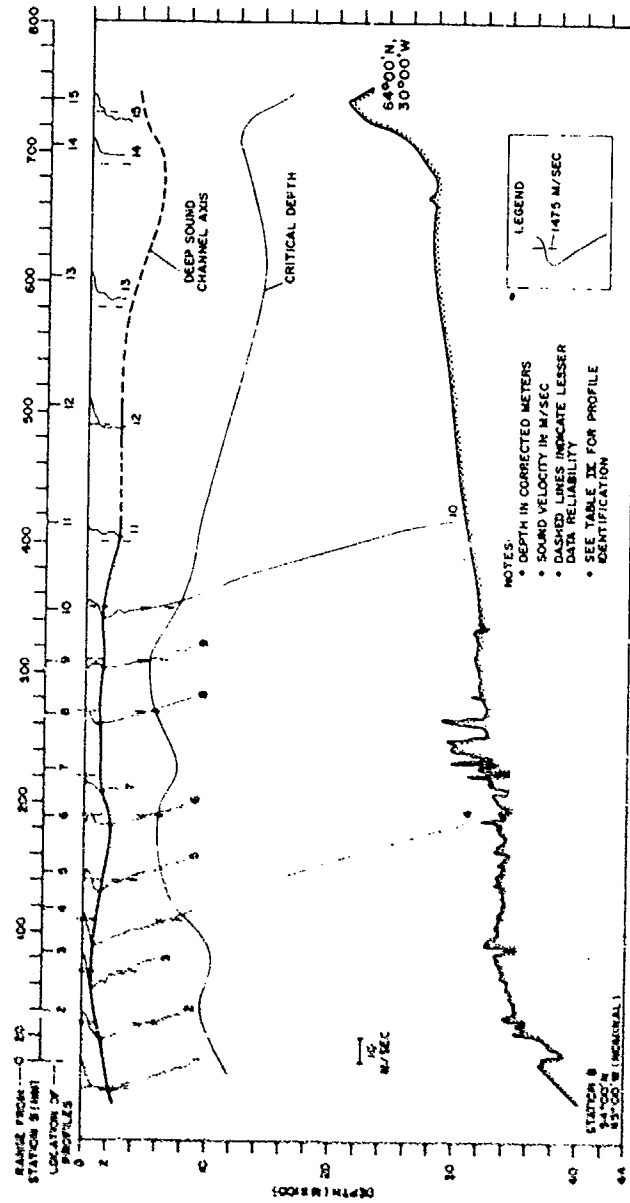
FIGURE 17. SOUND VELOCITY STRUCTURE BETWEEN STATION B AND DENMARK STRAIT DURING PHASE I (U)

47

PROFILE	OBSERVATION	DATE (1972)	TIME (GMT)	LAT (°N)	LONG (°W)
1	SANDS XBT 20	20 Jul	0037	53°59'	44°49'
2	SANDS XBT 21	20 Jul	0400	54°31'	44°24'
3	SANDS XBT 22	20 Jul	0800	55°11'	43°58'
4	SANDS SVP 2 (U)	20 Jul	2200	55°48'	43°23'
5	SANDS XBT 25	21 Jul	0400	56°08'	42°53'
6	SANDS XBT 26	21 Jul	0806	56°38'	42°02'
7	VXN 8 AXBT 22	21 Jul	1701	56°56'	40°47'
8	SANDS XBT 27	21 Jul	1600	57°44'	40°21'
9	SANDS XBT 28	21 Jul	2000	58°16'	39°25'
10	SANDS SVP 3 (U)	22 Jul	0430	58°42'	38°25'
11	VXN-8 AXBT 24	21 Jul	1820	59°41'	37°10'
12	VXN-8 AXBT 30	24 Jul	1147	60°59'	35°07'
13	VXN-8 AXBT 26	21 Jul	1946	62°19'	32°55'
14	VXN-8 AXBT 27	21 Jul	2029	63°42'	30°51'
15	VP-24 AXBT 66	28 Jul	1742	63°42'	28°19'

Note: (U) indicates upcast

TABLE IX.   IDENTIFICATION OF OBSERVATIONS USED IN STATION B TO
DENMARK STRAIT CROSS SECTION (PHASE I) (U)

(U) The overall sound velocity structure along the first half of station B to Denmark Strait track was not nearly as complex as that found in the primary OPAREA. A cell with sound velocities less than 1472 m/sec dominated the southern half of the track, and corresponded to the relatively stable Labrador Sea gyre. This cell was centered at a range of about 120 nm (profile 4). The large variations in sound velocity structure below the DSC axis in the contoured cross section surrounding profile 4 may be a result of data type (i.e., a SVP bracketed by two XBTs). The effects of the Subarctic Convergence can be seen in the upward tendency and closure of various isolines at ranges of about 400 nm from station B. At greater ranges, the overall sound velocity of the water column increased to the northeast. However, exact details of sound velocity structure at depths greater than 300 m are not available owing to the shallow depth of the AXBT data. NSOW effects expected at ranges greater than about 400 nm, should cause anomalous sound velocity structures at depths near or below 2200 m. Guthrie (1964) shows near-bottom sound velocity reversals in the Irminger Sea as far south as about 60°N (range of about 430 nm from station B). Along the northeastern half of the track, a complex sound velocity structure also would be expected near the depth of the DSC axis due to mixing along the lower boundary of the Irminger Current.

SOUND VELOCITY STRUCTURE EAST OF PRIMARY OPAREA

A. General Oceanography

(C) During Phases I and II of the exercise, SANDS and HAYES took lines of XBTs to the east-northeast and east of the primary OPAREA between station B and the Reykjanes Ridge. The Phase I track started in the North Atlantic Current gyre and crossed the Subarctic Convergence at ranges of about 15 and 280 nm from station B (figure 2). The Phase II track started on the edge of the relatively cold, dilute Labrador Sea gyre and crossed the Subarctic Convergence at a range of about 265 nm from station B (figure 3). The eastern halves of both the Phase I and II tracks lay in the warmer, more saline North Atlantic Current. Two T-S/sound velocity comparisons illustrate the dissimilar oceanographic conditions at opposite ends of these tracks: figure 7 at station B and figure 18 just east of the Reykjanes Ridge crest.

(U) At station B (figure 7) the depth of the DSC axis (160 m) coincides with the bottom of the ASaW layer. This layer overlies a layer of LCW that in turn overlies a layer of NACW below about 800 m. At station B, AIW is not discernable and NSOW does not have noticeable effects on the deep positive sound velocity gradient. Because the data shown in figure 7 were collected during Phase III of the exercise, this figure represents conditions in the colder, more dilute Labrador Sea gyre. East of the Reykjanes Ridge (figure 18), the warmer, more saline North Atlantic Current occupies the upper 800 m of the water column, causing considerably higher sound velocities. The depth of the DSC axis (470 m) corresponds to a salinity minimum in the NACW layer. The reason for this salinity minimum is not clear, but it may be a result of mixing over the eastern flank of the Reykjanes Ridge.
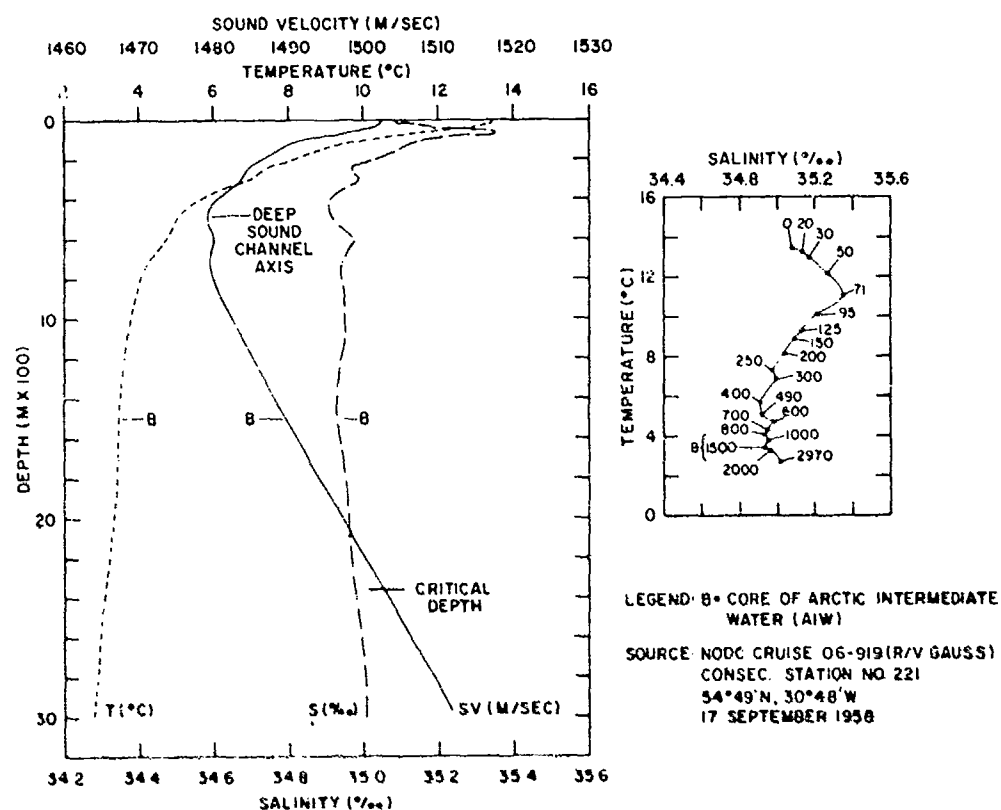
FIGURE 18. HISTORICAL SUMMER TEMPERATURE-SALINITY-SOUND
VELOCITY PROFILES AND T-S DIAGRAM OVER REYKJANES
RIDGE (U)

A second salinity minimum at 800 m marks the bottom of the NACW layer and results in a secondary sound velocity minimum below the DSC axis. The salinity maximum at 1000 m corresponds to the well mixed core of MIW that lies above the AIW salinity minimum (about 1500 m). Neither the MIW salinity maximum or the AIW salinity minimum have noticeable effects on the positive sound velocity gradient below the DSC axis. Between about 1600 and 3000 m, the sound velocities shown in figure 18 are up to 1.5 m/sec lower than those shown in figure 7. This is due to NSOW that enters the northeast Atlantic Ocean over the Faeroe-Iceland Ridge. This water mass flows south along the eastern flank of the Reykjanes Ridge before entering the Labrador Basin through the Gibbs Fracture Zone (Worthington and Volkmann, 1965; Garner, 1972). During summer, near-surface sound velocities can be more than 15 m/sec higher in the North Atlantic Current than in the Labrador Sea gyre. This results in much greater critical depths at the eastern end of the station B to Reykjanes Ridge track.

B.   Sound Velocity Structure Between Station B and Reykjanes Ridge

(U) Figure 19 shows a series of 10 sound velocity profiles plotted at their position of observation normal to the station B to Reykjanes Ridge track during Phase I of the exercise and a contoured cross section of these same data. The sound velocity profiles extend to a maximum depth of 1500 m and the contoured cross section to 1000 m. The bathymetric profile shown in figure 19 is from NAVOCEANO NAR chart 4, as is the bathymetric profile shown in figure 20 (Phase II). The observations used in figure 19 are identified in table X.

(C) During Phase I, surface sound velocities varied from less than 1477 m/sec in the Labrador Sea gyre to more than 1488 m/sec at the eastern end of the track. A mixed layer was absent on most of the profiles. The depth of the DSC axis varied from 90 m in the Labrador Sea gyre (profile 3) to about 650 m at the eastern end of the track (profile 10). The sound velocity at the DSC axis varied from about 1460 and 1482 m/sec between these same two profiles. However, the DSC structure shown on profile 10 is speculative since this profile is based on shallow AXBT data. The effects of the Sub-arctic Convergence are seen in rapid shoaling of sound velocity isolines below the DSC axis at ranges between 200 and 300 nm from station B. At a range of about 390 nm, these isolines deepen again, forming a domed structure centered on profile 9. This domed structure is apparently the result of an instrusion of warmer, more saline water at depths of 300 to 500 m. Critical depth decreased from about 1100 m at station B to 660 m at a range of about 70 nm from station B (center of Labrador Sea gyre) and then increased to 1400 m at the eastern end of the track. Except for the region directly over the crest of the Reykjanes Ridge, depth excess was adequate for convergence zone propagation from a near-surface source along the Phase I track.

FIGURE 19. SOUND VELOCITY STRUCTURE BETWEEN STATION B AND
REYJANES RIDGE DURING PHASE I (U)

PROFILE	OBSERVATION	DATE (1972)	TIME (GMT)	LAT (°N)	LONG (°W)
1	SANDS XBT 20	20 Jul	0037	53°59'	44°49'
2	SANDS XBT 21	20 Jul	0400	54°31'	44°24'
3	SANDS XBT 44	25 Jul	1300	54°19'	43°03'
4	SANDS XBT 43	25 Jul	0400	54°44'	40°36'
5	SANDS XBT 42	25 Jul	0000	54°58'	39°33'
6	SANDS XBT 41	24 Jul	2009	55°09'	38°19'
7	SANDS XBT 39	24 Jul	1600	55°20'	37°12'
8	SANDS XBT 38	24 Jul	1200	55°31'	35°53'
9	SANDS SVP 4 (D)	24 Jul	0200	55°50'	34°01'
10	VP-24 AXBT 62	28 Jul	1502	55°41'	31°49'

Note: (D) indicates downcast

TABLE X. IDENTIFICATION OF OBSERVATIONS USED IN STATION B TO
REYKJANES RIDGE CROSS SECTION (PHASE I) (U)

(C) Figure 20 shows a series of 8 sound velocity profiles plotted at their position of observation normal to the station B to Reykjanes Ridge track during Phase II of the exercise and a contoured cross section of these data. The observations used in figure 20 are identified in table XI. During Phase II, surface sound velocities varied from about 1480 m/sec at station B to about 1493 m/sec east of the Reykjanes Ridge. A mixed layer at depths between 20 and 40 m was found on most of the profiles. The depth of the DSC axis probably increased rapidly to about 600 m a few nautical miles east of profile 8. The sound velocity at the axis varied from about 1468 m/sec to about 1481 m/sec between station B and the eastern end of the track. The tongue with sound velocities less than 1472 m/sec found during Phase II is much less pronounced that the cell with similar sound velocities found during Phase I (figure 19). This is a direct result of the lesser eastward extent of the Labrador Sea gyre during Phase II (greater development of North Atlantic Current gyre). The effects of the Subarctic Convergence are not as obvious in figure 20 as they are in figure 19, probably due to the diminished extent of the Labrador Sea gyre during Phase II. Critical depth during Phase II varied from 1170 m at a range of about 150 nm from station B to 1840 m east of the Reykjanes Ridge. During Phase II, critical depths were 300 to 400 m deeper than those in Phase I due to increased surface insolation. However, except for the region directly over the Reykjanes Ridge crest, depth excess along the Phase II track was adequate for convergence zone propagation from a near-surface source.

(U) During Phase II of the exercise, sound velocity profiles at ranges between 200 and 300 nm from station B displayed a bichannel structure consisting of a sound velocity minimum (upper sound channel) and an intermediate sound velocity maximum above the DSC axis (profiles 5 and 6 of figure 20). Similar structures were found 20% to 80% of the time in the historical data of this region during summer by Fenner and Bucca (1971). The upper sound channel axis corresponded to the maximum depth of summer warming, while the intermediate sound velocity maximum coincided with a temperature inversion along the Subarctic Convergence (probably a NACW intrusion). During Phase I, similar sound velocity perturbations were found at ranges between 200 and 300 nm from station B, but at depths below the DSC axis (see profiles 6 and 7, figure 19). These perturbations apparently were caused by intrusions of NACW across the Subarctic Convergence into the ASaW/LCW layer (Fenner and Bucca, 1971).

(U) During Phase II, the DSC axis was deeper than during Phase I at ranges greater than about 260 nm from station B. At a range of about 460 nm from station B, the axis was nearly 400 m deeper during Phase II than it was in Phase I. However, in the same region, sound velocities at the axis were similar during both phases (i.e., 1476 to 1482 m/sec). This anomalous situation is not a function of data type, data spacing, or the relative position of the Subarctic Convergence.
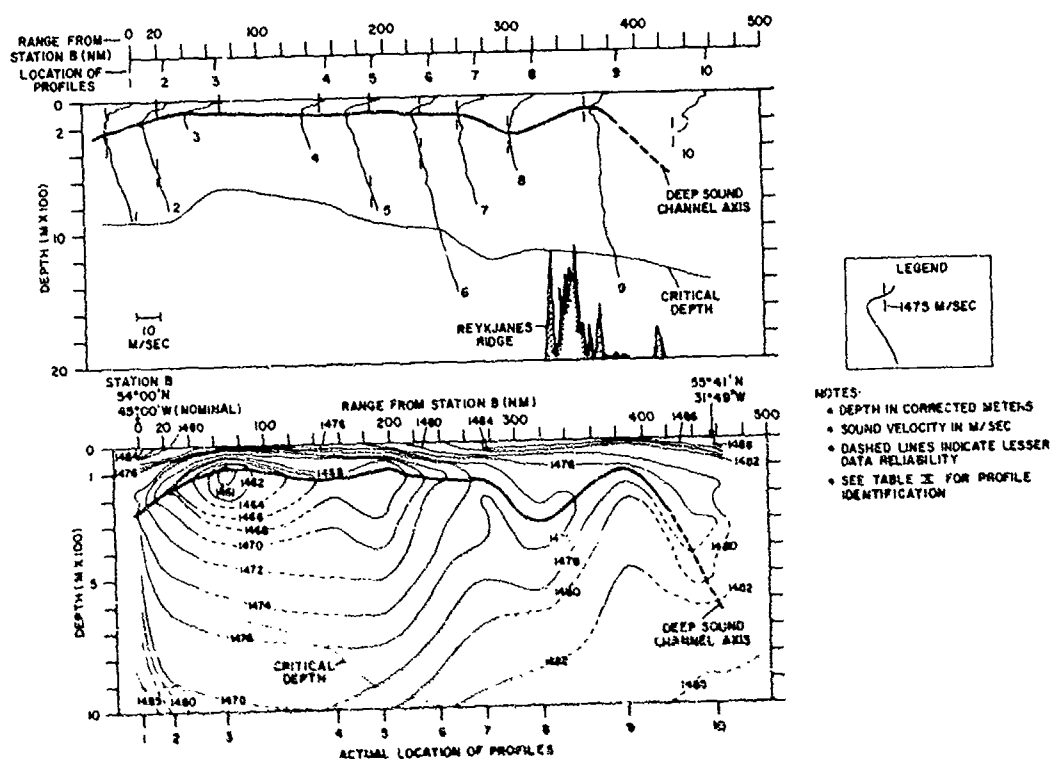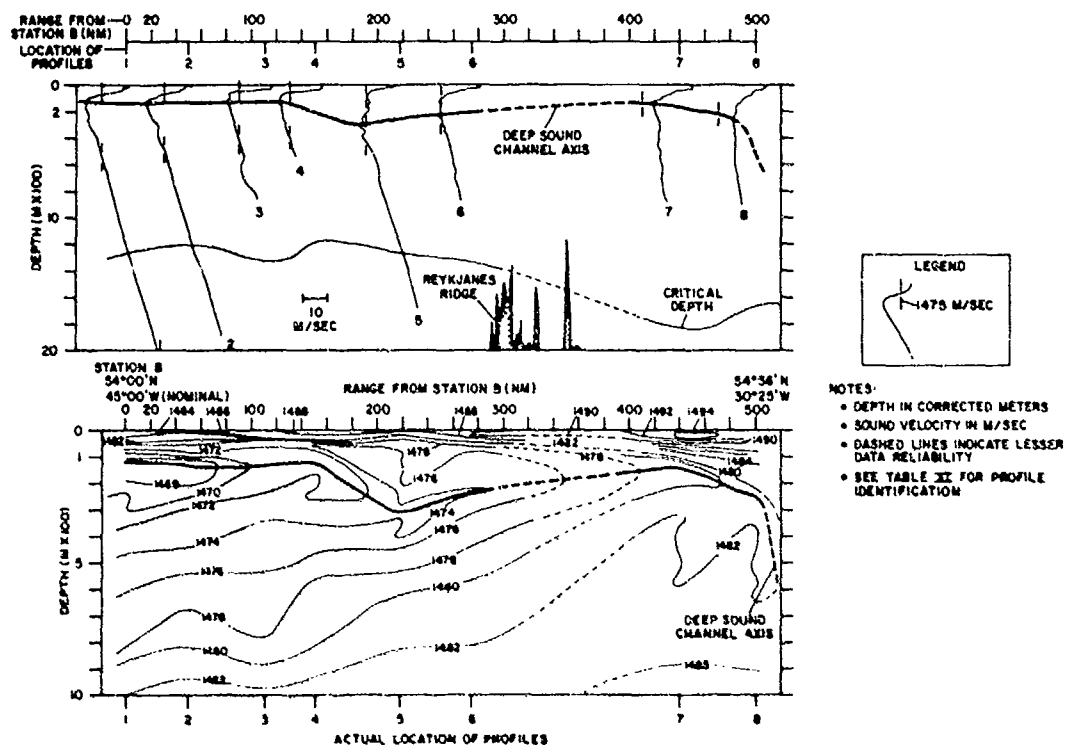
FIGURE 20. SOUND VELOCITY STRUCTURE BETWEEN STATION B AND
REYJANES RIDGE DURING PHASE II (U)

55

PROFILE	OBSERVATION	DATE (1972)	TIME (GMT)	LAT (°N)	LONG (°W)
1	SANDS SVP 5 (U)	31 Jul	0420	53°59'	44°51'
2	HAYES XBT 49A	3 Aug	0000	54°01'	43°18'
3	HAYES XBT 50	3 Aug	0400	54°06'	41°41'
4	HAYES XBT 51	3 Aug	0800	54°08'	40°25'
5	HAYES XBT 52	3 Aug	1200	54°13'	38°33'
6	HAYES XBT 53	3 Aug	1600	54°16'	36°54'
7	HAYES XBT 54	4 Aug	0400	54°29'	32°06'
8	HAYES XBT 55	4 Aug	0800	54°36'	30°25'

Note: (U) indicates upcast

TABLE XI. IDENTIFICATION OF OBSERVATIONS USED IN STATION B TO REYKJANES RIDGE CROSS SECTION (PHASE II) (U)

The DSC axis east of the Reykjanes Ridge corresponded to a salinity
minimum near the bottom of the NACW layer. However, a perturbation
below the DSC axis coincided with the bottom of the NACW layer (top of
MIW layer, figure 18). Mixing between NACW and transient cells of MIW
probably occurred at the eastern end of the Phase II track. Such
mixing has been observed farther to the south over the Mid-Atlantic
Ridge crest by Katz (1970). Mixing between NACW and MIW can cause
sound velocity perturbations below the DSC axis similar to those found
on profiles 7 and 8 of figure 20 (Fenner and Bucca, 1971). Sound
velocities associated with these perturbations were barely greater than
those at the DSC axis. This indicates that the depth of the DSC axis
is more sensitive to temporal and spatial fluctuations in the environ-
ment than is sound velocity at the axis. This sensitivity to mixing
is one possible explanation for the anomalously shallow depths of the
DSC axis at the eastern end of the station B to Reykjanes Ridge track
during Phase II of the exercise.

(U) The following sound velocity profile statistics (defined
in a previous section) summarize the track as a whole for Phases I and
II of the exercise:

	MINIMUM	MEAN	MAXIMUM	RANGE	NO. OF OBS.
MLV (m/sec)					
I	1476.5	1482.3	1488.3	11.8	10
II	1485.9	1489.6	1495.2	9.3	8
DSCD (m)					
I	90	150	290	200	9*
II	120	180	250	130	8
DSCV (m/sec)					
I	1460.4	1470.1	1477.0	16.6	9*
II	1468.2	1473.0	1480.9	12.7	8
CD (m)					
I	660	940	1400	740	10
II	1170	1380	1840	670	8

(*does not include profile 10)

Statistics on the depth and sound velocity at the DSC axis shown above
do not reflect speculative values of both parameters at the eastern ends
of the Phase I and Phase II tracks. The mean values of all four para-
meters were greater during Phase II than Phase I owing to increased

surface insolation and lesser development of Labrador Current gyre
during Phase II. The greater mean depth and sound velocity of the
DSC axis during Phase II indicates a seasonal effect on DSC structure
between station B and the Reykjanes Ridge. Variations of all four
parameters were greater during Phase I than Phase II, mainly because
of less uniform surface insolation in the region east of station B.
Owing to the disparity of oceanographic conditions at opposite ends
of the Phase I and Phase II tracks, variations in all four parameters
over the track were greater than similar variations at station B for
each phase.

SOUND VELOCITY STRUCTURE NORTHWEST OF PRIMARY OPAREA

A. General Oceanography

(C) During Phase III of NORLANT-72, QUEST took a continuous
line of 64 T-7 XBTs northwest of the primary OPAREA into Baffin Bay
and SANDS took a line of XBTs and one CTD/SV station northwest of
station B in the central Labrador Sea. Combined, these data describe
a track that extends nearly 1500 nm from station B to the Carey Islands
in northern Baffin Bay (figures 4A and 4B). The following T-S/sound
velocity comparisons have been chosen to illustrate the variable
oceanography along this track:

   • Figure 7, located at station B,

   • Figure 21, located at the edge of the Labrador Current
in the central Labrador Sea,

   • Figure 22, located in West Greenland Current in the
northern Labrador Sea,

   • Figure 23, located immediately south of the Davis
Strait sill,

   • Figure 24, located in central Baffin Bay; and

   • Figure 25, located immediately south of the Carey Islands.

Data shown in figures 7 and 21 were collected during Phase III of the
exercise. Data shown in figures 23, 24, and 25 were collected by USCG
EDISTO during August 1966 (Palfrey, 1968). Each of the T-S/sound
velocity comparisons represents conditions in distinct oceanographic
regimes along the 1500-nm track from station B to the Carey Islands.

(U) At station B (figure 7), ASaW overlies a layer of LCW
(160 to 800 m) that in turn overlies NACW. The DSC axis (160 m)
coincides with the bottom of the ASaW layer. A sound velocity
perturbation below the DSC axis at 240 m roughly corresponds with the
LCW core. Figure 7 represents oceanographic conditions just north of
the Subarctic Convergence during Phase III.

(U) In the central Labrador Sea (figure 21), the upper 1400 m
of the water column are comprised of LCW. The DSC axis (60 m) coincides
with the temperature minimum in the LCW core. A change in the positive
sound velocity gradient is discernable at about 1600 m, immediately
below the bottom of the LCW layer. This gradient change may be caused
by North Atlantic Deep and Bottom Water that is in the process of
sinking. Data shown in figure 21 were collected northwest of OWS
BRAVO (56°30'N, 51°00'W). According to Husby (1967), North Atlantic
Deep and Bottom Water is formed north of OWS BRAVO. At a depth of
3000 m, sound velocities shown in figure 21 are approximately 1.0 m/sec
less than those at station B (figure 7) due to a preferential flow
of NSOW under the Labrador Current (Worthington, 1970). Figure 21
represents oceanographic conditions in the Labrador Sea gyre between
about 56°N and 61°N.

(U) In the West Greenland Current (figure 22), the upper
1000 m of the water column consist of a derivative of NACW called West
Greenland Current Water (WGCW). This water mass is formed by mixing of
Irminger Current Water (another NACW derivative) with cold, dilute
waters carried by the East Greenland Current (figure 4A). The warming
effects of the West Greenland Current extend around the southern tip of
Greenland into the northern Labrador Sea, but are not manifest in the
near-surface layer north of about 64°N to 65°N. In the West Greenland
Current, the DSC axis (100 m) corresponds to the maximum depth of
summer warming. The core of WGCW is marked by a temperature and
salinity maximum at about 200 m that causes a sound velocity maximum
below the DSC axis. The AIW low-salinity core at about 1260 m has
no apparent effect on the deep positive sound velocity gradient.
However, at about 2500 m, sound velocities are approximately 2.0 m/sec
less than those at station B owing to a preferential flow of NSOW
under the West Greenland Current (Worthington, 1970). This preferential
flow is continuous with that found farther to the south under the
Labrador Current. Figure 22 represents oceanographic conditions off
the west coast of Greenland between about 61°N and 63°N.

(U) Oceanographic conditions just south of Davis Strait
(figure 23) are even more complex than those in the primary OPAREA,
because of intensive mixing between various water masses at all depths
and to tidal currents over the shallow Davis Strait continental slope.
The predominant surface current in this strait is the southerly Baffin
Land Current. The northerly flowing West Greenland Current is apparent
at the surface only on the far eastern side of Davis Strait in the
shallow water over the Greenland continental shelf (NAVOCEANO, 1958).
In this region, the DSC axis (50 m) coincides with the temperature
minimum in the Baffin Land Current Water (BLCW) core. The sound
velocity at the axis shown in figure 23 is nearly 35 m/sec less than
in the West Greenland Current (figure 22) and about 20 m/sec less than
in the Labrador Sea gyre (figure 21). This is due to the extremely
low temperature and salinity of the BLCW core (about -1.6°C and 34.45°/oo,
figure 23). In the deeper portions of Davis Strait, WGCW is present
as a relatively warm, saline core at depths between 300 and 400 m. This
core is about 2.0°C colder and nearly 0.5°/oo less saline than that

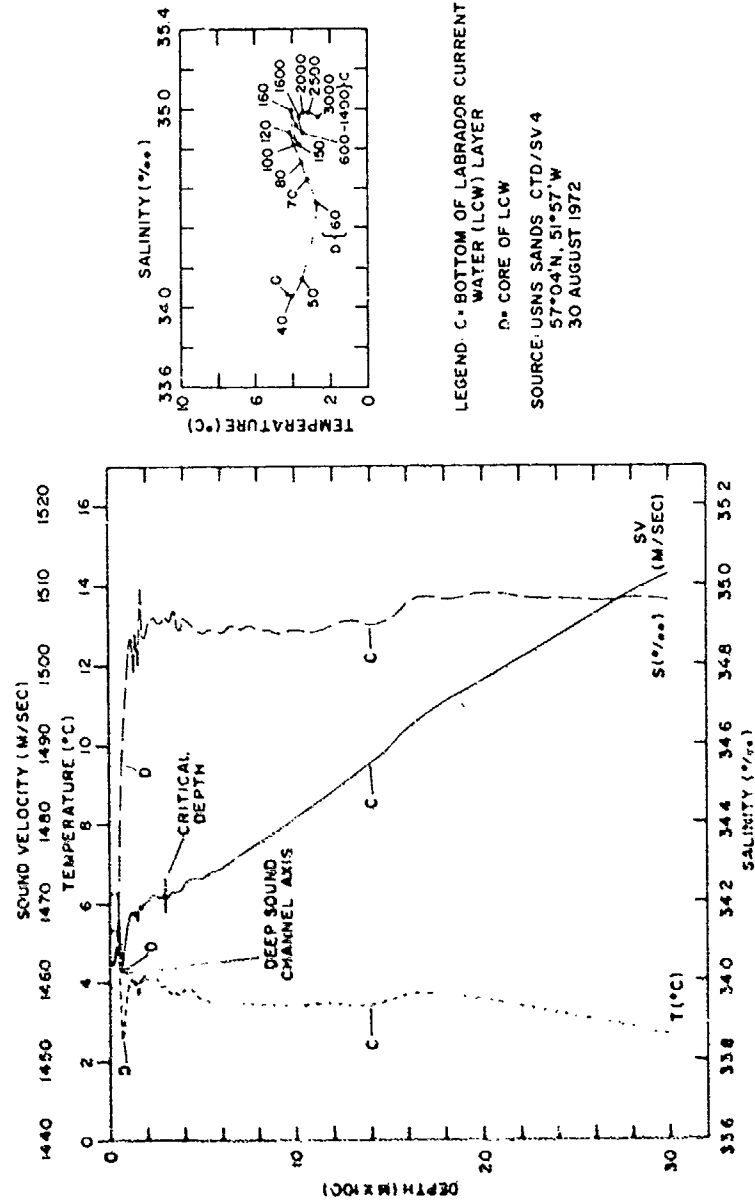FIGURE 21. TEMPERATURE-SALINITY-SOUND VELOCITY PROFILES AND T-S DIAGRAM IN CENTRAL LABRADOR SEA (EDGE OF LABRADOR CURRENT) DURING PHASE III (U)
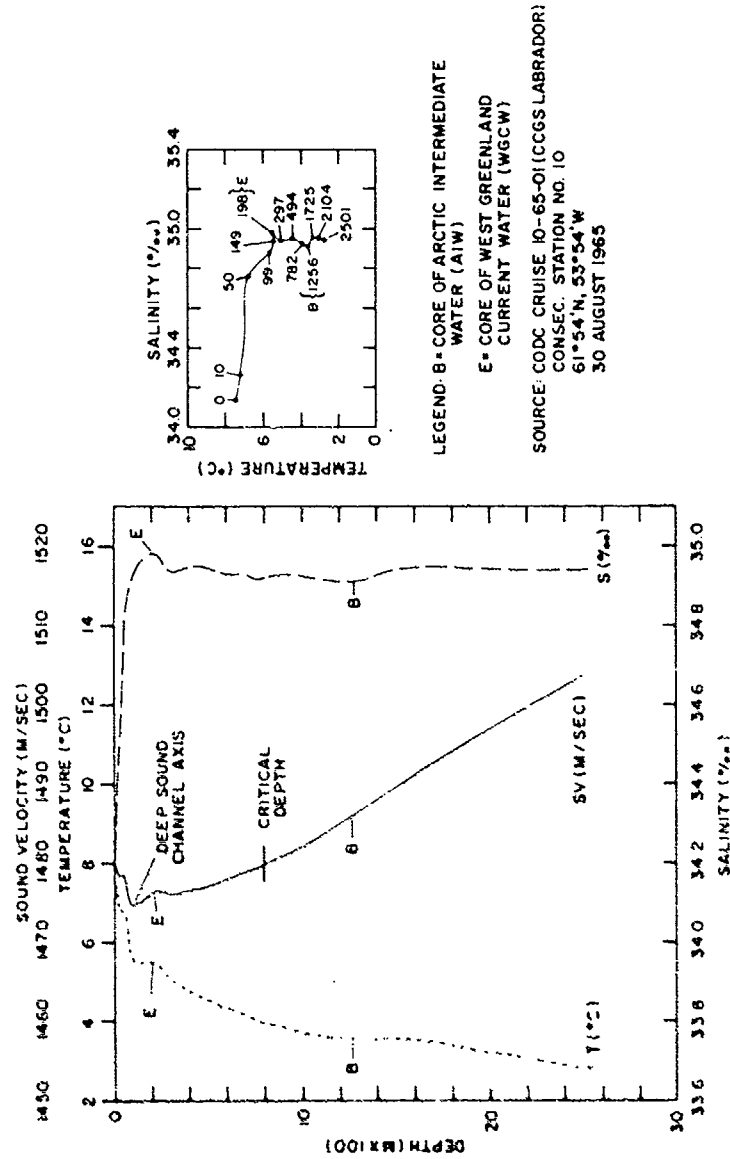
FIGURE 22. HISTORICAL SUMMER TEMPERATURE-SALINITY-SOUND VELOCITY PROFILES AND T-S DIAGRAM IN WEST GREENLAND CURRENT (NORTHERN LABRADOR SEA) (U)
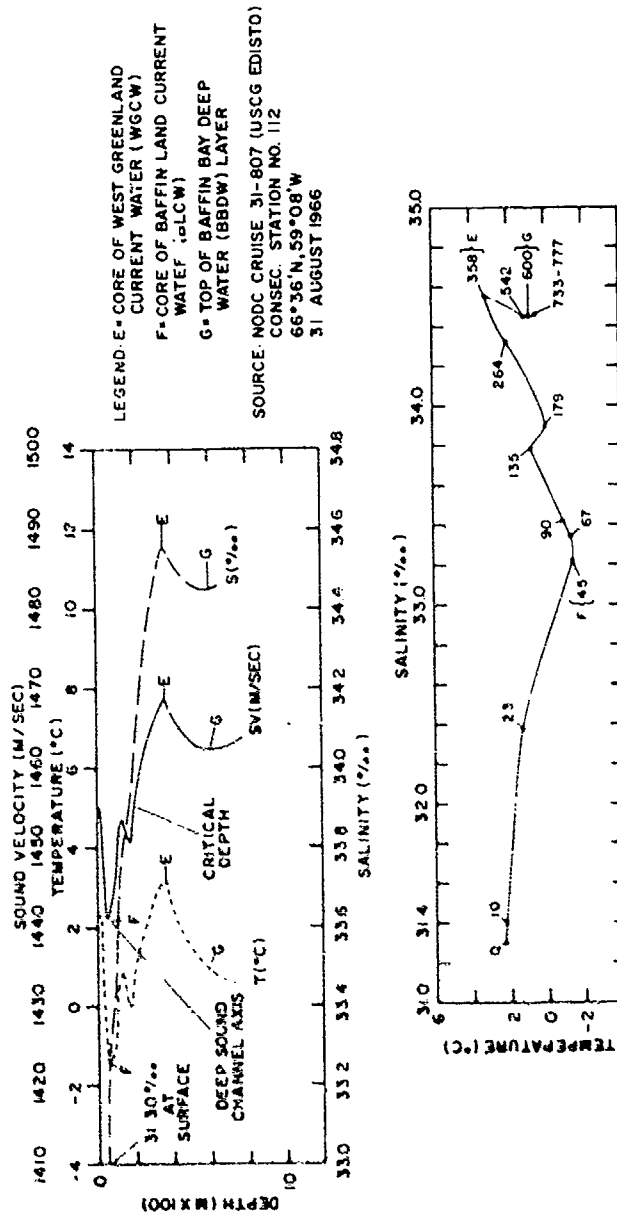
FIGURE 23. HISTORICAL SUMMER TEMPERATURE–SALINITY–SOUND VELOCITY PROFILES AND T–S DIAGRAM IN DAVIS STRAIT (U)

shown in figure 22 due to the substantial winnowing out of WGCW between 63°N and Davis Strait sill (a distance of approximately 250 nm). Palfrey (1968) shows an inflow of WGCW water on the eastern side of the strait and a substantial outflow of WGCW on the western side of the strait during the summer of 1966. Data shown in figure 23 are located in the WGCW outflow postulated by Palfrey. However, sections across Davis Strait shown by Bourkland (1968) for summer 1968 do not substantiate this outflow. In any case, the WGCW core in the environs of Davis Strait results in either a sound velocity maximum (as shown in figure 23 at 360 m) or in a marked change in the positive sound velocity gradient below the DSC axis. Below the WGCW core, the Davis Strait region is occupied by Baffin Bay Deep Water (BBDW). This water mass fills most of Baffin Bay below about 700 m, and is formed by sinking Arctic Water that enters northern Baffin Bay through Smith Sound (Bailey, 1956). BBDW is even colder and less saline than NSOW, having a temperature less than 0.8°C and a nearly uniform salinity of 34.45°/oo (Palfrey, 1968). Some BBDW boluses pulse over Davis Strait into the northern Labrador Sea to join the southerly flow of NSOW under the Labrador Current. BBDW can cause a sound velocity minimum or an isovelocity layer in the Davis Strait region and in southern Baffin Bay below the WGCW core. At a depth of about 800 m, the sound velocity shown in figure 23 is about 16 m/sec less than in the West Greenland Current (figure 22) and about 13 m/sec less than in the Labrador Sea gyre (figure 21) owing to the effects of BBDW.

(U) Figure 23 is specific only for oceanographic conditions in the immediate environs of Davis Strait (approximately 65°N to 67°N). An intense transitional zone occurs in the northern Labrador Sea between about 63°N and Davis Strait. In this transition zone, BLCW mixes with NGCW, obliterates most of the surface effects of the West Greenland Current, and causes WGCW to sink. This mixing can lead to complex and spurious sound velocity structures above and below the DSC axis. Furthermore, sinking WGCW and NACW below 500 to 600 m rapidly mix out boluses of BBDW that penetrate over Davis Strait sill. Mixing of BBDW with WGCW and NACW can cause abrupt changes in the near-bottom sound velocity structure.

(U) In central Baffin Bay (figure 24), oceanographic conditions are much less complex than those in the environs of Davis Strait. The upper 10 to 20 m of the water column in central Baffin Bay during summer frequently has a well-developed thermal mixed layer with temperature differences as great as 2°C. This thermal layer is superimposed on an extremely strong halocline (0.4°/oo or more per meter). These two factors combine to form a strong positive sound velocity gradient in the near-surface layer (about 1.3 m/sec/m in the case of figure 24). Surface effects of the West Greenland Current are confined to a narrow, poorly defined band off the west coast of Greenland. In central Baffin Bay, the Baffin Land Current is most pronounced off the east coast of Baffin Island, since its primary source is Lancaster Sound. This
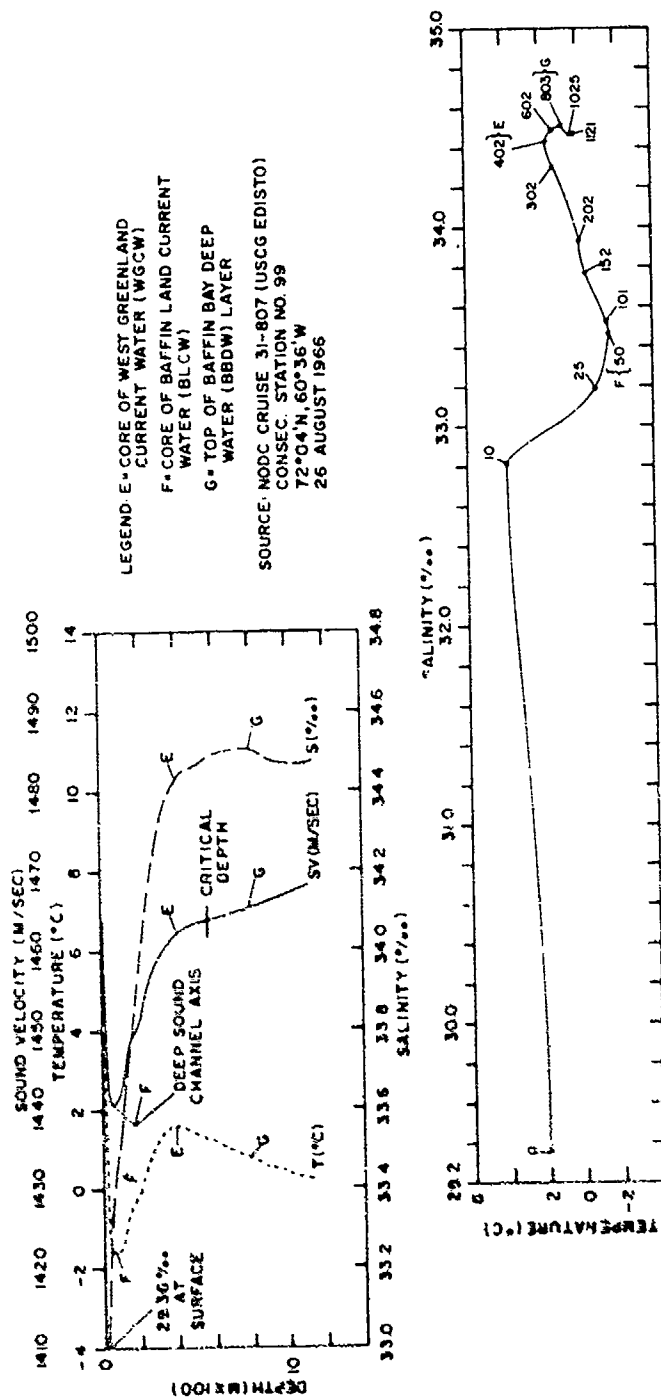
FIGURE 24. HISTORICAL SUMMER TEMPERATURE–SALINITY–SOUND VELOCITY PROFILES AND T-S DIAGRAM IN CENTRAL BAFFIN BAY (U)

results in a gyre in the center of Baffin Bay that circulates extremely cold, dilute BLCW. The DSC axis (50 m) coincides with the BLCW core. Sound velocity at the axis approximates that found in the Davis Strait region, but can be somewhat greater because of increased summer insolation in the Baffin Bay gyre. A strong thermocline and halocline occur between the bottom of the BLCW layer and the warmer, more saline WGCW core. This core is still present in central Baffin Bay, but in a much diminished form with temperatures nearly 2.0°C colder and salinities nearly 0.2°/$_{oo}$ less than those in Davis Strait (figure 23). In most of central Baffin Bay, WGCW causes an abrupt change in the slope of the positive velocity gradient below about 400 m. BBDW occupies the entire Baffin Basin below a depth of about 700 m. The extremely low temperature and salinity of this water mass and the well-developed surface mixed layer combine to cause anomalously deep critical depths over much of the Baffin Basin. Figure 24 represents general oceanographic conditions between about 71°N and 74°N. Between Davis Strait and 71°N, the upper 200 m of the water column is similar to that shown in figure 24, but WGCW is present in greater unmixed concentration between about 300 and 800 m. In this region, WGCW can cause a sound velocity maximum below the DSC axis and shallower critical depths than those in central Baffin Bay.

(U) In the region south of the Carey Islands (figure 25), the general oceanography is similar to that found in central Baffin Bay with two notable exceptions: the Baffin Land Current and BBDW are no longer present. In this region, the Baffin Land Current is replaced by the higher salinity Arctic Water Current (figure 4B) emanating from Smith Sound and BBDW is in the process of formation. The DSC axis (70 m) coincides with the Arctic Water core and occurs at slightly greater depths than in Central Baffin Bay. Only a slight remnant of well-mixed WGCW is found just above the bottom south of the Carey Islands. The sound velocity profile in figure 25 shows a perturbation below the DSC axis that roughly corresponds with a temperature maximum and minimum in the same depth range. This sound velocity perturbation may be caused by mixing of WGCW and sinking Arctic Water. At most depths below the DSC axis, sound velocities shown in figure 25 are lower than those found in central Baffin Bay (figure 24), largely due to cold Arctic Water throughout the water column. Generally speaking, figure 24 represents oceanographic conditions throughout northern Baffin Bay and southern Smith Sound.

(U) In summary, the overall sound velocity structure along the station B to Carey Islands track is least complicated in the Labrador Sea gyre, most complicated in the region between about 63°N and 71°N, and of intermediate complexity in central and northern Baffin Bay and in the immediate vicinity of station B. The greatest overall complexity in sound velocity structure occurs immediately south of the
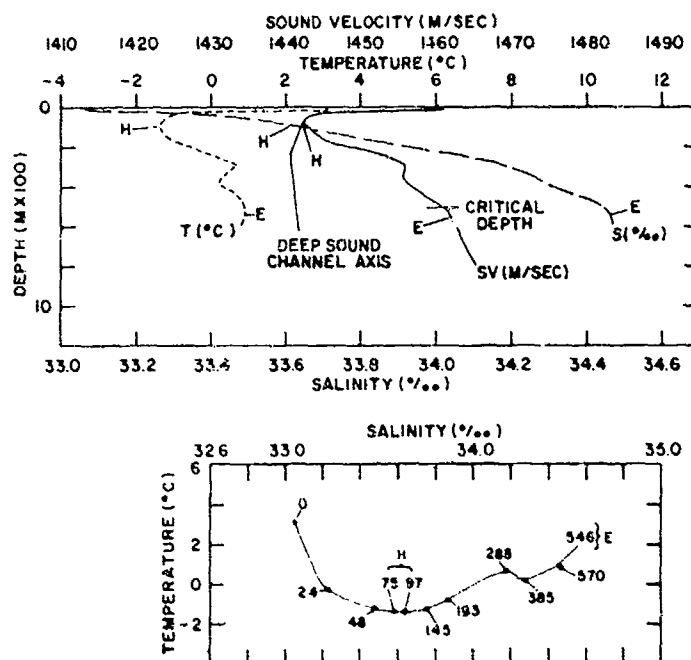
FIGURE 25. HISTORICAL SUMMER TEMPERATURE-SALINITY-SOUND
VELOCITY PROFILES AND T-S DIAGRAM SOUTH OF
CAREY ISLANDS, BAFFIN BAY (U)

Davis Strait sill (figure 23), where conditions are even more confused than those in the primary OPAREA. Extreme differences in sound velocities occur at all depths across Davis Strait, particularly at the DSC axis. Generally speaking, sound velocity at the DSC axis is greater than 1472 m/sec just north of the Subarctic Convergence and in the region between about 61°N and 63°N (West Greenland Current). The sound velocity at the DSC axis lies between 1460 and 1468 m/sec in the Labrador Sea gyre and between 1450 and 1472 m/sec in the intense transition zone south of Davis Strait (northern Labrador Sea). North of Davis Strait, sound velocity at the DSC axis is always less than 1450 m/sec and can be less than 1442 m/sec in regions of strong Baffin Land Current or Arctic Water Current influence.

B. Variability of Sound Velocity at Station E

(C) During Phase III of NORLANT-72, QUEST took a series of 8 T-7 XBTs during a 48-hour period on 24-26 August in the central Labrador Sea within about 20 nm of station E. Figure 26 shows a time series plot and a contoured presentation of these data. The time series plot and the contoured section extend to a maximum depth of about 1000 m. Data used in figure 26 are identified in table XII. Locations of these data relative to station E are shown in an insert to figure 26. Since QUEST was moving northeastward during most of the occupation, the sound velocity variability shown in figure 26 is a result of both temporal and spatial variability in the environment.

(C) During the station E occupation, the maximum depth of the DSC axis (80 m) occurred on profile 8, as did the maximum sound velocity at the DSC axis (about 1467 m/sec). The minimum depth and sound velocity at the DSC axis (40 m and about 1461 m/sec) occurred on profile 5. At station E, the DSC axis coincided with the temperature minimum in the LCW core. During the occupation, critical depth varied between 510 and 780 m and was sufficiently shallow to allow unrestricted convergence zone propagation from a near-surface source. The following sound velocity profile statistics summarize conditions over the 48-hour occupation:

	MINIMUM	MEAN	MAXIMUM	RANGE	NO. OF OBS.
MLV (m/sec)	1475.5	1476.6	1477.2	1.7	8
DSCD (m)	40	60	80	40	8
DSCV (m/sec)	1460.9	1462.9	1467.1	6.2	8
CD (m)	510	660	780	270	8

FIGURE 26. VARIABILITY OF SOUND VELOCITY AT STATION E DURING PHASE III (U)

68
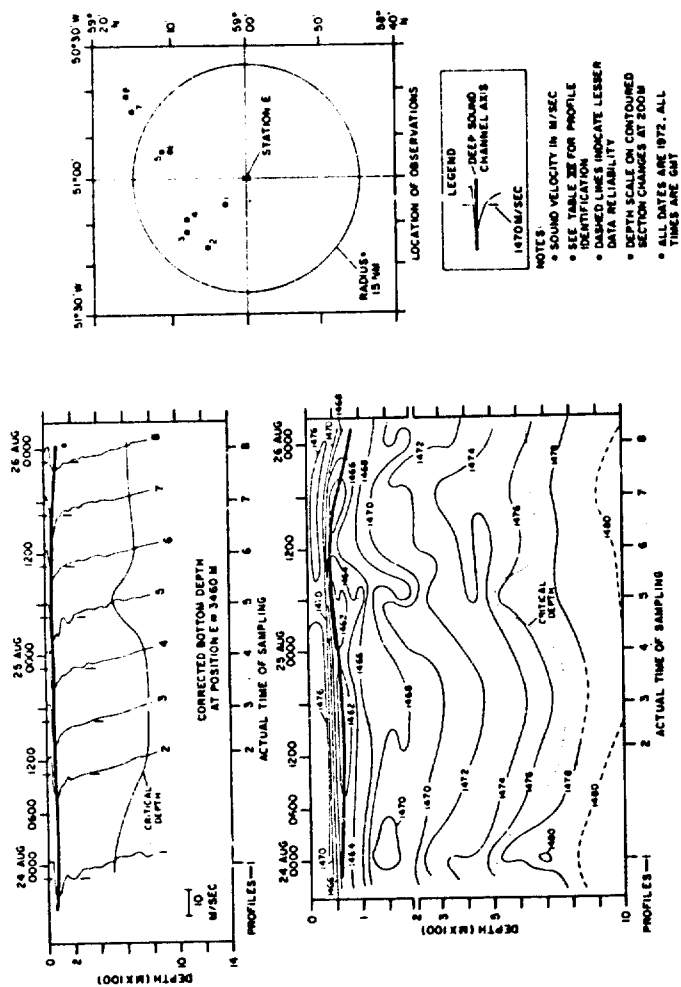
PROFILE	XBT NUMBER	DATE (1972)	TIME (GMT)	LAT (°N)	LONG (°W)	RANGE FROM STATION E (nm)
1	QUEST 7	24 Aug	0000	59°03'	51°06'	4
2	QUEST 9	24 Aug	1300	59°05'	51°16'	10
3	QUEST 10	24 Aug	1800	59°08'	51°12'	10
4	QUEST 11	25 Aug	0000	59°08'	51°10'	9
5	QUEST 12	25 Aug	0600	59°11'	50°54'	12
6	QUEST 13	25 Aug	1200	59°10'	50°54'	11
7	QUEST 14	25 Aug	1800	59°15'	50°45'	17
8	QUEST 15	26 Aug	0000	59°16'	50°42'	19

Note: Nominal position of station E is 59°00'N, 51°00'W

TABLE XII.   IDENTIFICATION OF OBSERVATIONS USED IN PHASE III
TIME SERIES STUDY AT STATION E (U)

(U) Variations in the maximum sound velocity in the mixed layer and in the depth of the DSC axis were much less than those at station B during Phases I and II of the exercise (figure 11). This is due to the greater stability of the near-surface layer in the Labrador Sea gyre and the relatively constant degree of surface in-solation found during late summer. However, variations in critical depth were of the same magnitude as those at station B during Phases I and II. This indicates variability in the sound velocity structure below about 500 m, and further indicates that critical depths at station E were more dependent on the positive velocity gradient below the DSC axis than on near-surface temperatures. Variation in the sound velocity at the DSC axis was greater at station E during Phase III than that at station B during either Phase I or II. This could be caused by intrusions of WGCW near the depth of the DSC axis or by internal motion. There is some evidence for internal waves with an approximately 18-hour period at station E in the form of the various sound velocity isolines below the DSC axis. However, intrusions of WGCW are a more likely explanation for the observed variations in sound velocity at the DSC axis. During the first 24 hours of the occupation, sound velocities in the upper 200 m of the water column were generally less than those during the second half of the occupation. The four profiles for the second half of the occupation (profiles 5 through 8) all lay to the northeast of station E, towards the main flow of the West Greenland Current (figure 4A). If an intrusion of WGCW occurred during the 48-hour occupation of station E, these pro-files would show the most pronounced effects of this intrusion. Sound velocity perturbations below the DSC axis on most of the profiles further indicate an intrusion of WGCW. The suspected WGCW intrusion may represent the initial turning of the West Greenland Current to the south and west to form the Labrador Sea gyre.

C. Variability of Sound Velocity at Station Q-3

(C) QUEST also took a series of 9 T-7 XBTs during a 48-hour period on 28-30 August within 20 nm of a station in the northern Labrador Sea. This is station Q-3 according to the operation plan for Phase III of NORLANT-72 (Naval Underwater Systems Center, 1972). Figure 27 shows a time series plot and contoured presentation of these data, both of which extend to the bottom (850 m according to NAVOCEANO NAR chart 4). Data used in figure 27 are identified in table XIII. Locations of the data relative to station Q-3 are shown in an insert to figure 27. Station Q-3 is located in the northern part of the intense oceanographic transition zone south of Davis Strait. In this transition zone, BLCW mixes with WGCW in the upper water column, and NACW and sinking WGCW mix with boluses of BBDW below 500 to 600 m. This can result in abrupt changes in sound velocity structures throughout the water column within relatively short distances. Furthermore, a strong horizontal front occurs in this region at depths of 100 to 300 m. This front marks the bottom of the BLCW layer and is a possible source of internal waves.
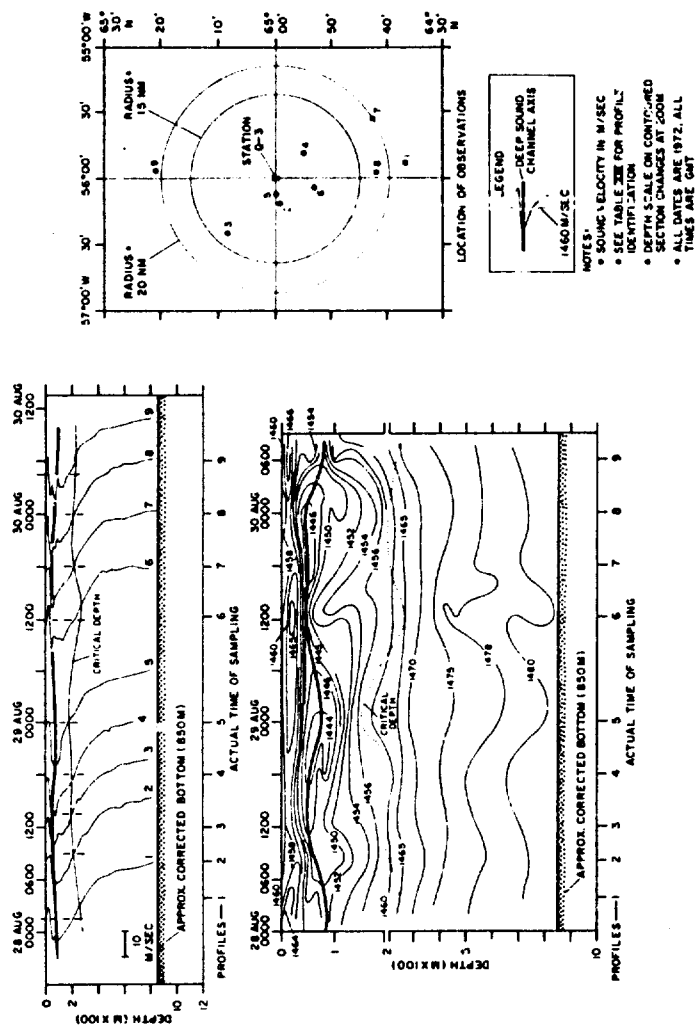
FIGURE 27. VARIABILITY OF SOUND VELOCITY AT STATION Q-3 DURING PHASE III (U)

PROFILE	XBT NUMBER	DATE (1972)	TIME (GMT)	LAT (°N)	LONG (°W)	RANGE FROM STATION Q-3 (nm)
1	QUEST 27	28 Aug	0410	64°37'	55°52'	23
2	QUEST 28	28 Aug	0800	64°59'	56°11'	4
3	QUEST 29	28 Aug	1200	65°08'	56°25'	12
4	QUEST 30	28 Aug	1800	64°55'	55°49'	7
5	QUEST 31	29 Aug	0000	65°00'	56°07'	3
6	QUEST 32	29 Aug	1230	64°53'	56°04'	7
7	QUEST 33	29 Aug	1800	64°43'	55°32'	20
8	QUEST 34	30 Aug	0000	64°42'	55°57'	18
9	QUEST 35	30 Aug	0400	65°21'	55°57'	21

Note: Nominal position of station Q-3 is 65°00'N, 56°00'W

TABLE XIII. IDENTIFICATION OF OBSERVATIONS USED IN PHASE III TIME SERIES STUDY AT STATION Q-3 (U)

CONFIDENTIAL

(C) The following sound velocity profile statistics summarize conditions during the 48 hour occupation of station Q-3:

	MINIMUM	MEAN	MAXIMUM	RANGE	NO. OF OBS.
MLV (m/sec)	1458.6	1461.5	1466.9	8.3	9
DSCD (m)	40	60	80	40	9
DSCV (m/sec)	1443.2	1446.7	1451.1	7.9	9
CD (m)	180	220	270	90	9

The maximum depth of the DSC axis (80 m) occurred on profiles 1 and 9, while the maximum sound velocity at the axis (about 1451 m/sec) occurred on profile 1. Sound velocity at the axis on profile 9 was only 0.5 m/sec greater than that for profile 1. The minimum depth of the axis (40 m) occurred on profiles 6 and 8, while minimum sound velocity at the axis (about 1443 m/sec) was found on profile 4. The diverse positions of these five profiles is an indication of extreme temporal and spatial variability in sound velocity at station Q-3. The DSC axis at this station coincided with the temperature minimum in the BLCW core. Both the depth and sound velocity at the DSC axis showed a 10- to 14-hour periodicity during the occupation, indicating possible effects of internal waves. Effects of internal waves also are evident in the form of the 1460 through 1480 m/sec sound velocity isolines below the DSC axis. These internal waves probably were generated along the front marking the bottom of the BLCW layer, and have a period approximating that of diurnal tides in the northern Labrador Sea (NAVOCEANO, 1965a). However, internal waves are not solely responsible for the observed variability in DSC structure. During the 5.5-hour period between 1230 and 1800 on 30 August the sound velocity at the DSC axis varied by 4.2 m/sec while the depth of the DSC axis remained at a constant 45 m. This variation is not a result of internal motion, but probably was caused by an intrusion of WGCW into the Baffin Land Current. The total variability in DSC structure at station Q-3 apparently was the result of temporal and spatial variations in the environment (i.e., caused by internal waves and intrusions of WGCW into the Baffin Land Current). Critical depths varied between 180 and 270 m, and also showed a 10- to 14-hour periodicity during part of the occupation of station Q-3. During the entire occupation, depth excess was adequate for convergence zone propagation from a near-surface source despite the shallow bottom depth (850 m).

73　　　　　　CONFIDENTIAL

(U) Overall variations in maximum sound velocity in the mixed layer and the sound velocity at the DSC axis at station Q-3 were greater than those at station E during Phase III (figure 26) or at station B during either Phases I or II (figure 11). This indicates that the sound velocity structure of the upper water column is more complex in the northern Labrador Sea than in the central Labrador Sea or in the region immediately north of the Subarctic Convergence. The statistics on the depth of the DSC axis at station Q-3 were identical to those at station E during Phase III. The DSC axis probably represents the maximum depth of summer warming at both stations. Variation in critical depth at station Q-3 was less than that at station E during Phase III, despite the much greater variation in near-surface sound velocity at station Q-3. This indicates that critical depths at station Q-3 are more dependent on the positive velocity gradient below the depth of the DSC axis than on near-surface temperatures, and that critical depth was relatively stable south of Davis Strait. At station Q-3, critical depth occurs at the approximate depth of the horizontal front demarking the bottom of the BLCW layer. Below the depth of this front, the sound velocity structure showed substantial variation due to mixing of NACW and sinking WGCW with boluses of BBDW descending south from Davis Strait. The nearly iso-velocity layer near the bottom on several profiles shown in figure 27 probably was the result of BBDW boluses mixing with NACW below the depth of the WGCW core. The WGCW core also caused the marked change in positive sound velocity gradient at depths below 400 m at station Q-3.

(U) The 7.9 m/sec variation in sound velocity at the DSC axis during the 48-hour occupation of station Q-3 is of the same general magnitude as the 9.5 m/sec variation in this parameter at station D over about 48 hours during Phase I (figure 10). The magnitude of both variations is approximately double that at station B during Phases I or II. At station D, about 45% of the total variability in DSC structure was attributable to internal wave action, the remaining 55% to spatial variations in the position of the Subarctic Convergence. At station Q-3, probably about half of the variability in DSC structure was caused by internal waves. The other half apparently resulted from intrusions of WGCW into the Baffin Land Current. About 60 nm north of station Q-3 on the southern edge of Davis Strait, oceanographic conditions are even more complex than those at station Q-3 or in the primary OPAREA (figure 23). Even greater variability in DSC structure would be expected at about 66°N than 60 nm southward at station Q-3.

D. Sound Velocity Structure Between Station B and Carey Islands

(C) Figure 28 shows a series of 39 sound velocity profiles plotted at their position of observation along a track from station B to Carey Islands, Baffin Bay, during Phase III of the exercise and a contoured cross section of these same data. This section is not a straight line, but rather a series of six doglegs that describe the

CONFIDENTIAL

track of QUEST (figures 4A and 4B). The sound velocity profiles ex-
tend to a maximum depth of 2000 m in the case of profile 1 and to a
maximum depth of about 850 m for the remainder of the observations.
The contoured sound velocity cross section extends to a depth of 1000 m.
Observations used in figure 28 are identified in table XIV. The bathy-
metric profile shown in this figure was taken from the following
sources:

> ● NAVOCEANO NAR Chart 4,

> ● NAVOCEANO Bathymetric Contour (BC) Chart 415,

> ● General Bathymetric Chart of the Ocean (GEBCO) Chart B-1, and

> ● Canadian Hydrographic Service Chart 896 (Arctic Bathymetry
north of 72°, 0° to 90°W).

The three major physiographic features along the track are the Labrador
Basin, the Davis Strait sill, and the Baffin Basin.

(C) Since figure 28 extends 1500 nm across several distinct
and diverse oceanographic regimes, it will be discussed in the following
sections:

1. Near-Subarctic Convergence section, ranging 140 nm
northwestward from station B (about 54°N to 56°N along the figure 28
track),

2. Labrador Sea gyre section, ranging from 140 to 520 m
(about 56°N to 61°N),

3. West Greenland Current section, ranging from 520 to
620 nm (about 61°N to 63°N),

4. North Labrador Sea section, ranging from 620 to
760 nm (about 63°N to 65°N),

5. Davis Strait section, ranging from 760 to 880 nm
(about 65°N to 67°N),

6. Southern Baffin Bay section, ranging from 880 to
1130 nm (about 67°N to 71°N),

7. Central Baffin Bay section, ranging from 1130 to
1380 nm (about 71°N to 75°N), and

8. Northern Baffin Bay section, ranging from 1380 nm to
the Carey Islands (about 75°N to about 76°45'N).

PROFILE	XBT NUMBER	DATE (1972)	TIME (GMT)	LAT (°N)	LONG (°W)
1	SANDS 122	1 Sep	0010	53°58'	44°46'
2	SANDS 120	21 Aug	1600	54°25'	45°57'
3	SANDS 119	31 Aug	1200	54°50'	46°48'
4	SANDS 118	31 Aug	0800	55°17'	47°55'
5	QUEST 1	22 Aug	2011	55°55'	47°37'
6	QUEST 3	23 Aug	0400	56°38'	47°30'
7	QUEST 4	23 Aug	1200	57°37'	48°51'
8	QUEST 5	23 Aug	1600	58°07'	49°40'
9	QUEST 6	23 Aug	2000	58°36'	50°25'
10	QUEST 7	24 Aug	0000	59°03'	51°06'
11	QUEST 16	26 Aug	0400	59°29'	51°30'
12	QUEST 17	26 Aug	0800	60°00'	52°14'
13	QUEST 18	26 Aug	1200	60°23'	53°07'
14	QUEST 21	27 Aug	0300	50°53'	54°04'
15	QUEST 22	27 Aug	0800	61°31'	54°14'
16	QUEST 23	27 Aug	1240	62°23'	54°38'
17	QUEST 24	27 Aug	1600	62°53'	54°59'
18	QUEST 25	27 Aug	2000	63°32'	55°15'
19	QUEST 26	28 Aug	0200	64°13'	55°44'
20	QUEST 27	28 Aug	0410	64°37'	55°52'
21	QUEST 29	28 Aug	1200	65°08'	56°25'
22	QUEST 36	30 Aug	0800	65°55'	55°56'
23	QUEST 39	31 Aug	0045	66°25'	57°56'
24	QUEST 40	31 Aug	0410	66°56'	58°23'
25	QUEST 41	31 Aug	0800	67°40'	58°54'
26	QUEST 42	31 Aug	1200	68°23'	59°15'
27	QUEST 43	31 Aug	1600	68°58'	60°03'
28	QUEST 44	31 Aug	2000	69°32'	60°14'
29	QUEST 45	1 Sep	0000	70°05'	61°07'
30	QUEST 48	1 Sep	2115	70°35'	61°40'
31	QUEST 51	2 Sep	1215	71°08'	63°14'
32	QUEST 52	2 Sep	1600	71°34'	65°09'
33	QUEST 53	2 Sep	2000	72°00'	67°00'
34	QUEST 56	4 Sep	0415	73°05'	65°00'
35	QUEST 57	4 Sep	0800	73°38'	64°35'
36	QUEST 60	5 Sep	0000	74°18'	66°12'
37	QUEST 61	5 Sep	0400	74°40'	68°29'
38	QUEST 64	5 Sep	1800	74°59'	71°00'
39	QUEST 65	6 Sep	0000	75°27'	70°28'

TABLE XIV. IDENTIFICATION OF OBSERVATIONS USED IN STATION B TO
CAREY ISLANDS CROSS SECTION (PHASE III) (U)

All eight sections are indexed in figures 4A and 4B. Sections 1, 2, 3, 5, 7, and 8 are represented by T-S/sound velocity comparisons that have been discussed previously (figures 7, 21, 22, 23, 24, and 25, respectively). Sections 4 and 6 are regions of transition located on either side of Davis Strait. Sound velocity profile statistics on the maximum sound velocity in the mixed layer, the depth and sound velocity of the DSC axis, and critical depth for each of the eight sections are summarized in table XV. Statistics for sections 3, 5, and 8 may be misleading owing to the small number of observations.

(U) Section 1 of figure 28 extends northwest of station B to a range of about 140 nm and includes profiles 1 through 5. Although the entire section lay on the cold side of the Subarctic Convergence during Phase III of NORLANT-72, it was influenced by a tongue of the North Atlantic Current gyre (figure 4A), particularly at a range of about 80 nm from station B. A mixed layer occurred along the entire section between depths of 20 and 50 m and at sound velocities between about 1479 and 1488 m/sec. The mixed layer was best defined near the Subarctic Convergence. The depth of the DSC axis varied between 100 and 180 m and generally decreased to the northwest. The sound velocity at the axis decreased to the northwest from about 1472 m/sec near the Subarctic Convergence to about 1466 m/sec at 56°N. Critical depth varied between 820 and 1250 m and generally decreased to the northwest of station B. Along this section, the DSC axis coincided with the bottom of the ASaW layer (figure 7), and the positive sound velocity gradient below the DSC axis was relatively free of perturbations. The effect of the Subarctic Convergence can be seen in the domed sound velocity structure on either side of profile 2 below the axis.

(U) Section 2 of figure 28 extends northwestward across the Labrador Basin between ranges of 140 and 520 nm from station B, and includes profiles 6 through 14. Station E lies in the approximate center of this section. The entire section lay within the relatively stable Labrador Sea gyre during Phase III, and was bounded on the north by a strong oceanographic front demarking the southwest wall of the West Greenland Current. This front extended to depths of at least 500 m. A mixed layer occurred throughout the section at about 40 m depth with sound velocities between about 1474 and 1482 m/sec. This mixed layer was best developed in the northern half of the section. The depth of the DSC axis varied between 60 and 80 m and did not show any marked dependence on increasing latitude. Sound velocity at the axis generally decreased to the northwest from greater than 1465 m/sec at 56°N to less than 1460 m/sec along the West Greenland Current front. Depth and sound velocity at the axis showed less variation in section 2 than in section 1 because of more stable oceanographic conditions in the Labrador Sea gyre. Critical depth varied from 1060 to 390 m

SOUND VELOCITY AT DSC AXIS (m/sec)

SECTION	MIN.	MEAN	MAX.	RANGE	NO. OF OBS.
1	1466.0	1469.2	1471.9	5.9	5
2	1461.0	1463.4	1465.4	4.4	8 (a)
3	1463.4	1467.9	1473.8	10.4	3
4	1445.6	1454.4	1466.5	20.9	5 (b)
5	1440.7	1442.7	1445.5	4.8	3
6	1440.4	1441.9	1444.5	4.1	6
7	1440.2	1442.5	1444.5	4.3	6
8	1440.8	1441.0	1441.5	0.7	3

CRITICAL DEPTH (m)

SECTION	MIN.	MEAN	MAX.	RANGE	NO. OF OBS.
1	820	1040	1250	430	5
2	390	670	1060	670	8 (a)
3	100	165	270	170	3
4	100	170	250	150	5 (b)
5	140	190	240	100	3
6	190	220	240	50	6
7	380	750	920	540	6
8	250	310	390	140	3

DEPTH OF DSC AXIS (m)

SECTION	MIN.	MEAN	MAX.	RANGE	NO. OF OBS.
1	100	140	180	80	5
2	60	70	80	20	8 (a)
3	60	70	80	20	3
4	40	60	80	40	5 (b)
5	70	70	80	10	3
6	40	60	90	50	6
7	40	70	130	90	6
8	50	80	110	60	3

MAXIMUM SOUND VELOCITY IN MIXED LAYER (m/sec)

SECTION	MIN.	MEAN	MAX.	RANGE	NO. OF OBS.
1	1478.9	1484.2	1487.7	8.8	5
2	1473.6	1477.9	1481.6	8.0	8 (a)
3	1469.3	1471.7	1475.6	6.3	3
4	1459.3	1463.9	1470.1	10.8	5 (b)
5	1451.2	1455.0	1461.4	10.2	3
6	1452.3	1456.1	1459.2	6.9	6
7	1461.6	1466.7	1468.8	7.2	6
8	1457.9	1459.2	1460.4	2.5	3

Notes: o (a) does not include profile 14 which is atypical
o (b) includes profile 17, in common with section 3

TABLE XV. SUMMARY OF SOUND VELOCITY PROFILE STATISTICS BETWEEN STATION B AND CAREY ISLANDS (U)

northwest across the Labrador Basin. The 670 nm variation in critical
depth observed over section 2 (maximum for any section) was mainly
caused by variations in the positive sound velocity gradient below the
DSC axis. In this section, the DSC axis coincided with the depth of
the temperature minimum in the LCW core (figure 21). Frequent
perturbations in the sound velocity profile immediately below the
axis probably were caused by intrusions of WGCW into the Labrador Sea
gyre. Such intrusions were observed during a 48-hour occupation of
station E in Phase III (figure 26). Mean values of maximum sound
velocity in the mixed layer, the depth and sound velocity of the DSC
axis, and critical depth at station E agreed well with mean values
of these parameters over the extent of section 2. This indicates
that station E was a representative site for the Labrador Sea gyre
during Phase III.

(U) Section 3 of figure 28 extends up the continental slope
of the northern Labrador Sea between ranges of 520 and 620 nm from
station B. This section includes profiles 15, 16, and 17. Section 3
lay within the flow of the West Greenland Current during Phase III,
and was bounded on the south by a strong oceanographic front
separating this relatively warm, high-salinity current and the
colder, less saline Labrador Sea gyre. At about 63°N this section
merged into the intense northern Labrador Sea transition zone. A
mixed layer occurred on all three profiles at a depth of about 40 m
with sound velocities between about 1469 and 1476 m/sec. The depth
of the DSC axis fluctuated between 60 and 80 m across the section,
while sound velocity at the axis varied from about 1474 m/sec (profile 15)
to about 1469 m/sec (profile 16) over a distance of about 44 nm. Critical
depth continued to shoal to the north from 270 m at about 61°N to 100 m
at about 63°N. Profile 15 represents the maximum effects of the West
Greenland Current along the station B to Carey Islands track and
generally agrees with historical summer data for the West Greenland
Current in the northern Labrador Sea shown in figure 22 and in
NAVOCEANO (1965b). Sound velocity at the DSC axis on profile 15
was about 15 m/sec greater than that on profile 14 (section 2).
These two profiles were separated by the strong West Greenland
Current/Labrador Sea gyre front. This front caused the closure of
the 1460 through 1472 m/sec sound velocity isolines and resulted in
the pronounced domed structure of the 1474 through 1480 m/sec iso-
lines below the DSC axis. Profile 14 is atypical for the Labrador
Sea gyre and probably lay in a detached, well mixed gyre of the Baffin
Land Current that penetrated the Labrador Sea gyre during Phase III.

(U) Section 4 of figure 28 extends up the relatively shallow continental slope south of Davis Strait between ranges of 620 and 760 nm from station B, and includes profiles 18 through 21. Station Q-3 lies at the northern end of this section. This section crossed the intense oceanographic transition zone in the northern Labrador Sea found during Phase III. Since profile 17 represents the effects of the West Greenland Current in this transition zone, the profile has been included in all section 4 sound velocity profile statistics. Within this transition zone, the Baffin Land Current mixes with and obliterates the surface effects of the West Greenland Current. This leads to sinking of the WGCW core. Below about 500 m, sinking WGCW and NACW mix with and obliterate boluses of BBDW descending from the Davis Strait sill. In addition, tidal effects in the relatively shallow water south of Davis Strait can induce formation of internal waves along the horizontal front that marks the bottom of the BLCW layer.

(U) Extremely large temporal and spatial variations in the overall sound velocity structure occurred south of Davis Strait during Phase III. A mixed layer occurred on four of the five sound velocity profiles at a depth of about 20 m, and was best developed on the northern two profiles of the section. Over the section as whole, sound velocity at the mixed layer showed a variation of 10.8 m/sec, the maximum such variation on any section of figure 28. This extreme variation was caused by intense mixing in the near-surface layer. The depth of the DSC axis varied between 40 and 80 m and coincided with the BLCW temperature minimum on all five profiles. Sound velocity at the axis varied from less than 1467 m/sec on profile 17 to about 1446 m/sec on profile 21. Critical depth increased from 100 m at about 63°N to 220 m at about 65°N and generally corresponded to the horizontal front marking the bottom of the BLCW layer. A similar situation was observed at station Q-3 during Phase III (figure 26).

(C) The 20.9 m/sec variation in sound velocity at the DSC axis across section 4 is the maximum variation in this parameter found anywhere in the exercise area. This variation is more than twice the magnitude of that at station Q-3 during Phase III (figure 26). It is also about twice the maximum variation in the sound velocity at the DSC axis found in the primary OPAREA (9.5 m/sec at station D during Phase I, figure 10). This remarkably large variation occurred over a distance of about 155 nm within 20 hours. Such a phenomenal amount of change could only be the result of tremendous amounts of mixing between various intrusive water masses. Much of this mixing must have been induced by internal waves. This mixing is apparent in the irregular and varied shapes of sound velocity profiles 17 through 21 and in the confused pattern of sound velocity isolines throughout section 4. The intense sound velocity variability south of the Davis Strait should have pronounced effects on sound transmission.

(C) Section 5 of figure 28 spans the shallow Davis Strait sill between ranges of 760 and 880 nm from station B, and includes profiles 22, 23, and 24. The overall sound velocity profiles in this region were very complex, but only below the DSC axis. Various perturbations in the positive sound velocity gradient below about 100 m were caused by inflowing WGCW, outflowing BBDW, or mixing of these water masses (figure 23). A well-developed mixed layer occurred on all three profiles at about 20 m depth and at sound velocities between about 1451 and 1461 m/sec. The 10.2 m/sec range in the sound velocity at the mixed layer was caused by mixing between the West Greenland Current and Baffin Land Current in the near-surface layer. The mean depth of the DSC axis was 70 m. Sound velocity at the axis varied between about 1441 and 1446 m/sec. The magnitude of this variation is about one-fifth that of section 4. The greater stability of the DSC axis along section 5 was due to the overwhelming presence of BLCW at depths of about 30 to 200 m. On all three profiles, the DSC axis coincided with the BLCW temperature minimum. Critical depth in section 5 varied between 140 and 240 m owing to variations below the BLCW core and variations in the near-surface layer. The near-bottom sound velocity maximum on profile 23 was caused by WGCW flowing north-ward over the Davis Strait sill into southern Baffin Bay. The near-bottom isovelocity layer on profile 24 resulted from mixing of WGCW and BBDW. Inflow of WGCW over the Davis Strait sill is evident in the form of the 1464 through 1472 m/sec sound velocity isolines below the DSC axis, particularly in the region just north of the Davis Strait sill. Although near-bottom flow does not directly affect critical depth over the Davis Strait sill, limited depth excess (less than 200 m) and variation of the near-bottom sound velocity profile could impede underwater sound transmission between the Labrador Sea and Baffin Bay during Phase III.

(U) Section 6 of figure 28 extends generally north-northwestward across southern Baffin Bay between ranges of 880 and 1130 nm from station B, and includes profiles 25 through 30. In this region, the upper 200 m of the water column are dominated by BLCW. Between about 200 and 700 m, BBDW mixes with a tongue of inflowing WGCW and eventually winnows out most of the WGCW core. Below about 700 m, southern Baffin Bay is occupied by relatively uniform BBDW. During Phase III, a well-developed mixed layer was found on all profiles in this section at 10 to 20 m depth with sound velocities between about 1452 and 1459 m/sec. On profile 25, sound velocity varied from 1441.6 m/sec at the surface to 1457.7 m/sec at 20 m (gradient of about 0.8 m/sec/m). This was the maximum such gradient observed in the NORLANT-72 data and was caused by a temperature maximum inbedded in an extremely strong halocline. Even stronger positive sound velocity gradients in the near-surface layer were observed in historical data (figure 24). The DSC axis

generally deepened to the north across section 6 from 40 m at about 67°N to 90 m at about 71°N. This abnormal increase probably was caused by a less pronounced flow of the Baffin Land Current in the northern part of the section (southern edge of Baffin Bay gyre). Sound velocity at the DSC axis varied between about 1440 and 1445 m/sec, and was generally less in the southern part of the section. Critical depth remained relatively constant across the section (mean depth of 220 m) and corresponded to the horizontal front marking the bottom of the BLCW layer. Below about 300 m, the northerly flow of WGCW is strongly indicated by the shapes of the 1464 through 1472 m/sec sound velocity isolines. At a range of about 1060 nm from station B, this inflow apparently was forced to rise in the water column by a flow of BBDW (sound velocities less than 1467 m/sec). Mixing of WGCW and BBDW caused extremely irregular sound velocity structures below about 300 m throughout southern Baffin Bay.

(U) Section 7 of figure 28 extends north-northwestward to northwestward across central Baffin Bay at ranges between 1130 and 1380 nm from station B, and includes profiles 31 through 36. This section lies over the relatively deep water of Baffin Basin and within the Baffin Bay gyre. The upper 200 m of the water column along section 7 is dominated by the Baffin Land Current. However, in central Baffin Bay, this current is far better defined off the east coast of Baffin Island (figure 4B). In central Baffin Bay, the WGCW core is much less pronounced than the core farther to the south. The entire Baffin Basin below about 700 m is occupied by BBDW. During Phase III, a well developed mixed layer at depths of 10 to 20 m was found on all profiles at sound velocities between about 1462 and 1469 m/sec. Mean sound velocity in the mixed layer in section 7 exceeded that in sections 4, 5, or 6, due to decreased surface effects of the Baffin Land Current and extremely low salinities in the upper 20 m of the water column (generally less than 30°/oo, figure 24). The depth of the DSC axis varied between 40 m on profile 35 and 130 m on profile 36. This 90-m variation (maximum variation for any section of figure 28) probably caused by variations in the flow of the Baffin Land Current. Sound velocity at the DSC axis generally increased to the north from about 1440 m/sec on profile 31 to about 1444 m/sec on profile 36. Mean critical depth for section 5 (750 m) was greater than that on any other section except section 1. Anomalously deep critical depths in central Baffin Bay were caused by an increase in the sound velocity of the near-surface layer and the predominance of cold, dilute BBDW over WGCW at intermediate depths. Critical depth approximately corresponded to the top of the BBDW layer throughout the section. The large variation in critical depth (540 m) along section 7 was caused mainly by changes in the near-surface sound velocity structure. The marked change in the positive sound velocity gradient between about 300 and 500 m corresponded to the depth of the much diminished WGCW core in central Baffin Bay.

84

(C) The final section (section 8) of figure 28 extends north-westward from a range of 1380 nm from station B to the Carey Islands in northern Baffin Bay. This section includes profiles 37, 38, and 39. The general sound velocity structure of northern Baffin Bay is similar to that in central Baffin Bay despite the absence of the Baffin Land Current and BBDW. These water masses are replaced by Arctic Water from Smith Sound. Only a slight, well-mixed core of WGCW is present south of the Carey Islands (figure 25). During Phase III, a mixed layer at about 10 m depth was found on all three profiles at sound velocities of about 1458 to 1460 m/sec. The variation in the maximum sound velocity in the mixed layer (2.5 m/sec) was the minimum such variation found in any section due to the surface stability of the Arctic Water Current. The depth of the DSC axis decreased to the north across section 8 from 110 m on profile 37 to 50 m on profile 39 and coincided with the temperature minimum in the Arctic Water core. The sound velocity at the axis also decreased to the north, but varied only 0.7 m/sec. This extremely small variation (minimum for any section of the track) further indicates the stability of the Arctic Water Current. Sound velocity perturbations below the DSC axis on profiles 37 and 38 probably were caused by mixing of Arctic Water and the well-mixed WGCW core. Critical depth also decreased to the north along section 8 from 390 to 260 m and generally corresponded to the bottom of the Arctic Water layer. However, owing to the shallow bathymetry of northern Baffin Bay, convergence zone propagation from a near-surface source probably was impeded north of about 75°N during Phase III.

(C) Over the 1500 nm track from station B to Carey Islands in northern Baffin Bay, maximum sound velocity in the mixed layer varied from 1487.7 m/sec (near station B) to 1451 m/sec (in Davis Strait). The maximum value of this parameter was found in close proximity to the North Atlantic Current gyre, the minimum occurred in the Baffin Land Current. The depth of the DSC axis varied from 180 m (near station B) to about 40 m at several locations north of Davis Strait and frequently coincided with the depth of a temperature minimum in the LCW, BLCW, or Arctic Water cores. However, the relatively constant depth of the axis along the track (variation of only 140 m) indicates that this parameter generally corresponded to the maximum depth of summer warming in the region northwest of the primary OPAREA. Sound velocity at the DSC axis varied from 1473.8 m/sec (in West Greenland Current) to 1440.2 m/sec (in central Baffin Bay), a total variation of 33.6 m/sec. Critical depth generally shoaled from 1250 m near station B to 100 m south of Davis Strait. Over the Davis Strait sill and in southern Baffin Bay, critical depth remained relatively constant between 140 and 240 m. However, over the Baffin Basin, critical depth increased markedly to a maximum of 920 m because of higher sound velocities in the near-surface layer and the effects of extremely cold, dilute BBDW. In northern Baffin Bay, the mean critical depth was 310 m. Generally, critical depths along the track were as dependent on the positive sound velocity gradient below the DSC axis as they were on near-surface temperatures. Except for regions over the Davis Strait sill and just south of the Carey Islands, depth excess was adequate for convergence zone propagation from a near-surface source during Phase III.

85

CONFIDENTIAL

(C) Along the entire track, overall sound velocity structure
was least variable in the Labrador Sea gyre (section 2) and most
variable south of Davis Strait (section 4). Sound velocity at the
DSC axis varied by 20.9 m/sec over a distance of about 155 nm south
of Davis Strait. This variation is about twice the magnitude of the
maximum variation found in the primary OPAREA and is more than three
times that at station E in the Labrador Sea gyre. Furthermore, this
variation is about two-thirds that over the track as a whole. Such a
phenomenal amount of variation can only be caused by intensive mixing
between several water masses. About half of this mixing probably is
induced by internal waves. An intense oceanographic transition zone
south of Davis Strait should have profound effects on sound propagation
in the northern Labrador Sea and on transmission of underwater sound
from the Labrador Sea across Davis Strait into Baffin Bay during
summer.

SUMMARY

(C) From July through September 1972, 3 STDs, 6 CTD/SVs, 10 SVPs,
266 XBTs, and 154 AXBTs were collected in the Labrador Sea, Irminger
Sea, and Baffin Bay as part of the NORLANT-72 Exercise. These ob-
servations were collected during three phases that corresponded to
early, middle, and late summer. Sound velocity profiles were
calculated for 163 XBT and AXBT traces using the equation of Wilson
(1960) and historical salinity correction factors. Agreement was
generally good between calculated sound velocity profiles and sound
velocities measured directly by the CTD/SV and SVP systems. However,
calculated sound velocities below the DSC axis were 0.5 to 1.0 m/sec
higher than measured values in several instances, possibly because of
an error in Wilson's equation and XBT system inaccuracies. Data were
adequate for intensive sound velocity analyses in the following
regions:

   ● The primary OPAREA (50°N to 55°N between 44°W and 49°W)
including stations A, B, and D,

      ● A track between station B and Denmark Strait,

      ● A track between station B and Reykjanes Ridge, and

      ● A track between station B and the Carey Islands in
northern Baffin Bay.

In the primary OPAREA, data were collected during all three phases of
the exercise. On the track from station B to the Reykjanes Ridge, data
were available during Phases I and II. Data were adequate for analysis
during Phase I to the northeast of station B and during Phase III to
the northwest of this station.

(U) During all three phases the primary OPAREA was dominated by the meandering Subarctic Convergence. This strong oceanographic front separated an unstable gyre of the relatively warm, saline North Atlantic Current from the colder, less saline Labrador Sea gyre. Intensive mixing of North Atlantic Central Water (NACW), Labrador Current Water (LCW), and Atlantic Subarctic Water (ASaW) across the Subarctic Convergence caused very complex and spurious sound velocity profiles in the primary OPAREA throughout the exercise. Near-bottom sound velocity profiles in much of the primary OPAREA were affected by a flow of cold, dilute Norwegian Sea Overflow Water (NSOW) that enters the western North Atlantic through Denmark Strait. This water mass caused lower sound velocities below a depth of about 2200 m that were most pronounced in the North Atlantic Current gyre and under the main flow of the Labrador Current, but did not directly affect critical depths.

(C) At stations A, B, and D, the DSC axis coincided with the bottom of the ASaW layer whether the stations lay on the warm or cold side of the Subarctic Convergence. At station A during Phase III, the depth of the DSC axis varied between 150 and 220 m, and sound velocity at the axis varied from 1470.4 to 1474.7 m/sec (variation of 4.3 m/sec). At station B during Phases I and II, the depth of the DSC axis varied between 80 and 360 m, while its sound velocity varied between 1469.3 and 1473.6 m/sec (also a variation of 4.3 m/sec). Station A lay astride the Subarctic Convergence during Phase III, as did station B during Phase I. During Phase II, station B lay just north of this front. At station D during Phase I, the DSC axis varied between 100 and 380 m during the total occupation and its sound velocity varied between 1466.7 and 1476.2 m/sec (a variation of 9.5 m/sec over less than 48 hours). Station D also lay astride the Subarctic Convergence during Phase I, but in close proximity to the center of the unstable North Atlantic Current gyre. The unstable nature of this gyre and mixing across the Subarctic Convergence were responsible for the maximum variation in sound velocity at the DSC axis found anywhere in the primary OPAREA. About 45% of the variation in DSC structure at station D during Phase I was attributable to temporal effects (mixing induced by internal waves with a period approximating that of the diurnal tide). The other 55% was due to spatial effects (changes in the position of the meandering Subarctic Convergence). Depth excess was adequate for convergence zone propagation from a near-surface source at all three stations throughout the exercise.

(C) Data were adequate during all three phases to construct a sound velocity cross section from station B to station A (due south) to Grand Banks (southwest of station A). This section crossed the North Atlantic Current gyre and the Labrador Current northeast of Grand Banks during each phase. A sporadic mixed layer at depths between 10 and 70 m occurred along the track throughout the exercise. This layer was best developed and most persistent during Phase III in

response to increased surface insolation. The depth of the DSC axis along the track remained somewhat similar during each phase, and varied from a maximum of 320 to 420 m in the North Atlantic Current gyre to a minimum of 30 to 50 m northeast of Grand Banks. In the Labrador Current, the DSC axis coincided with a temperature minimum in the LCW core. Sound velocity at the axis along the track showed a significant variation between phases of the exercise. In the North Atlantic Current gyre, this parameter varied between 1475.4 m/sec (Phase I) and 1480.2 m/sec (Phase III). In the Labrador Current, the sound velocity at the axis varied between 1444.6 m/sec (Phase II) and 1455.4 m/sec (Phase I). These variations are attributable to changes in position of the Subarctic Convergence, fluctuations in Labrador Current flow, and increased development of the North Atlantic Current gyre. Critical depths along the track were about 400 m deeper during Phase III than during Phase I owing to increased surface insolation. However, depth excess along the entire track was adequate for convergence zone propagation from a near-surface source during each of the three phases of NORLANT-72, except at the southwest end of the track (over the Grand Banks continental slope). Along the station B to station A to Grand Banks section, sound velocity profiles were most complicated in the North Atlantic Central gyre, least complicated in the Labrador Current, and of intermediate complexity in numerous tongues of the Labrador Sea gyre that protruded into the primary OPAREA.

(U) Along that portion of the above section that extended due south from station B to station A, temporal and spatial variations in the depth and sound velocity at the DSC axis were greatest during Phase III (260 m and 8.9 m/sec, respectively) and least during Phase I (130 m and 4.2 m/sec, respectively). This was caused by greater development of the unstable North Atlantic Current gyre between station B and station A during Phase III. Maximum variability in sound velocity at the axis along the station B to station A track (8.9 m/sec during Phase III) is of the same magnitude as the maximum temporal and spatial variation of this parameter at any station in the primary OPAREA (9.5 m/sec at station D during Phase I). These variations are caused by the predominance of the unstable North Atlantic Current gyre. About half the variability in DSC structure at station D during Phase I was attributable to temporal variations (by internal wave action). About half the variability in DSC structure encountered in the vicinity of stations A and B during NORLANT-72 probably was also temporal in nature. The other half probably was caused by fluctuations in position of the Subarctic Convergence.

(C) During Phase I of NORLANT-72, a line of XBTs and AXBTs were collected between station B and a position just south of Denmark Strait in the Irminger Sea. This track started in the North Atlantic Current gyre just south of the Subarctic Convergence, spanned the Labrador Current gyre, paralleled the Subarctic Convergence, and ended in the relatively warm, saline Irminger Current. A variable mixed layer occurred along the first half of the track but was generally absent north of 60°N. The depth of the DSC axis generally increased to the

northeast from 70 m in the Labrador Current gyre to about 600 m at
54°N, 45°W. In the Irminger Sea, the DSC axis coincided with the
bottom of the Irminger Current Water layer (a derivant of NACW).
Sound velocity at the axis also increased to the northeast from less
than 1465 m/sec to more than 1480 m/sec. Critical depth varied from
1150 m at station B to 520 m in the Labrador Sea gyre to 1640 m in the
Irminger Current. However, depth excess along the entire track was
adequate to ensure convergence zone propagation from a near-surface
source. At the northern end of the track, the near-bottom sound
velocity profile should be markedly influenced by NSOW overflow from
Denmark Strait. Historical data for this region show a near-bottom
sound velocity maximum corresponding to the top of the NSOW layer
(Guthrie, 1964). Generally, the overall sound velocity structure was
most complicated in the Irminger Sea, least complicated in the Labrador
Sea gyre, and of intermediate complexity along the Subarctic Convergence.

(C) During Phases I and II of NORLANT-72, two lines of XBTs were
taken between station B and separate positions just east of the crest
of the Reykjanes Ridge. These two lines trended east-northeast and
due east of station B, respectively. The Phase I track started in the
North Atlantic Current gyre, spanned the Labrador Sea gyre, and then
crossed the Subarctic Convergence into the main flow of the North
Atlantic Current. The Phase II track started at the edge of the Labrador
Sea gyre and ended in the North Atlantic Current. A mixed layer was
absent along the Phase I track, but did occur between 20 and 40 m along
most of the Phase II track. The depth of the DSC axis over much of
both tracks was approximately the same and varied from about 100 m
at station B to about 300 m just east of the Reykjanes Ridge. At
the eastern end of both tracks, the depth of the DSC axis increased
rapidly to about 600 m and coincided with the bottom of the NACW
layer. This occurred at about 35°W during Phase I and at about 30°W
during Phase II. Between these locations, the DSC axis was as much
as 400 m deeper during Phase I than during Phase II. This anomalous
situation probably is the result of sensitivity of DSC axis depth to
temporal and spatial fluctuations in the environment. Large-scale
fluctuations in sound velocity structure would be expected in the
upper 1000 m in the relatively shallow water over the eastern flank
of the Reykjanes Ridge because of mixing between NACW and transient
cells of Mediterranean Intermediate Water. Sound velocity at the
DSC axis along the track increased to the east from 1460.4 to
1477.0 m/sec during Phase I and from 1468.2 to 1480.9 m/sec during
Phase II. Greater sound velocities at the axis during Phase II were
mainly the result of the lesser extent of the Labrador Sea gyre to
the south and west. Critical depths along the station B to Reykjanes
Ridge track were about 400 m deeper during Phase II than during Phase I
due to increased surface insolation. However, depth excess along both
tracks was adequate for convergence zone propagation from a near-surface
source, except over the crest of the Reykjanes Ridge. Generally, sound
velocity structure along the track was most complicated in the vicinity
of the Subarctic Convergence (just west of the Reykjanes Ridge).

(C) During Phase III of the exercise, a line of XBTs was taken extending 1500 nm northwest of station B to the Carey Islands in northern Baffin Bay. This track crossed the following distinct oceanographic regimes:

1. Near-Subarctic Convergence (station B to about 56°N),

2. Labrador Sea gyre (about 56°N to 61°N),

3. West Greenland Current (about 61°N to 63°N),

4. Northern Labrador Sea transition zone (about 63°N to 65°N),

5. Davis Strait sill (about 65°N to 67°N),

6. Southern Baffin Bay (about 67°N to 71°N),

7. Central Baffin Bay (about 71°N to 75°N), and

8. Northern Baffin Bay (about 75°N to the Carey Islands).

Oceanographic conditions changed markedly within and between several of these regimes. The Labrador Sea gyre and the West Greenland Current were separated by a strong oceanographic front extending to at least 500 m depth. The northern Labrador Sea transition zone was even more complex oceanographically than the primary OPAREA. In this region, the Baffin Land Current obliterated surface effects of the West Greenland Current and caused West Greenland Current Water (WGCW) to sink. Sinking WGCW and NACW obliterated boluses of Baffin Bay Deep Water (BBDW) descending from the Davis Strait sill. In addition, tidal effects in the relatively shallow water south of Davis Strait induced formation of internal waves along the horizontal front marking the bottom of the Baffin Land Current Water (BLCW) layer. In southern and central Baffin Bay, the upper 200 m were dominated by BLCW. However, oceanographic conditions below about 300 m were quite variable due to mixing of the northerly flowing WGCW core with extremely cold, dilute BBDW. Just south of the Carey Islands, BLCW and BBDW disappeared and were replaced by more saline Arctic Water.

(C) During Phase III, data were adequate to examine sound velocity variations at two stations along the station B to Carey Islands track. At station E in the center of the Labrador Sea gyre, the depth of the DSC axis varied between 40 and 80 m and coincided with the LCW temperature minimum. Sound velocity at the axis varied between 1460.9 and 1467.1 m/sec (6.2 m/sec). This relatively large variation in the stable Labrador Sea gyre was caused by intrusions of WGCW into the gyre. At station Q-3 immediately south of the Davis Strait sill, the DSC axis again varied between 40 and 80 m, but coincided with the very

cold BLW core. Sound velocity at the axis varied between 1443.2 and 1451.1 m/sec (7.9 m/sec). This variation is of the same general magnitude as the maximum variation found in the primary OPAREA (9.5 m/sec at station D during Phase I). About half of the variability in DSC structure at station Q-3 probably was caused by internal waves. The other half apparently resulted from intrusions of WGCW into the Baffin Land Current. Below the DSC axis, sound velocity profiles at station Q-3 displayed frequent perturbations caused by mixing of WGCW, NACW, and BBDW. At both stations, depth excess was adequate for convergence zone propagation from a near-surface source.

(C) A mixed layer occurred between 10 and 50 m on most profiles along the station B to Carey Islands track. This layer reached maximum development in southern Baffin Bay, where a positive sound velocity gradient of about 0.8 m/sec/m occurred in the upper 20 m. This strong gradient was caused by a temperature maximum imbedded in an extremely strong halocline. The depth of the DSC axis varied from 180 m near station B to about 40 m at several locations north of the Davis Strait sill and coincided with a temperature minimum in the LCW, BLCW, or Arctic Water core over most of the track. The relatively constant depth of the axis along the track (variation of only 140 m) indicates that this parameter generally corresponded to the maximum depth of summer warming in the region northwest of the primary OPAREA. Sound velocity at the DSC axis varied from 1473.8 m/sec in the West Greenland Current to 1440.2 m/sec in central Baffin Bay (33.6 m/sec). In the intense transition zone south of Davis Strait, this parameter varied 20.9 m/sec over a distance of about 155 nm. This latter variation is about twice the magnitude of the maximum variation found at any single station in the primary OPAREA and about two-thirds that found over the track as a whole. Such a phenomenal amount of variation can only be caused by intensive mixing between several water masses. About half of this mixing probably was induced by internal waves. Critical depth generally shoaled to the north from 1250 m near station B to 100 m south of Davis Strait. Over the Davis Strait sill and in southern Baffin Bay, critical depth remained relatively constant (140 to 240 m) and generally corresponded to the horizontal front marking the bottom of the BLCW layer. In central Baffin Bay, critical depth increased to a maximum of 920 m as a result of higher sound velocities in the near-surface layer and the effects of extremely cold, dilute BBDW. South of the Carey Islands, critical depth shoaled to 250 m. Depth excess along most of the track was adequate for convergence zone propagation from a near-surface source, except just south of the Carey Islands and over the shallow Davis Strait sill. The intense oceanographic transition zone south of Davis Strait and the shallow sill depth of this strait may preclude meaningful underwater sound transmission between the Labrador Sea and Baffin Bay during summer.

CONFIDENTIAL

CONCLUSIONS

1. (U) The general oceanography of the NORLANT-72 area is more complicated than in most of the North Atlantic Ocean. This leads to complex and variable sound velocity structures throughout much of the exercise area.

2. (U) Sound velocity profiles calculated from XBT temperature traces and historical salinity profiles using Wilson's equation generally agree well with measured sound velocity profiles.

3. (U) T-7 XBTs (maximum depth of 760 m) are excellent sampling devices for the NORLANT-72 area owing to the relatively shallow DSC axis. However, more salinity profiles collected during the exercise would have simplified sound velocity analysis.

4. (C) Sound velocity profiles are most complex and variable in the primary OPAREA (50°N to 55°N between 44°W and 49°W) and in the region just south of Davis Strait. A similar situation would be expected south of the Denmark Strait sill.

5. (U) In the primary OPAREA, sound velocity variability is related to the position of the meandering Subarctic Convergence that separates the relatively warm, saline North Atlantic Current gyre from the colder, less saline Labrador Sea gyre. The Labrador Sea gyre is far more stable oceanographically than the North Atlantic Current gyre.

6. (U) South of Davis Strait, sound velocity variability is related to mixing between the West Greenland Current and the Baffin Land Current in the upper 200 m. Below this depth, mixing of North Atlantic Central Water with Baffin Bay Deep Water boluses also causes substantial variations in sound velocity structure. Sound velocity profiles south of Davis Strait are even more complex and variable than those in the primary OPAREA.

7. (U) Temporal and spatial variability appear to be equally significant in controlling DSC structure throughout the NORLANT-72 Exercise area.

8. (C) Depth excess is adequate for convergence zone propagation from a near-surface source throughout most of the exercise area during NORLANT-72. Exceptions to this general rule occur over the Grand Banks continental slope, over the crest of the Reykjanes Ridge, across the sills of Denmark and Davis Straits, and in northern Baffin Bay.

9. (C) The shallow sill depth of Davis Strait and the intense oceanographic transition zone in the northern Labrador Sea may preclude meaningful sound transmission between the Labrador Sea and Baffin Bay during summer.

10. (C) Because of its location astride the meandering Subarctic
Convergence, the primary OPAREA does not appear to be an optimum site
for summer acoustic exercises. This also applies for station B
situated just north of this front during most of the NORLANT-72
Exercise. A better location for summer acoustic exercises would be
at about 56°N, 45°W in the relatively stable Labrador Sea gyre where
sound velocity profiles should be much less complex and variable.

REFERENCES (U)

Bailey, W. D., On the origin of deep Baffin Bay water, J. Fish. Res. Bd. Can., 13(3), 303-308, 1956.

Bourkland, M. T., Oceanographic cruise summary, Davis Strait, July-August 1968, Nav. Oceanogr. Off., Informal Rep., IR 68-117, Washington, DC, 1968 (unpublished).

Bubnov, V. A., Intermediate subarctic waters in the northern part of the Atlantic Ocean, Okeanol. Issled., 19, 136-153, 1968 (translated from Russian as Nav. Oceanogr. Off. Trans. 545, Washington, DC, 1973).

Carnvale, A., P. Bowen, M. Basileo, and J. Sprenke, Absolute sound velocity measurements in distilled water, J. Acoust. Soc. Am., 44(4), 1098-1102, 1968.

Fenner, D. F. and P. J. Bucca, The sound velocity structure of the North Atlantic Ocean, Nav. Oceanogr. Off., Informal Rep., IR 71-13, Washington, DC, 1971 (unpublished).

Fenner, D. F. and P. J. Bucca, NORLANT-72 environmental measurements and preliminary sound velocity analysis, Nav. Oceanogr. Off., Tech. Note, TN 7005-2-72, Washington, DC, 1972 (unpublished).

Garner, D. M., Flow through Charlie-Gibbs Fracture Zone, Mid-Atlantic Ridge, Can. J. Earth Sci., 9, 116-121, 1972.

Guthrie, R. C., Sound velocity distribution in the Irminger Sea, in Proc. First Navy Symp. Mil. Oceanogr., 1, 97-111, Nav. Oceanogr. Off., Washington, DC, 1964.

Husby, D. M., Oceanographic observations, North Atlantic Ocean station BRAVO, October 1965 - September 1966, Coast Guard Oceanogr. Unit, Oceanogr. Rep. 14 (CG-373-14), Washington, DC, 1967.

Husby, D. M., Oceanographic observation   North Atlantic Ocean station CHARLIE, May 1966 - March 1967, Coast Guard Oceanogr. Unit, Oceanogr. Rep. 17 (CG-373-17), Washington, DC, 1968.

Katz, E. J., Diffusion of the core of Mediterranean water above the Mid-Atlantic Ridge crest, Deep-Sea Res., 17, 611-625, 1970.

La Fond, E. C., Internal waves, part 1, in The sea, 1, edited by N. M. Hill, chap. 22, 731-751, Interscience, New York, 1962.

REFERENCES (cont'd)

NAVOCEANO, Oceanographic atlas of the polar seas, part II, Arctic,
Nav. Oceanogr. Off., H.O. Pub. No. 705, Washington, DC, 1958.

NAVOCEANO, Tables of sound speed in sea water, Nav. Oceanogr. Off.,
Spec. Pub., SP-58, Washington, DC, 1962.

NAVOCEANO, Oceanographic atlas of the North Atlantic Ocean, section I,
tides and currents, Nav. Oceanogr. Off., H.O. Pub. No. 700,
Washington, DC, 1965a.

NAVOCEANO, An interim report on sound velocity distribution in the
North Atlantic Ocean, Nav. Oceanogr. Off., Tech. Rep., TR-171,
Washington, DC, 1965b.

Naval Underwater Systems Center, NORLANT-72 phase 3 operation plan (U),
Nav. Underw. Sys. Cen., Tech. Doc. 4371, New London, Conn., 1972.
CONFIDENTIAL

Nunn, S. O., III, Study of the oceanic polar front in the Denmark Strait,
Nav. Postgraduate School, MS thesis, Monterey, Cal. 1968.

Palfrey, K. M., Jr., Oceanography of Baffin Bay and Naires Strait in
the summer of 1966, Coast Guard Oceanogr. Unit, Oceanogr. Rep. 16
(CG-373-16), 1-74, Washington, DC, 1968.

Sverdrup, H. U., M. W. Johnson, and R. H. Fleming, The oceans, their
physics, chemistry, and general biology, Prentice-Hall, Englewood
Cliffs, N. J., 1942.

Wilson, W. D., Equation for the speed of sound in sea water, J. Acoust.
Soc. Am., 32(10), 1357, 1960.

Worthington, L. V., The Norwegian Sea as a mediterranean basin, Deep-
Sea Res., 17, 77-84, 1970.

Worthington, L. V. and G. H. Volkman, The volume transport of Norwegian
Sea overflow water in the North Atlantic, Deep-Sea Res., 12,
667-676, 1965.

Worthington, L. V. and W. R. Wright, North Atlantic Ocean atlas of
potential temperature and salinity in the deep water including
temperature, salinity, and oxygen profiles from the ERIKA DAN
cruise of 1962, Woods Hole Oceanogr. Inst., Atlas Series, Vol. II,
Woods Hole, Mass., 1970.

DISTRIBUTION LIST (U)

CNO (OP-95) (1)

MASWSP (ASW-11) (1)

OCEANAV (Dr. J. Boosman) (1)

NAVELECSYSCOM (PME-124/TA) (1)

NAVFACENGCOM (Code FPO-1) (1)

NAVSEASYSCOM (SEA-06H1) (1)

ONR Codes:
    102-OS   (1)
    102-OSC   (2)
    400   (1)
    412   (1)
    AESD   (1)

DIRNRL (1)

NRL Codes:
    2000   (1)
    8100   (1)
    8160   (2)
    8174   (1)

COMNAVAIRDEVCEN (1)

NAVAIRDEVCEN (P. VanSchuyler) (1)

COMNUC (1)

NUC (Code 502) (1)

OICNUSC (1)

NUSC Codes:
    TA   (1)
    TA11   (2)
    J. Syck   (1)

DDC (1)

DDC-TSR (1)

COMOCEANSYSLANT (1)

COMNCSL (1)

NAVPOSTGRADSCOL (1)

DIRMPL, SIO (1)

U. Miami (Dr. S. C. Daubin) (1)

WHOI (Dr. E. E. Hayes) (1)

ADL (Dr. G. A. Raisbeck) (1)

B.K. Dynamics (A. E. Fadness) (1)

Raff Assoc. (Dr. J. I. Bowen) (1)

Tracor (J. T. Gottwald) (1)

TRW Systems Group (R. Brown) (1)

Underwater Systems, Inc.
    (Dr. M. S. Weinstein) (1)

Xonics (Dr. N. L. Moise) (1)

PRECEDING PAGE BLANK-NOT FILMED

MEMORANDUM FOR DISTRIBUTION LIST

Subj: DECLASSIFICATION OF LONG RANGE ACOUSTIC PROPAGATION PROJECT (LRAPP) DOCUMENTS

Ref: (a) SECNAVINST 5510.36

Encl: (1) List of DECLASSIFIED LRAPP Documents

1. In accordance with reference (a), a declassification review has been conducted on a number of classified LRAPP documents.

2. The LRAPP documents listed in enclosure (1) have been downgraded to UNCLASSIFIED and have been approved for public release. These documents should be remarked as follows:

> Classification changed to UNCLASSIFIED by authority of the Chief of Naval Operations (N772) letter N772A/6U875630, 20 January 2006.

> DISTRIBUTION STATEMENT A: Approved for Public Release; Distribution is unlimited.

3. Questions may be directed to the undersigned on (703) 696-4619, DSN 426-4619.

BRIAN LINK
By direction

Subj: DECLASSIFICATION OF LONG RANGE ACOUSTIC PROPAGATION PROJECT
        (LRAPP) DOCUMENTS

DISTRIBUTION LIST:
        NAVOCEANO (Code N121LC – Jaime Ratliff)
        NRL Washington (Code 5596.3 – Mary Templeman)
        PEO LMW Det San Diego (PMS 181)
        DTIC-OCQ (Larry Downing)
        ARL, U of Texas
        Blue Sea Corporation (Dr.Roy Gaul)
        ONR 32B (CAPT Paul Stewart)
        ONR 3210A (Dr. Ellen Livingston)
        APL, U of Washington
        APL, Johns Hopkins University
        ARL, Penn State University
        MPL of Scripps Institution of Oceanography
        WHOI
        NAVSEA
        NAVAIR
        NUWC
        SAIC

Declassified LRAPP Documents

Report Number	Personal Author	Title	Publication Source (Originator)	Pub. Date	Current Availability	Class.
Unavailable	Beam, J. P., et al.	LONG-RANGE ACOUSTIC PROPAGATION LOSS MEASUREMENTS OF PROJECT TRANSLANT I IN THE ATLANTIC OCEAN EAST OF BERMUDA	Naval Underwater Systems Center	740612	ADC001521	U
Unavailable	Cornyn, J. J., et al.	AMBIENT-NOISE PREDICTION. VOLUME 2. MODEL EVALUATION WITH IOMEDEX DATA	Naval Research Laboratory	740701	AD0530983	U
Unavailable	Unavailable	COHERENCE OF HARMONICALLY RELATED CW SIGNALS	Naval Underwater Systems Center	740722	ADB181912	U
Unavailable	Banchero, L. A., et al.	IOMEDEX SOUND VELOCITY ANALYSIS AND ENVIRONMENTAL DATA SUMMARY	Naval Oceanographic Office	740801	ADC000419	U
3810	Unavailable	CONSTRUCTION AND CALIBRATION OF USRD TYPE F58 VIBROSEIS MONITORING HYDROPHONES SERIALS 1 THROUGH 7	Naval Research Laboratory	741002	ND	U
ARL-TM-73-11; ARL TM-73-12	Ellis, G. E., et al.	ARL PRELIMINARY DATA ANALYSIS FROM ACODAC SYSTEM; ANALYSIS OF THE BLAKE TEST ACODAC DATA	University of Texas, Applied Research Laboratories	741015	ADA001738; ND	U
Unavailable	Mitchell, S. K., et al.	QUALITY CONTROL ANALYSIS OF SUS PROCESSING FROM ACODAC DATA	University of Texas, Applied Research Laboratories	741015	ADB000283	U
Unavailable	Unavailable	MEDEX PROCESSING SYSTEM. VOLUME II. SOFTWARE	Bunker-Ramo Corp. Electronic Systems Division	741021	ADB000363	U
Unavailable	Spofford, C. W.	FACT MODEL. VOLUME I	Maury Center for Ocean Science	741101	ADA078581	U
Unavailable	Bucca, P. J., et al.	SOUND VELOCITY STRUCTURE OF THE LABRADOR SEA, IRMINGER SEA, AND BAFFIN BAY DURING THE NORLANT-72 EXERCISE	Naval Oceanographic Office	741101	ADC000461	U
Unavailable	Anderson, V. C.	VERTICAL DIRECTIONALITY OF NOISE AND SIGNAL TRANSMISSIONS DURING OPERATION CHURCH ANCHOR	Scripps Institution of Oceanography Marine Physical Laboratory	741115	ADA011110	U
Unavailable	Baker, C. L., et al.	FACT MODEL. VOLUME II	Office of Naval Research	741201	ADA078539	U
ARL-TR-74-53	Anderson, A. L.	CHURCH ANCHOR EXPLOSIVE SOURCE (SUS) PROPAGATION MEASUREMENTS (U)	University of Texas, Applied Research Laboratories	741201	ADC002497; ND	U
MCR106	Cherkis, N. Z., et al.	THE NEAT 2 EXPERIMENT VOL 1 (U)	Maury Center for Ocean Science	741201	NS; ND	U
MCR107	Cherkis, N. Z., et al.	THE NEAT 2 EXPERIMENT VOL 2 - APPENDICES (U)	Maury Center for Ocean Science	741201	NS; ND	U
Unavailable	Mahler, J., et al.	INTERIM SHIPPING DISTRIBUTION	Tetra, Tech, BB&N, & PSI	741217	ND	U
75-9M7-VERAY-R1	Jones, C. H.	LRAPP VERTICAL ARRAY - PHASE IV	Westinghouse Electric Corp.	750113	ADA008427; ND	U
AESD-TN-75-01	Spofford, C. W.	ACOUSTIC AREA ASSESSMENT	Office of Naval Research	750201	ADA090109; ND	U